CHALMERS
UNIVERSITY OF TECHNOLOGY

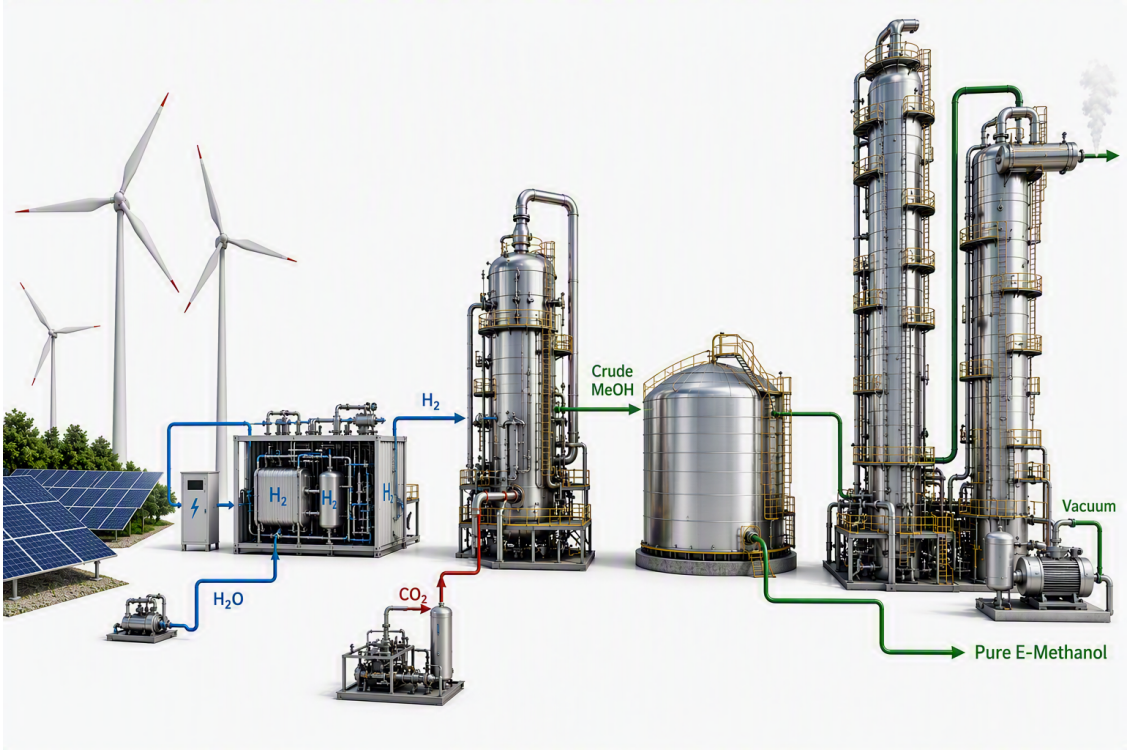

E-Methanol Vacuum Distillation

Techno-Economic Evaluation and Process Design of Flexible Vacuum Distillation under Renewable-Driven Feed Variability in E-Methanol Production

Master's thesis in Innovative Sustainable Energy Engineering (Nordic Master), Master of Science (Technology)

ABDUL MOEEZ

DEPARTMENT OF ENVIRONMENTAL AND ENERGY SCIENCES
CHALMERS UNIVERSITY OF TECHNOLOGY
Gothenburg, Sweden 2026
www.chalmers.se

Master's thesis 2026

Flexible Vacuum Distillation for E-Methanol Purification

Techno-Economic Evaluation and Process Design of Flexible Vacuum Distillation under Renewable-Driven Feed Variability in E-Methanol Production

ABDUL MOEEZ



CHALMERS
UNIVERSITY OF TECHNOLOGY

Department of Environmental and Energy Sciences
Chalmers University of Technology
Gothenburg, Sweden 2026

Techno-Economic Evaluation and Process Design of Flexible Vacuum Distillation under Renewable-Driven Feed Variability in E-Methanol Production

© ABDUL MOEEZ, 2026.

Supervisor: Dr. Thomas Kohl, Andritz OY
Prof. Ville Alopaeus, Aalto University, Finland
Examiner: Prof. Simon Harvey, Assistant Head of Department, Environmental and Energy Sciences

Master's Thesis 2026
Department, Environmental and Energy Sciences
Chalmers University of Technology
SE-412 96 Gothenburg
Telephone +46 31 772 1000

Typeset in LaTeX
Printed by Chalmers Digitaltryck
Gothenburg, Sweden 2026

Techno-Economic Evaluation and Process Design of Flexible Vacuum Distillation under Renewable-Driven Feed Variability in E-Methanol Production

Abdul Moeez
Department, Environmental and Energy Sciences
Chalmers University of Technology

Abstract

E-methanol synthesis from green hydrogen and captured biogenic CO_2 offers a low-carbon route to methanol, but purification, the second most energy-intensive step after electrolysis, is complicated by the intermittent hydrogen supply typical of renewable electricity. This thesis examines whether 85 °C waste heat from the cooling water of an alkaline electrolyzer can fully replace utility steam in e-methanol distillation, benchmarks this configuration against conventional three-column distillation, and develops a dynamic optimization framework to reconcile fast upstream hydrogen fluctuations with the column's stable ramp rate of ±5%/h.

A steady-state rate-based RadFrac design in Aspen Plus achieves 99.995 wt% methanol purity, meeting IMPCA specifications with an over-design margin while operating down to 57.5% of nominal feed capacity. As the electrolyzer stream covers only about half of the vacuum reboiler duty, an ammonia closed-cycle heat pump was designed to upgrade the remaining low-grade heat. Its viability is strongly location-dependent: a 2-year payback in the Nordics against a 17-year payback in South America, driven by the difference in steam cost.

To manage crude e-methanol feed mass flow-rate variability, three buffering strategies – intermediate storage, product recycling, and a hybrid of the two – were formulated and solved dynamically over one year of hourly 2025 electricity prices for both markets. The hybrid model consistently achieved the lowest annualised cost and reduced the required tank size relative to the intermediate storage model.

The techno-economic analysis favours conventional distillation in South America, where steam is inexpensive and hydrogen supply is comparatively stable, and vacuum distillation in the Nordics, where steam is costly and electrifying the reboiler duty provides available synthesis-loop steam for CO_2 capture. Waste-heat-driven vacuum distillation is therefore not universally advantageous: it pays off only where steam is expensive enough relative to electricity to offset the energy penalty of vacuum operation.

Keywords: E-Fuels, Waste Heat Recovery, Heat Integration, Dynamic Process Modeling and Optimization, Heat Pump Dynamic Analysis, Mathematical Modeling and Simulations, Mixed-Integer Linear and Non-Linear Programming, and Techno-Economic Analysis.

Acknowledgements

I would like to express my sincere gratitude to Dr. Thomas Kohl, Director of Technology, e-Fuels at Andritz Oy, for giving me the opportunity to carry out this thesis and for serving as my advisor throughout the work. He allowed me to work independently, in the way I was most comfortable, while always remaining supportive and appreciative of my progress.
I am also deeply grateful to my supervisors, Prof. Ville Alopaeus from Aalto University and Prof. Simon Harvey from Chalmers University of Technology, for their guidance and support throughout this thesis.
My sincere thanks go to Otto Greis, my adviser, who consistently brought new ideas to the table and provided valuable feedback throughout our meetings. I would also like to thank Dr. Pavel Maksimov, Manager of Technology, e-Fuels, who was always ready to help and worked through every problem alongside me during the course of this thesis. His personal interest and support in my thesis, offered like that of an older brother, meant a great deal to me. I am also thankful to Anubhuti Goel and Arun Mohanan, process engineers at Andritz, who were always available to help.
I would like to especially thank Prof. Mika Järvinen, who motivated me to pursue a thesis within a company and supported me throughout the process of finding and securing it.
Finally, I want to thank my two friends, Mustaneer and Tanzeel ur Rehman, whom I met in Finland — they have truly been a source of support for me since we met.

Abdul Moeez, Gothenburg, September 2026

Contents

Abstract 4

Preface 6

Contents 7

1 Introduction 17
- 1.1 Scope . . . 18
- 1.2 Objectives . . . 18
- 1.3 Outline of the Thesis . . . 19

2 Literature Review 21
- 2.1 E-Methanol: Physical Properties . . . 21
  - 2.1.1 E-Methanol: Production Pathways . . . 21
- 2.2 Methanol Synthesis . . . 23
  - 2.2.1 Crude Methanol . . . 23
- 2.3 E-Methanol Distillation . . . 24
  - 2.3.1 Thermodynamic Principles . . . 24
  - 2.3.2 Fractional Distillation . . . 25
- 2.4 Column Sizing and Design . . . 26
  - 2.4.1 Tray Columns . . . 26
  - 2.4.2 Packed Column . . . 28
  - 2.4.3 Columns Configurations for E-Methanol Distillation . . . 28
- 2.5 Operating Conditions . . . 31
  - 2.5.1 Flow Regime: Tray Columns . . . 31
  - 2.5.2 Flow Regime: Packed Columns . . . 32
- 2.6 Vacuum Distillation . . . 32
- 2.7 Transient Distillation Process . . . 34
  - 2.7.1 Distillation Column Design Options . . . 35
- 2.8 Distillation Heat Duty Availability . . . 36
  - 2.8.1 Mechanical Vapour-Compression Heat Pump . . . 36

3 Assumptions 39
- 3.1 Process Simulation . . . 39
- 3.2 Optimization Models . . . 39
- 3.3 Techno-Economic Analysis . . . 41
- 3.4 Heat Pump Analysis . . . 44

4 Methodology 46
- 4.1 Vacuum Distillation: Process Design and Simulation . . . 46
  - 4.1.1 Topping Column . . . 46
    - 4.1.1.1 Number of Stages and Feed Stage . . . 47
    - 4.1.1.2 Reboiler and Condenser Temperature . . . 47

4.1.1.3 Turn-Down Ratio . . . 49
4.1.2 Refining Column . . . 50
4.1.2.1 Number of Stages and Feed Stage . . . 51
4.1.2.2 Reboiler and Condenser Temperature . . . 53
4.1.2.3 Fusel Oils Side stream . . . 54
4.1.2.4 Turn-Down Ratio . . . 55
4.2 Base Case: Conventional Distillation . . . 56
4.2.1 Base Case 1: Process Design and Simulation . . . 56
4.2.2 Base Case 2: Process Design and Simulation . . . 57
4.2.3 Turn-Down Ratio . . . 58
4.3 Crude Methanol Feed Variability . . . 59
4.3.1 Problem Statement . . . 60
4.3.2 Optimization Modeling Approach . . . 61
4.3.3 Intermediate Storage Tank Model . . . 63
4.3.4 Product Recycling Model . . . 66
4.3.5 Hybrid Model . . . 68
4.4 Heat Pump Modeling . . . 72
4.4.1 Electrolyzer Waste Heat Variability . . . 74
4.4.2 Annual Dynamic Performance of the Heat Pump . . . 76
4.5 Techno-Economic Analysis . . . 79

5 Results and Discussion **81**
5.1 Conventional Distillation . . . 81
5.2 Case Study: South America . . . 81
5.2.1 Vacuum Distillation . . . 82
5.2.2 Process Optimization: Distillation Feed Mass Flowrate . . . 83
5.2.3 Techno-economic Analysis . . . 84
5.3 Case Study: Nordics . . . 85
5.3.1 Vacuum Distillation . . . 85
5.3.2 Process Optimization: Distillation Feed Mass Flowrate . . . 87
5.3.3 Techno-economic Analysis . . . 88

6 Conclusion **90**
6.1 Limitations . . . 91

7 Appendix **99**
7.1 Vacuum Case Appendix . . . 99
7.2 Optimization Model Appendix . . . 104
7.2.1 Storage Initial Inventory Estimator . . . 104
7.2.2 Storage Optimization . . . 107
7.2.3 Product Recycling . . . 114
7.2.4 Hybrid Model Optimization . . . 121
7.3 Heat Pump Sample Calculation for 100 % Electrolyser Capacity (South American Case) . . . 131

List of Figures

1 E-Methanol production process via captured biogenic CO_2 Hydrogenation from electrolyzer H_2 inside a catalytic reactor [24] 22
2 Simplified methanol synthesis loop showing reactor effluent cooling, crude methanol condensation and removal, synthesis-gas recycle, and purge for inert removal. 23
3 Comparison of two configurations: (a) two-column design and (b) three-column design [33]. 29
4 Four-column double-effect methanol distillation scheme (C1, light ends column; C2, pressured column; C3, atmospheric column; C4, water column). 30
5 Five-column methanol distillation scheme (PC, light ends column; AC-1, Medium pressured column; HC, high pressure column; AC-2, atmospheric column; RC, alcohol diluting column). 30
6 Tray-column operating envelope and associated hydraulic limits. . . 31
7 Packed-column operating envelope and associated hydraulic limits . 32
8 Closed-cycle mechanical vapour-compression heat pump links the electrolyser waste heat stream (evaporator source) to the vacuum-distillation reboiler (condenser sink). Adapted schematically from the standard four-component vapour-compression layout used in the process heat-pump literature [51, 50]. 37
9 Monthly grid electricity price in MWh. 43
10 Electricity consumption and the corresponding share of green versus grey e-methanol (including the PPA green mix) for (a) the Nordic market and (b) the South American market. 44
11 Topping column optimized parameters: (a) Shows effect on reboiler duty as feed stage changes, (b) Shows effect on concentration of acetone in bottom stream as feed stage changes, and (c) Shows effect on concentration of acetone in bottom stream as number of stages increases. 47
12 Changing the condenser pressure effects on: (a) Amount of methanol wasted in distillate of topping column and (b) bottom temperature of the topping column *Appendix Table 29*. 48
13 Effect of changing condenser temperature on methanol waste in the distillate of the topping column *Appendix Table 30*. 49
14 Topping Column with changing nominal feed capacity: (a) Reboiler duty in MW and (b) Mole reflux ratio of the column *Appendix Table 31*. 50
15 Distillate and bottom temperature versus changing condenser pressure. 51
16 For 100% stage efficiency, the concentration of ethanol in distillate vs: (a) Mole Reflux Ratio, and (b) Number of stages required. . . . 51
17 Effect of mole reflux ratio on ethanol concentration in the refining column distillate (ppm). 52

18 Feed stage vs concentration of ethanol in the distillate of the refining column . . . 53
19 Number of stages vs mass fraction of impurities in liquid phase . . . 55
20 Variable feed capacity effects on (a) Mole reflux ratio and (b) Reboiler duty of the refining column Table 32. . . . 56
21 Three-Column Conventional distillation (Base case 01) . . . 57
22 Three-Column Conventional distillation (Base case 02) . . . 58
23 Variable feed-capacity effects on Base case 01 and 02 steam cumulative heat-duty (Low pressure and medium pressure) consumption. . . . 59
24 Feed fluctuation comparison for South American and Nordic electricity markets for the year 2025 (Weekly moving average). . . . 59
25 Dynamic optimization framework for evaluating storage, recycle, and hybrid buffering strategies under hourly crude methanol production variability . . . 61
26 Conceptual Schematic of the Intermediate Storage Tank. . . . 63
27 Workflow of the Intermediate Storage Tank Optimization Model. The model is attached in *Appendix* subsubsection 7.2.1 and subsubsection 7.2.2 . . . 64
28 Conceptual Schematic of the product recycling Model. . . . 67
29 Conceptual Schematic of the Hybrid (Storage + Recycling) Model. . . 69
30 Workflow of the Hybrid Optimization Model. . . . 70
31 Schematic of the vacuum distillation reboiler duty requirement. . . . 73
32 Schematic of the ammonia (R717) closed-loop compression heat pump used to upgrade low-grade electrolyzer waste heat to the temperature level required by the vacuum column reboiler . . . 74
33 Mass and energy balance of the waste-heat recovery system at 100% electrolyzer capacity (71 MW, 483 kg/s), showing the direct heat-exchanger duty, the heat-pump branch, and the surplus flow rejected through the parallel cooler. . . . 75
34 Mass and energy balance at the minimum electrolyzer load (17 MW, 116 kg/s), where the entire cooling-water stream is required by the heat-pump branch, and the bypass carries zero flow, defining the design limit of the integration. . . . 76
35 Framework for techno-economic analysis. . . . 79
36 Reboiler heat duty for the South American vacuum distillation: (a) presents the overall heat duty required, and (b) presents the amount of heat recovered from waste electrolyzer heat and additional heat required. 82
37 Comparison of hourly operational cost for LP steam generation versus heat-pump electricity consumption, South America. . . . 83
38 Comparison of operational cost (including annualised buffer CAPEX and buffer OPEX) across the storage, product-recycling, and hybrid flexibility strategies for the South American: (a) vacuum case and (b) Base Case 2. . . . 84

39 Reboiler heat duty for the Nordic's vacuum distillation: (a) presents the overall heat duty required, and (b) presents the amount of heat recovered from waste electrolyzer heat and additional heat required. 86
40 Comparison of hourly operational cost for LP steam generation versus heat-pump electricity consumption, Nordics. 86
41 Comparison of operational cost (including annualised buffer CAPEX and buffer OPEX) across the storage, product-recycling, and hybrid flexibility strategies for the Nordic: (a) vacuum case and (b) Base Case 2. 88
42 Comparison between 100% and 60% stage efficiency based on the concentration of ethanol in the distillate of the refining column paragraph 4.1.2.1. 100
43 Vacuum distillation process flow diagram paragraph 4.1.2.4. 101
44 Three-Column Conventional distillation (Base case 01). subsection 4.2 102
45 Three-Column Conventional distillation (Base case 02). subsubsection 4.2.2 103

List of Tables

3 Physical properties of methanol relevant to distillation design. . . . 21
4 Crude Methanol Impurities 24
5 A summary of findings from literature [35, 36, 37]: Effects on parameters and design implications for vacuum methanol distillation using an 85 °C electrolyzer heat source. 33
6 Utility cost comparison between Nordic and South American regions. 42
7 PPA and electricity transmission costs for Nordic and South American regions. 42
8 Green versus grey e-methanol share for the Nordic and South American cases. 43
9 Column internals with pressure drop and bottom temperature. 48
10 Cooling water mass flow rate at different minimum approach temperatures. 49
11 Cooling water optimization for condenser duty of 1.6 MW (C_p = 4180 J/kg·K, U = 1000 W/m^{2}K). 49
12 Total number of stages required and ethanol concentration in distillate at varying reflux ratios. 52
13 Packing geometry and product purity at condenser pressure of 0.30 bar(a). 53
14 Pressure drop and column temperatures for different packings at condenser pressure of 0.30 bar(a). 53
15 Effective HETP values for the refining column. 54
16 Impurities in the feed stream. 54
17 Side stream effect on fusel oil impurities and methanol production. . 55
18 Specifications of distillation columns. 57
19 Condenser and reboiler duties for distillation columns. 57
20 Specifications of distillation columns. 58
21 Condenser and reboiler duties for distillation columns. 58
22 Available nominal feed capacity per hour for the Nordics and South America. 60
23 Annual steam consumption comparison: Base Case 1 vs Base Case 2. 81
24 Heat-pump economic performance: South America (500 €/kW$_{th}$, 6% discount rate). 83
25 Techno-economic Analysis: Base Case 2 vs Vacuum Case (South America). 85
26 Heat-pump economic performance — Nordics (500 €/kW$_{th}$, 6% discount rate). 87
27 Economic comparison — Base Case 2 vs Vacuum Case (Nordics). . 89
28 Column internals and the corresponding model equations used paragraph 4.1.1.2. 99
29 Methanol loss with light gases as a function of condenser pressure and bottom temperature Figure 12. 99

30 Methanol loss with light gases as a function of condenser temperature Figure 13. 99
31 Topping column performance at varying feed rates (distillate temperature constant at 40°C *Figure 14* 100
32 Refining column performance at varying feed rates (distillate temperature constant at 36.53 °C, Figure 20). 100
33 Stream summary for the refining column paragraph 4.1.2.4. 101
34 Condenser cooling requirements and cost for Base Case 1 (heat-integrated TC/RC) at varying feed loads (South America). 104
35 Condenser cooling requirements and total cooling cost for the Vacuum Case at varying feed loads. Cooling duty of the topping column for vacuum distillation is not included here, which has a temperature difference of 10 K and only imposes a 6-3 €/hr additional cost of cooling water (South America). 104
36 Step-by-step calculation of heat pump performance for the sizing hour (hour 151). 132
37 Summary of sample hour (hour 151, 100% electrolyser capacity). . . 133

Symbols and Abbreviations

Symbols

A	total column cross-sectional area (m^2)
A_d	downcomer area (m^2)
C	capacity factor
C_o	orifice coefficient (0.65–0.85)
C_t^{cool}	cooling cost at time t (€/hr)
D_c	column diameter (m)
D_T	column diameter (m)
D_t	distillation feed rate at time t (kg/h)
E_o	overall tray efficiency
E_{HP}	annual heat supplied by heat pump (MWh)
F_{Design}	design factor (0.6–0.8)
F_t	crude methanol feed rate at time t (kg/h)
H_c	column height (m)
H_{column}	total column height (m)
H_{tray}	pressure drop per tray (mbar)
K	variable coefficient for storage sizing
LP_t^{avail}	available low-pressure steam at time t (MW)
LP_t^{buy}	purchased low-pressure steam at time t (MW)
LP_t^{req}	low-pressure steam requirement at time t (MW)
MP_t^{avail}	available medium-pressure steam at time t (MW)
MP_t^{buy}	purchased medium-pressure steam at time t (MW)
MP_t^{req}	medium-pressure steam requirement at time t (MW)
$M\&S$	Marshall & Swift index
N_{stages}	number of stages
P	system pressure (bar a)
P_i^{sat}	saturation vapor pressure of component i (bar)
P_t	pumping cost at time t (kg/h)
P_{comp}	compressor electrical power (MW_{el})
R_t	recycled methanol flow rate at time t (kg/h)
R_{max}	maximum ramp rate ($0.05D_{\text{max}}$) (kg/hr)
S_t	storage inventory at time t (kg)
S_{max}	maximum storage capacity (kg)
S_{annual}	annual operating-cost saving from heat pump (€)
T	time horizon (h)
T_{cond}	heat-pump condensing temperature (°C)
T_{evap}	heat-pump evaporating temperature (°C)
T_{lim}	direct heat exchanger cutoff temperature (°C)
T_{reb}	reboiler operating temperature (°C)
T_{src}	minimum source-stream temperature for evaporator (°C)

V_{Mass}	vapor mass flow rate (kg/s)
$\dot{V}_{\text{NC}}$	volumetric flow of non-condensables (m^3/s)
W_{el}	annual compressor electricity consumption (MWh)
c_p	pumping cost (€/kg)
c_R	recycle pumping cost (€/kg)
c_s	storage cost (€/kg)
c_{cap}	tank capital cost (€/m^3)
c_{spec}	specific heat-pump equipment cost (€/kW)
h_d	dry tray loss (mbar)
h_l	liquid head loss (mbar)
h_{ow}	liquid height over weir (m)
h_w	weir height (m)
l_{weir}	weir length (m)
m	design margin for heat-pump sizing
p_h	hourly electricity price (€/MWh)
t_{MeOH}	annual operating hours (h)
v_{flood}	flooding velocity (m/s)
x_i	liquid mole fraction of component i
y_i	vapor mole fraction of component i
z_{recycle}	binary variable for product recycling
z_{storage}	binary variable for storage
α	relative volatility; recycle water-to-methanol ratio
γ_i	activity coefficient of component i
ΔH	enthalpy change (kJ/mol)
ΔP	pressure drop (mbar)
ΔT_{LM}	log mean temperature difference (°C)
ΔT_{lift}	temperature lift (K)
ΔT_{min}	minimum approach temperature (K)
ε	numerical tolerance for heat-pump feasibility
η	second-law (Carnot) efficiency of heat pump
μ_L	liquid viscosity (cP)
ρ	density (kg/m^3)
ρ_L	liquid density (kg/m^3)
ρ_V	vapor density (kg/m^3)
ϕ	minimum-load fraction for electrolyzer
$\dot{Q}_{\text{avail}}$	heat available to evaporator (MW)
$\dot{Q}_{\text{dir}}$	direct heat-exchanger duty (MW)
$\dot{Q}_{\text{ELY}}$	electrolyzer waste heat (MW)
$\dot{Q}_{\text{evap}}$	heat-pump evaporator duty (MW)
$\dot{Q}_{\text{HP}}$	heat-pump condenser duty (MW)
$\dot{Q}_{\text{peak}}$	peak hourly heat-pump duty (MW)
$\dot{Q}_{\text{reb}}$	reboiler heat requirement (MW)
$\dot{Q}_{\text{res}}$	residual heat to cooling water (MW)
$\dot{W}_h$	compressor work at hour h (MW_{el})

Abbreviations

ACL	Free Market (South America)
AEL	Alkaline Electrolyzer
CAPEX	Capital Expenditure
CBC	COIN-OR Branch-and-Cut (solver)
CCEE	Chamber of Electric Energy Commercialization (Brazil)
COP	Coefficient of Performance
CRF	Capital Recovery Factor
CW	Cooling Water
DME	Dimethyl Ether
EJ	Exajoule
EPC	Engineering, Procurement, and Construction
ENTSO-E	European Network of Transmission System Operators for Electricity
FUG	Fenske–Underwood–Gilliland (shortcut method)
GHG	Greenhouse Gas
GWP	Global Warming Potential
HETP	Height Equivalent to Theoretical Plate
HTHP	High-Temperature Heat Pump
IMPCA	International Methanol Producers and Consumers Association
IPCC	Intergovernmental Panel on Climate Change
IRR	Investment Rate of Return
LCO	Levelized Cost
LCO-MeOH	Levelized Cost of Methanol
LP	Low Pressure
LPro	Linear Programming
MILP	Mixed Integer Linear Programming
MP	Medium Pressure
MTO	Methanol-to-Olefins
NIST	National Institute of Science and Technology
NPV	Net Present Value
NRTL	Non-Random Two-Liquid (activity coefficient model)
NRTL–RK	NRTL–Redlich–Kwong (property method)
ODP	Ozone Depletion Potential
OPEX	Operational Expenditure
PLD	Difference Settlement Price (Brazil)
PPA	Power Purchase Agreement
PTM	Power to Methanol
RED III	Renewable Energy Directive III
RFNBO	Renewable Fuels of Non-Biological Origin
SOS2	Special Ordered Set of type 2
TAC	Total Annual Cost
TEA	Techno-Economic Analysis
VLE	Vapor-Liquid Equilibrium

1 Introduction

For many years, methanol, along with other fossil fuels, has been used as a feedstock in chemical industries and as a fuel in the transportation sector. Approximately 110 million metric tonnes of methanol are produced annually; around 70% is used as a raw material for chemical manufacturing, while the remainder is consumed as fuel. The chemical industry converts methanol into a broad range of products, including formaldehyde, acetic acid, and plastics via the methanol-to-olefins (MTO) route [1]. In the near future, the road and maritime sectors are expected to increasingly use methanol as a fuel, driven by environmental regulations and the rapid development of green methanol, which together create substantial potential for its wider adoption [2].

With recent developments in the Power-to-Methanol (PTM) process, which synthesizes e-methanol using green hydrogen and captured carbon dioxide (CO_2) from industrial sources or directly from the air, [3], e-methanol is increasingly regarded as a promising substitute for conventional fossil resources in the energy sector, the chemical industry, and particularly in hard-to-abate sectors such as maritime [4] [5].

The production of e-methanol is attracting significant interest because it can reduce greenhouse gas (GHG) emissions, which are the major contributors to climate change. According to the Intergovernmental Panel on Climate Change (IPCC) [6], the industrial sector contributes 32% of the world's greenhouse gas (GHG) scope 1 and 2 emissions and approximately one third of the global energy use, which is predicted to increase from 156 EJ in 2020 to 207 EJ in 2050. The industrial sector accounts for 32 % of global scope 1 and 2 GHG emissions, and approximately one-third of total global energy use, which is projected to increase from 156 EJ in 2020 to 207 EJ in 2050 [7].

Within this context, the European Union recognizes methanol as an essential energy carrier to support transportation decarbonization through its regulatory framework. The Renewable Energy Directive (RED III) requires that fuel suppliers in EU ports provide at least 1.2 % renewable fuels of non-biological origin (RFNBOs) to shipping by 2030, while the complementary FuelEU Maritime Regulation imposes a binding 80 % well-to-wake GHG reduction target for ships by 2050. Life cycle assessment studies indicate that e-methanol can meet the 2050 RED III e-fuels target, albeit at higher costs and with greater toxicity risks compared to some other e-fuels [8].

Developing energy-efficient plants will be crucial for the emerging e-methanol sector. Although electrolysis is the most dominant process in e-methanol production, this thesis focuses on distillation-process optimization because distillation is the dominant separation technology in industry and accounts for 90–95 % of all separation, purification, and recovery processes [9].

Research on e-methanol technology demonstrates its potential to substantially reduce greenhouse gas emissions; however, only a limited number of demonstration plants are currently in operation, including the first e-methanol plant in Denmark [10], the Haru Oni facility in Chile, which began operating in 2022, and several CRI-licensed projects in China (e.g., Anyang and Jiangsu) that utilize hydrogen from industrial waste and electricity from grey sources [11]. To meet future e-methanol consumption needs, the industrial community must collaborate closely with technology developers

to establish large-scale production facilities [12].

1.1 Scope

This thesis presents an approach to building an e-methanol distillation plant that can operate in transient mode, allowing the electrolyzer and methanol reactor to contribute to changes in the feed conditions of the distillation columns. The problems that needed to be addressed are as follows;

1. The e-methanol distillation process is an energy-intensive process and requires reboiler duty at high temperatures, especially in the case of a three-column configuration where the middle rectifying column is at 5-10 bar pressure [13, 14].

2. Supply of Green hydrogen, which is required for e-methanol synthesis, depends on renewable electricity and hence is intermittent. So, it is necessary to design a distillation process that can work efficiently under varying feed loads.

1.2 Objectives

The main objective of this thesis is to develop and evaluate a transient-capable e-methanol distillation system that can operate under variable feed conditions while utilizing low-grade waste heat from the electrolyzer. The detailed list of objectives is as follows:

1. To evaluate the feasibility of using electrolyzer waste heat at 85 °C as the sole heat source for the distillation reboilers under vacuum operation, with cooling water used as the utility at a supply temperature of 25 °C.

2. To verify that the final methanol product meets International Methanol Producers and Consumers Association (IMPCA) specifications and the additional over-design margin. Accordingly, ethanol must be below 35 ppm and acetone below 10 ppm, compared with the IMPCA limits of 50 ppm and 20 ppm, respectively.

3. To design a distillation system capable of operating with a lowest possible turndown ratio (at least 60% of the nominal feed capacity).

4. To evaluate the techno-economic implications of operating the distillation system under vacuum conditions compared to conventional distillation process models.

5. To ensure that the distillation system maintains stable operation under transient conditions despite limited column ramp rates (±5%/h), and to assess buffering strategies such as recycle and intermediate storage for decoupling upstream variability from downstream separation. The analysis focused on hourly production fluctuations arising from variable renewable electricity supply and evaluated a series of representative operating scenarios rather than a fully dynamic process-control simulation. Annual trends were addressed through

the optimization framework, while detailed control dynamics, equipment start-up/shutdown behavior, and controller interactions were outside the scope of this work. A ramp rate of 5%/h was assumed based on consultations with prominent vendors in the methanol distillation sector and a review of the literature, including Yu-Ying [15], and S. Skogestad [16, 17].

6. To perform a sensitivity analysis of steam and electricity prices across different process configurations to determine the conditions under which vacuum distillation is economically feasible.

1.3 Outline of the Thesis

This thesis is organized into five main sections and an Appendix that contains supporting figures, tables, and stream data.

Literature Review builds the technical foundation and defines the boundaries for the design work that follows. It begins with the physical and thermodynamic properties of e-methanol and the pathways used to produce it, then moves through crude methanol composition, distillation fundamentals, and the column configurations used industrially for methanol purification. Vacuum distillation is then introduced as a purification route, together with the transient nature of hydrogen production and the resulting feed-load variability; the reboiler's isothermal heat demand is met directly by the electrolyser's waste heat where the temperature allows, with a closed-cycle vapour-compression heat pump brought in if needed to cover the remaining duty, and the chapter closes by outlining the buffering strategies proposed to address that variability.

Assumptions present the key inputs and design criteria adopted for the process simulation, optimization, and techno-economic analysis. These include the feed composition, thermodynamic models, equipment sizing criteria, operational constraints, economic parameters, and market conditions used throughout the study to provide a consistent basis for evaluating the different distillation configurations and flexibility strategies.

Methodology sets out how the vacuum distillation system was designed and evaluated. It discusses the Aspen Plus simulation results and the development of the topping and refining columns under reduced pressure, the conventional base-case columns used for comparison, and the optimization models developed to match the variable upstream feed to the distillation column's operating limits. The main outputs carried forward to the Results section are the distillation CAPEX and annual OPEX. The methodology for the heat pump dynamic modeling and analysis is also included in this section, and the chapter concludes with the techno-economic framework used to compare all cases.

Results and Discussion compares the distillation CAPEX and OPEX of the vacuum configuration with those of the conventional base cases and evaluates the full techno-economic performance, including all relevant cost components, through the Techno-economic Analysis (TEA). The chapter also presents the results of the Python-based dynamic optimization of feed variability and assesses the use of a heat

pump when waste heat from the alkaline electrolyzer is insufficient to meet the vacuum distillation heat demand.

Conclusion summarizes the extent to which the thesis objectives were met, states the main technical and economic findings, and identifies the limitations of the current analysis together with directions for future considerations.

2 Literature Review

2.1 E-Methanol: Physical Properties

The physical properties of e-methanol are identical to those of conventional methanol. The prefix "e" highlights the use of renewable electricity and captured biogenic CO_2 in its production, which distinguishes it from fossil-fuel-based conventional methanol. E-methanol is a colorless liquid that is soluble in water. The properties relevant for distillation column design are summarized in Table 3[18]. More detailed information on pure methanol and its mixtures can be found in the literature [19], [20].

Table 3: Physical properties of methanol relevant to distillation design.

Property	Value
Molecular weight	32.04 g/mol
Normal boiling point (1 atm)	64.7 °C
Latent heat of vaporization (at 64.7 °C)	1101 kJ/kg
Liquid density (20 °C)	791 kg/m^3
Vapor density (at boiling point, ideal gas)	~1.17 kg/m^3
Specific heat capacity (liquid, 25 °C)	2.55 kJ/(kg·K)
Thermal conductivity (liquid, 20 °C)	0.202 W/(m·K)
Surface tension (20 °C)	0.0226 N/m
Liquid viscosity (20 °C)	0.55 cP
Critical temperature	239.5 °C
Critical pressure	8.09 MPa (a)

2.1.1 E-Methanol: Production Pathways

Conventionally, methanol is produced by gasification of coal or reforming of natural gas to produce syngas, composed of CO, CO_2, and H_2, which is then catalytically reacted to produce methanol [21]. Currently, 99% of methanol is produced from fossil fuels [22], but in order to meet the IPCC and Paris Agreement vision, it is important to eliminate the dependency of methanol production on fossil fuels. This leads to a new pathway to produce methanol via catalytically reacting captured biogenic CO_2 from industrial sites or directly from air with hydrogen gas (H_2) from a renewable-powered electrolyzer [4], [3].

Bio-methanol is also produced as a by-product of the digestion process in kraft pulp mills. It is typically combusted in the recovery boiler or discharged to wastewater streams. However, it can be recovered and purified to IMPCA grade, allowing it to be used as an alternative to natural gas and potentially reducing the plant's operating costs significantly [23]. In addition to the formation in the digester, methanol is also produced in other parts of the mill, such as during biomass gasification, cooking, O_2 delignification, and partly in the evaporation plant. Methanol is likewise formed in the bleaching plant, although this methanol is typically not recovered. This is an interesting pathway, but the core focus of this study is e-methanol that is produced

with biogenic CO_2 from pulp mills and H_2 from an electrolyzer, which in our case is an alkaline electrolyzer. Figure 1 shows the process flow diagram of e-methanol production, integrating green hydrogen from renewable-powered electrolysis with captured CO_2 (via DAC or flue-gas capture). These streams are compressed and routed through the methanol synthesis loop and distillation section, with internal heat integration and external heat supply used to produce the final methanol product.

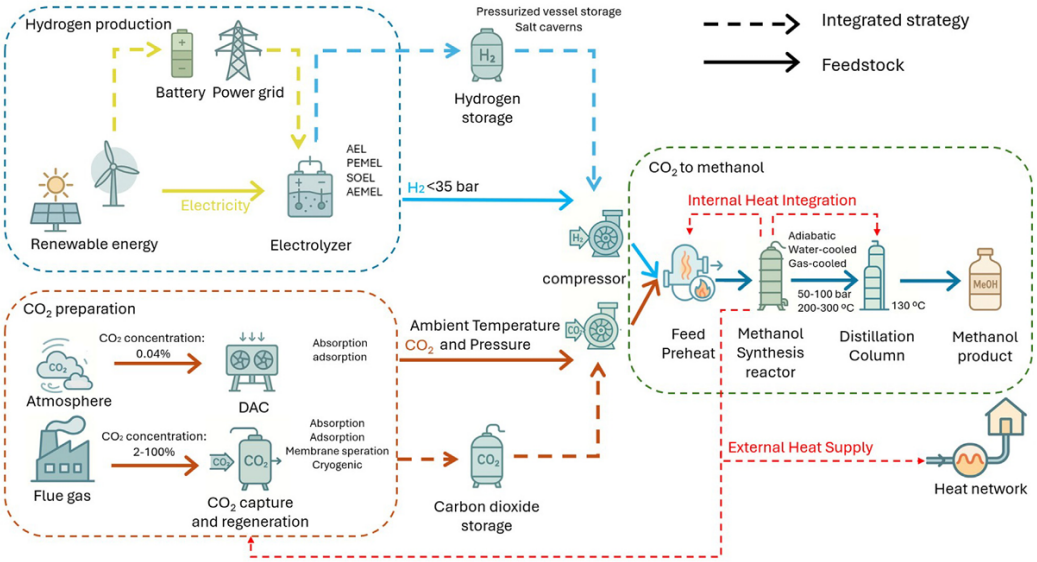

Figure 1: E-Methanol production process via captured biogenic CO_2 Hydrogenation from electrolyzer H_2 inside a catalytic reactor [24]

CO_2 hydrogenation takes place in the presence of a catalyst (typically $Cu/Zn/Al_2O_3$) in the reactor under 50-100 bar pressure and 200-300°C temperature. The equilibrium reactions are as follows:

$$CO_2 + 3H_2 \rightleftharpoons CH_3OH + H_2O \qquad \Delta H_{300K} = -49.16 \text{ kJ/mol} \tag{1}$$

$$CO_2 + H_2 \rightleftharpoons CO + H_2O \qquad \Delta H_{300K} = 41.21 \text{ kJ/mol} \tag{2}$$

$$CO + 2H_2 \rightleftharpoons CH_3OH \qquad \Delta H_{300K} = -90.77 \text{ kJ/mol} \tag{3}$$

All three reactions follow Le Chatelier's principle, which states that a system at equilibrium will adjust to counteract imposed changes in temperature, pressure, or composition. Reactions (1) and (2) are the main reactions in the CO_2-to-methanol pathway, while reaction (1) can be regarded as the overall reaction obtained by combining the independent reactions (2) and (3). Reaction (2) is also known as the reverse water–gas shift reaction and is endothermic in nature. The CO produced in this step undergoes hydrogenation via reaction (3) to form e-methanol [18, 24]. Side reactions, which lead to by-products such as dimethyl ether, methyl formate, formic acid, acetone, methane, ethanol, and higher alcohols, can also occur depending on the catalyst formulation and operating conditions.

2.2 Methanol Synthesis

Industrial methanol plants operate a synthesis loop to maximize methanol production from carbon monoxide, carbon dioxide, and hydrogen, as shown in Figure 28. The reactor effluent contains methanol, water, and unreacted synthesis gas, which is initially cooled so that methanol and water condense. The resulting liquid phase, referred to as crude methanol, is separated and sent to downstream purification, while the uncondensed gases are compressed and recycled back to the reactor.

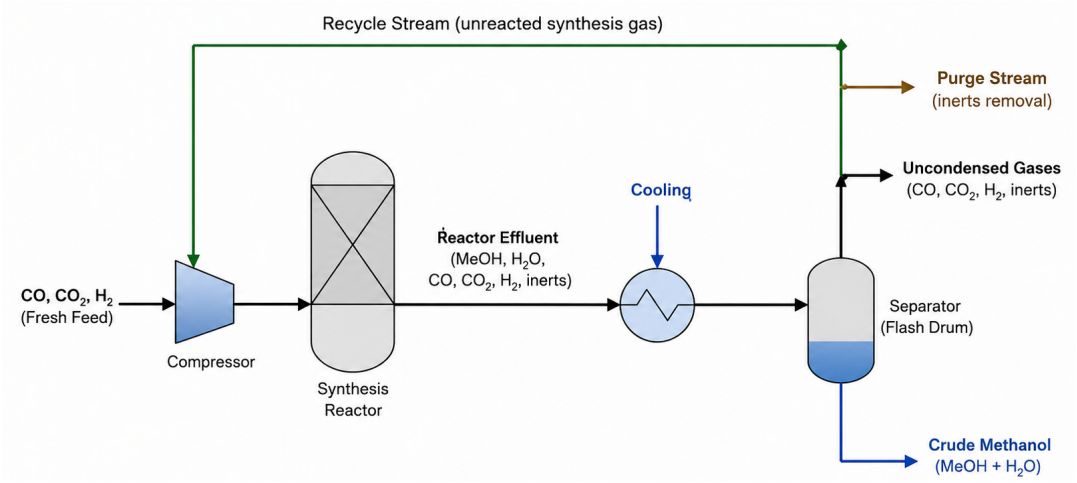

Figure 2: Simplified methanol synthesis loop showing reactor effluent cooling, crude methanol condensation and removal, synthesis-gas recycle, and purge for inert removal.

In the synthesis loop, crude methanol is continuously removed through condensation, and a purge stream is withdrawn to prevent the accumulation of inert components. Due to the relatively low single-pass conversion in the reactor, a large recycle stream is required. This recycle stream improves reactant utilization, maintains stable reactor inlet conditions, and influences both the crude methanol production rate and its impurity composition [18].

2.2.1 Crude Methanol

The e-methanol stream leaving the reactor is not a pure e-methanol stream. It is diluted with water and has some impurities as well. The amount and composition of these impurities are not fixed but depend strongly on how the reactor is operated. In particular, they are influenced by the lifetime of the catalyst (aging and deactivation change selectivity and promote side reactions), the quality and composition of the feed stream (e.g., $CO/CO_2/H_2$ ratio and trace contaminants), and the operating conditions of the reactor (temperature, pressure, etc). Crude methanol is slightly alkaline in nature, as a small fraction of caustic soda is added to neutralize lower molecular weight carboxylic acids and also partially hydrolyze esters.

Crude methanol contains light, medium, and heavy-end impurities, which are listed in Table 4. Water is not mentioned as an impurity, as its concentration is quite high and needs to be distilled out. The light ends consist of gases that are dissolved under

high pressure and volatile organic compounds like acetone, which can be removed easily at room temperature. The heavy ends, also known as fusel oils, include higher alcohols, esters, and hydrocarbons that have high boiling points and low volatility. These impurities remain at the bottom during distillation, and methanol is distilled out from the top of the column [18].

Table 4: Crude Methanol Impurities

Category	Representative Species
Light Ends	Dissolved gases (CO_2, H_2, CO, N_2, O_2) Dimethyl ether (DME) Methyl formate Acetone
Medium Alcohols	Ethanol Propanol & other ethers
Heavy Ends	Higher alcohols: Butanol, S-Butanol, Pentanol Long-chain hydrocarbons (mostly >C8) Higher ketones and esters of lower alcohols with formic, acetic, and propionic acids

Some compounds with boiling point are closer to that of methanol can form an azeotrope with it and need to be considered in distillation process. Acetone, ethyl formate, methyl acetate, ethyl acetate, etc., are the compounds that make an azeotrope with methanol [25].

2.3 E-Methanol Distillation

Distillation is a thermal separation process in which liquid mixtures containing components of different volatilities are separated through repeated cycles of evaporation and condensation, with the phase compositions at each stage governed by vapor–liquid equilibrium (VLE). To achieve an efficient and economical separation, key design and operating variables—such as operating pressure, relative volatility, column configuration, and reflux ratio—must be selected and optimized carefully [26], [18].

2.3.1 Thermodynamic Principles

Vapor-liquid equilibrium (VLE) is very important for methanol distillation [27] because methanol and water form a **non-ideal mixture**, where water is polar, and methanol is polar on the -OH side, but the CH_3 side is nonpolar. Hence, the VLE for this mixture deviates from Raoult's law [28]. To account for these non-ideal behaviors, the extended Raoult's law is given by:

$$y_i P = x_i \gamma_i P_i^{sat}(T) \tag{4}$$

here x_i and y_i are the liquid and vapor mole fractions, respectively, P is the system pressure, γ_i is the activity coefficient, and P_i^{sat} is the saturation vapor pressure of component i. Considering the Antoine equation for the vapor pressure and the sum of the vapor and liquid mole fractions in both phases is unity, the bubble point and dew point curves in the Txy (temperature versus liquid, x, and vapor, y, composition at fixed pressure) diagram are obtained from these equations:

$$P = \sum x_i \gamma_i P_i^{sat}(T) \tag{5}$$

$$1 = \sum \frac{y_i P}{\gamma_i P_i^{sat}(T)} \tag{6}$$

The methanol–water system shows major nonideal behavior because hydrogen bonding occurs between its components, which change both its **relative volatility** (α) and its VLE characteristics. The separation of methanol and water through conventional distillation achieves effective results, although it is important to consider nonideal behavior during process design [27].

One of the most useful ways of representing a VLE is relative volatility, which can be applied to both binary and multi-component mixtures. In binary systems, relative volatility between light and heavy ends gives the composition in the liquid and vapor phases, respectively. The equation for the methanol-water case, which includes non-ideal behavior considerations, is given by:

$$\alpha = \frac{\gamma_{\mathrm{MeOH}} P^{\mathrm{sat}}_{\mathrm{MeOH}} / x_{\mathrm{MeOH}}}{\gamma_{\mathrm{H_2O}} P^{\mathrm{sat}}_{\mathrm{H_2O}} / x_{\mathrm{H_2O}}} \tag{7}$$

A value of α greater than 1 means that the components can be separated by distillation. Although the value of α is not constant, for a 50 % methanol in water binary mixture at atmospheric conditions, it is 2.98, which indicates that it is easy to separate [29].

2.3.2 Fractional Distillation

Crude e-methanol consists almost entirely of methanol and water, with only trace impurities [30]. Since this study focuses solely on e-methanol production, extractive and azeotropic distillation are not considered. These techniques are required only when a distillation boundary prevents the desired separation; in the methanol–water system, any azeotropes present are of the saddle type, which do not act as separation boundaries and therefore do not hinder purification by conventional distillation [28].

Conventionally, methanol is purified using fractional distillation, where the mixture is continuously evaporated and condensed at multiple stages. This produces vapor that reaches the top of the column, rich in methanol, which is then condensed. The temperature of the mixture plateaus around 64–67 °C until most of the methanol has been distilled, after which it rises sharply toward 100 °C, the boiling point of water. This type of distillation is suitable for close-boiling methanol–water mixtures [31], [32].

2.4 Column Sizing and Design

A fractional distillation column is the most suitable type of distillation for crude e-methanol distillation. Both tray and packed columns can be used for the separation process based on the operating conditions.

2.4.1 Tray Columns

In tray columns, the length of the weir on each tray governs the height of liquid and its flow between trays. Tray efficiency is a critical parameter in the initial design stages, which is calculated using the O'Connell correlation [26], [27]. It is an empirical relationship based on data collected from operating columns; it is derived for bubble-cap trays and is conservative for sieve and valve trays. The correlation relates the overall column efficiency to the product of the liquid (feed) viscosity and the relative volatility of the key components, both evaluated at the arithmetic mean of the column top and bottom temperatures, where higher viscosity leads to lower efficiency due to reduced mass-transfer potential. The equation is given by:

$$E_o = 0.492\,(\mu_L\,\alpha)^{-0.245} \tag{8}$$

where:

- E_o = overall tray efficiency (dimensionless)
- μ_L = liquid viscosity in cP at the mean column temperature
- α = relative volatility of the key components at the mean column temperature

The estimated efficiency is considered in the initial stages of the design and can be changed later on using rate-based computational calculations. **Flooding velocity** is the maximum velocity at which a column can operate, and after that, the efficiency decreases as the vapor causes entrainment or weeping occurs through holes or downcomer. The flooding velocity is given by:

$$v_{\text{flood}} = C\sqrt{\frac{\rho_L - \rho_V}{\rho_V}} \tag{9}$$

where:

- v_{flood} = flooding velocity of vapor (m/s)
- C = capacity factor (The fair correlation uses empirical charts for the C value, offering a reliable method for design of a tray column)
- ρ_L = liquid density (kg/m^3)
- ρ_V = vapor density (kg/m^3)

The **column diameter** can be estimated using:

$$D_T = \sqrt{\frac{4V_{\text{Mass}}}{V_{\text{Flood}}\, F_{\text{Design}}\, \pi\, \rho \left(1 - \frac{A_d}{A}\right)}} \tag{10}$$

where:

- D_T = column diameter (m)
- V_{Mass} = vapor mass flow rate (kg/s)
- v_{Flood} = flooding velocity (m/s)
- F_{Design} = design factor (fraction of flooding velocity, typically 0.6–0.8)
- ρ = vapor density (kg/m^3)
- A_d = downcomer area (m^2)
- A = total column cross-sectional area (m^2)

The column diameter requirements can be determined through this equation, which uses vapor flow data and flooding limits. The term $\left(1 - \frac{A_d}{A}\right)$ accounts for the reduction in active area because the downcomer area does not participate in mass transfer operations. The design factor ensures the column operates safely below flooding conditions, which typically occur between 60 and 80 % of the flooding velocity [28]. It is important to estimate and consider pressure drop, especially in reduced-pressure cases. The **total pressure drop** per tray is the sum of vapor and liquid head losses:

$$H_{\text{tray}} = h_d + h_l \tag{11}$$

Dry tray loss (h_d) is due to the resistance of vapor flow through tray holes, which is calculated as:

$$h_d = 0.186 \frac{\rho_V}{\rho_L} \frac{V_{\text{hole}}^2}{C_o^2} \tag{12}$$

where C_o (0.65–0.85) is an orifice coefficient [26].

Liquid head loss (h_l) is considered for liquid height and frothing:

$$h_l = \beta(h_w + h_{ow}) \tag{13}$$

where $\beta \approx 0.6$ (aeration factor), h_w the weir height, and h_{ow} the liquid height over the weir [26].

Liquid height over the weir can be estimated by:

$$h_{ow} = 0.48 \left(\frac{L}{l_{\text{weir}}}\right)^{2/3} \tag{14}$$

where L is liquid flow rate and l_{weir} the weir length.

The final parameter, which must be evaluated, deals with the **height**, which depends on both tray spacing and stage count. Total column height is based on the number of stages and tray spacing, which is given by:

$$H_{\text{column}} = N_{\text{stages}} \times \text{tray-spacing} + \text{additional allowances}, \tag{15}$$

[28] Standard tray spacing measures between 0.45 and 0.61 m. Furthermore, extra height must be provided for vapor disengagement (approximately 20 % of the total column height) and for liquid holdup at the base of the column [26].

2.4.2 Packed Column

Packed columns use the height equivalent to a theoretical plate (HETP) as the primary performance measure, which depends on the packing material characteristics and flow conditions rather than on tray efficiency (relevant only for tray columns). Packed columns typically tolerate higher gas velocities and flooding better than tray columns; flooding in packed columns is associated with liquid holdup and accumulation within the packing, and its prediction relies on correlations that depend on the specific packing geometry, rather than on vapor flow through tray holes and downcomers. The high specific surface area of the packing enhances mass transfer and generally allows for smaller column diameters. Moreover, because the entire column is filled with packing, mass transfer occurs continuously along the column height rather than only at discrete trays. Although the pressure drop per unit height is usually lower than in tray columns, it is distributed over the entire packed section.

The total column height is determined by the required number of theoretical stages and the HETP, eliminating the need for tray spacing; however, for tall packed columns, additional internal devices such as liquid collectors and redistributors are required every few meters to prevent channeling and to ensure adequate liquid wetting. Packed columns are also often recommended for column diameters below approximately 0.9 m for economic reasons. These columns can achieve high mass transfer efficiency, relatively low pressure drop, and simpler internals compared with tray columns of similar duty, provided that an appropriate packing type and HETP value are selected for the specific operating conditions [26].

2.4.3 Columns Configurations for E-Methanol Distillation

There are not many examples of industrial-scale projects, but a lot of different configurations and optimizations have been carried out and documented in recent years. The most basic option, a single-column distillation of crude methanol, typically achieves only about 90.5 % methanol purity. This limitation arises because dissolved light gases (e.g., CO, CO_2, and light hydrocarbons) remain in the overhead product and cannot be fully separated in one column without excessive reflux and energy input. As a result, the column must operate with relatively high reflux ratios and reboiler duties to approach chemical-grade e-methanol purity levels, leading to considerably high operating costs [14].

In contrast, a two-column configuration, in which the first column is dedicated to removing light gases and other low-boiling components and the second column serves as the main refining column, can achieve chemical-grade methanol with a purity of about 99.9 %. In this arrangement, the first (degasifying or light-ends) column operates under conditions optimized for stripping out volatile impurities, thereby reducing the impurity load entering the main refining column. The second column can then be designed and operated specifically for the separation of methanol from water and heavier components, with more favorable internal compositions and lower impurity concentrations. This staged separation not only enables higher product purity but can also be more energy-efficient overall, since each column can be operated closer to its optimal pressure, temperature, and reflux regime for the particular separation task.

Figure 3 shows the 2- and 3-column configuration, where in the 3-column configuration, the middle column is operating at a 6 – 19 bar pressure range to have hot enough vapors coming out of the top to integrate and reboiler duty to other columns. By doing so, not only does the operating cost decrease but also there is no need of condenser for the middle column. These heat-integrated columns can save up to 40 % of operational cost when the distillation process is considered alone [33].

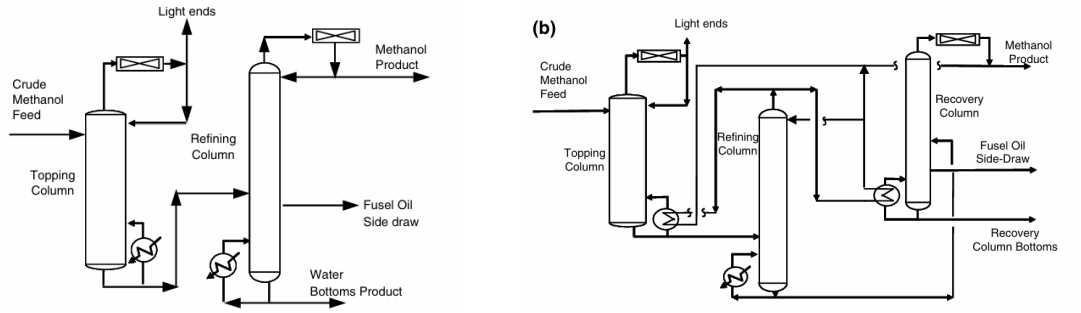

Figure 3: Comparison of two configurations: (a) two-column design and (b) three-column design [33].

In recent years, it has also been proved computationally that a 4-column configuration works significantly better than a 3-column configuration by providing much better control of fusel oils removal and higher recovery of methanol, as shown in Figure 4 [34].

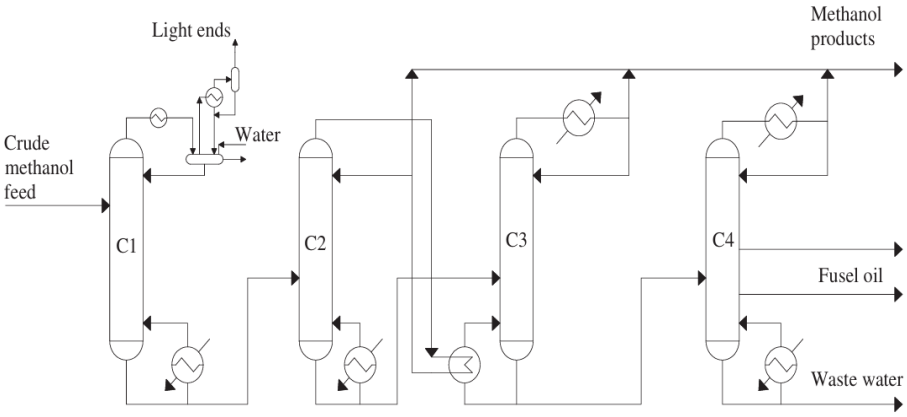

Figure 4: Four-column double-effect methanol distillation scheme (C1, light ends column; C2, pressured column; C3, atmospheric column; C4, water column).

The major disadvantage of the 4-column configuration is that the feed to the last water column is very small, and to maintain stable operation, the reflux ratio needs to be high, which increases operating costs by around 9 %. Five-column configurations have also been investigated, in which a medium-pressure column is placed between the light-ends column and the high-pressure column, which achieves a 15.23 % reduced energy consumption and 21.5 % reduced exergy losses [34]. As shown in Figure 5, an alcohol-dilution technique is employed instead of a side draw to achieve higher methanol recovery, rather than utilizing the fusel oils for combustion [14]. Although four- and five-column configurations offer high energy efficiency, they have not been widely adopted in industry because of their complexity and control challenges.

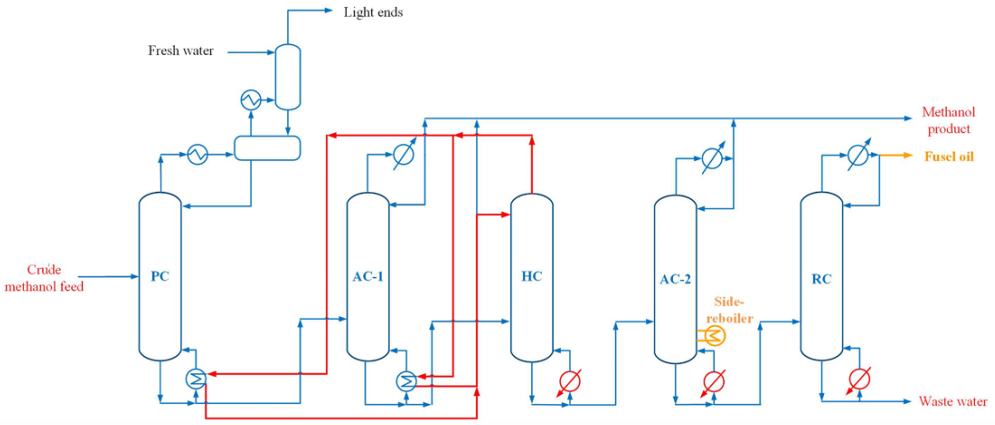

Figure 5: Five-column methanol distillation scheme (PC, light ends column; AC-1, Medium pressured column; HC, high pressure column; AC-2, atmospheric column; RC, alcohol diluting column).

2.5 Operating Conditions

The performance of a distillation column depends on various factors, which include the feed conditions, operating pressures and the reflux ratio, along with the vapor flow behavior and the internal as well as external environmental conditions [26]. The feed composition and required condenser and reboiler duties, along with the required composition of product as distillate and bottom streams, determine the required number of stages and the most optimal feed stage because any major changes from design conditions will result in decreased separation performance. Reference [35] also documents that a saturated liquid feed entering the column close to its bubble point improves mass transfer and helps achieve high purity without disturbing the internal vapour–liquid equilibrium (VLE). The reflux ratio governs the trade-off between separation efficiency and energy consumption: a higher reflux ratio reduces the number of stages required but increases the reboiler duty. The research suggests that the better economic operation of columns requires approximately 1.2 to 1.5 times the minimum reflux ratio when operating close to 1 atm [27, 28].

2.5.1 Flow Regime: Tray Columns

The interaction between vapor and liquid traffic determines the operational performance of tray distillation columns, as described by operating diagrams. At low vapor flow rates, weeping occurs when the vapor velocity is too low to retain liquid on the tray, causing liquid to leak through perforations and reducing mass transfer efficiency. As the vapor flowrate increases, entrainment begins: vapor carries liquid droplets upward to higher trays, which decreases separation efficiency and increases the risk of overhead product contamination. At very high vapor rates, the column experiences flooding because liquid accumulates and obstructs normal downflow, leading to a sharp increase in pressure drop and operational instability. Figure 6 [27] illustrates that these phenomena define an operating window between weeping and flooding, which is a key constraint for designing tray spacing and column diameter.

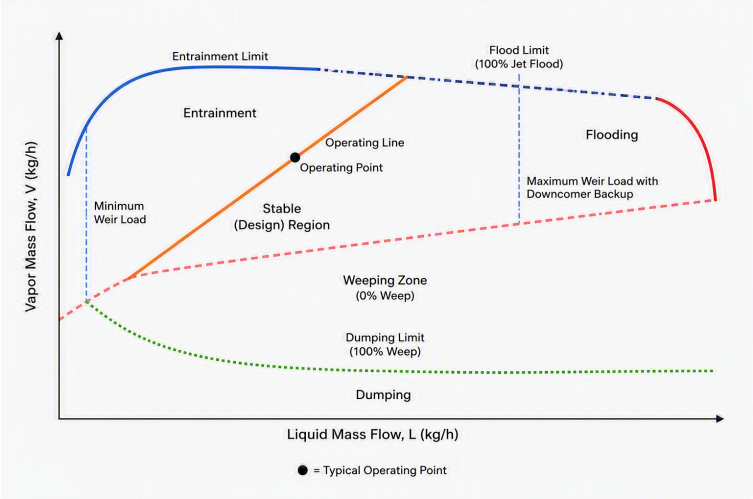

Figure 6: Tray-column operating envelope and associated hydraulic limits.

The constant V/L line illustrates how coupled vapor–liquid flows determine the feasible operating point. Because operating conditions directly influence tray efficiency and stage performance, designers must establish a safe operating range that covers all expected variations in vapor and liquid loads over time [26].

2.5.2 Flow Regime: Packed Columns

The performance of packed columns depends on vapor–liquid interaction, but operational limits differ from those of tray systems because there is a continuous separation in packed columns. At low vapor rates, liquid maldistribution and channeling may occur, which leads to a reduction of effective surface area and mass transfer efficiency. The packing material experiences both entrainment and flooding at high vapor rates, which results in two specific outcomes: liquid holdup reaches excessive levels, and pressure drop across the bed increases sharply. The flooding curve, shown in Figure 7, establishes the operational boundary because it indicates the point at which all packaging material reaches maximum capacity, which leads to a reduction in mass transfer performance.

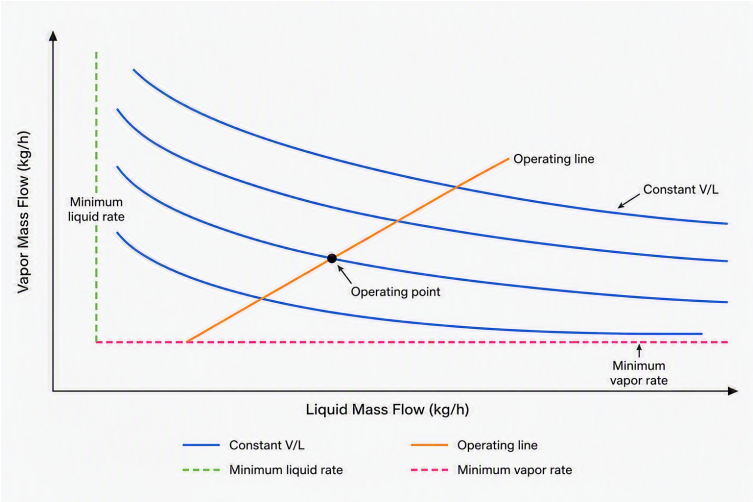

Figure 7: Packed-column operating envelope and associated hydraulic limits

The performance of packed columns depends on liquid load because higher liquid rates establish thicker films, which create greater pressure drops that decrease vapor flow capacity. The operating point must therefore be selected within the safe hydraulic region defined by packing flooding correlations, which ensures stable counter-current flow and maintains operational efficiency under diverse operating conditions.

2.6 Vacuum Distillation

Very little research has been conducted on vacuum distillation for e-methanol, since the process does not involve heat-sensitive compounds. As the components are thermally stable and not prone to degradation at higher temperatures, vacuum operation offers

little benefit. This might not be lucrative in terms of energy efficiency and has less heat integration potential between columns, but can be economically feasible as the electrolyzers, especially alkaline electrolyzers, which are the main source of H_2 in the project, need to be at 90 °C all the time, which provides cooling water at 85 °C. This cooling water stream is typically cooled using the cooling tower, which imposes an additional cooling duty on the plant. Luyben [36] compared methanol and water binary mixture distillation at atmospheric and vacuum conditions, and concluded that due to reduced pressure, the reflux drum temperature decreases, re-boiler duty decreases, condenser area increases a lot, and the column diameter needs to be large due to smaller vapor density. In the end, the total capital cost increases by 20-30% when comparing the pressure of 1,01 bar to 0,52 bar.

Even though the capital cost increased but vacuum distillation concept provides a pathway to use this excess low-grade energy to be integrated with the re-boilers of the distillation column and reduce the operating expenditure (OPEX). The capital cost increases to accommodate the large vapor flow under reduced pressures. The design of vacuum distillation columns requires large column diameters and wide tray spacing [26]. Based on all the theoretical review and fundamentals of distillation discuss previously, a very robust set of implications on the column parameters if used under vacuum or reduced pressure conditions is included in Table 5.

Table 5: A summary of findings from literature [35, 36, 37]: Effects on parameters and design implications for vacuum methanol distillation using an 85 °C electrolyzer heat source.

Parameter	**Effect**	**Design / Operational Implication**
Reboiler temperature on the process side	Limited to 75 °C; Pressure needed to be reduced	Vacuum operation; size re-boilers for lower ΔT, increasing CAPEX
Boiling point	Reduced at lower pressures	Optimize column parameters (tray/packed) to maintain efficiency
ΔT	Moderate (8–10 °C)	Larger heat exchanger area required
Column height	Might remain the same or need to be increased slightly if efficiency drops	Optimize trays/packing to meet 99.99% purity
Vapor velocity	Vapor density reduces under vacuum	Diameter needs to increase to maintain operations
Flooding	Lower flooding risks; weeping possible	Optimize design to balance vapor–liquid flows
Columns: Heat integration	85 °C water stream supplies heat	No possible heat integration between columns
Operational control	Sensitive to feed, vacuum, and heat fluctuations	Monitor pressure, reflux, purity, and temperature for stable operation

The **reflux ratio** is one of the key parameters to consider when designing a distillation column. There are three different scenarios, as follows:

- At constant feed, increasing the reflux ratio raises the reboiler duty, since the two are directly coupled.
- At reduced feed rates, the reflux ratio remains constant and the reboiler duty decreases proportionally with throughput until the column reaches its turndown limit.
- Below the turndown limit, the reboiler duty is held constant at its minimum stable value to maintain sufficient vapor load, which prevents tray weeping but forces the reflux ratio to increase.

Vacuum distillation's 85°C heat source and low-pressure vapor density limit heat integration and stable multi-column operation, making a two-column process (light-gas removal plus methanol-water separation/polishing, optionally with a water column for fusel oil disposal below 75°C) could be the optimal configuration [14, 32, 33, 34].

2.7 Transient Distillation Process

An electrolyzer is used to produce H_2, which is powered by a wind- and solar-based PPA that does not guarantee a constant electricity supply. The renewable electricity supply fluctuates on an hourly basis as it is dependent on weather conditions as well as the region [7]. The operational mode of modern electrolyzers is often termed as grid-forming load control where it provides stability to the grid while producing hydrogen [38]. This means the electrolyzer only uses the electricity or part of it when renewable energy is available. This load is expected to swing between 20% and 100% of rated capacity on an hourly basis, with required to build electrolyzers with larger ramp rates to cope with renewable intermittency.

The minimum load of the **alkaline electrolyzer (AEL)** is limited to 20–25% of nominal hydrogen production. This lower bound is caused by hydrogen diffusing laterally across the diaphragm to the oxygen side, which, at low production rates, increases the hydrogen-in-oxygen concentration toward a flammable mixture and triggers a safety shutdown [38, 39]. According to Buttler [38] and Taranin [39], the alkaline electrolyzer can potentially ramp at 0.2%/s (equivalent to 720%/hr). A load change from 100% to the 20% minimum therefore corresponds to an 80% swing completed in $80/0.2 = 400$ s ≈ 6.7 min, which is effectively instantaneous relative to the hourly dispatch resolution used in this work.

The electrolyzer must operate at a minimum of 20% of its nominal capacity during certain periods of the year when renewable electricity is insufficient. In these periods, electricity must be imported from the grid, as 20% represents the minimum stable operating point of the synthesis loop. This leads us to the situation where, if we have 70 MW of excess heat at 85 °C at 100 % capacity, now we only have 14 MW of it. The important aspect is that the outlet temperature of the cooling water of the electrolyzer remains constant at 85°C regardless of load to maintain the stack temperature at 90°C [40]. This ensures that the temperature is not going to be a constraint, provided that the distillation is carried out under reduced pressure and at around 75°C column bottom temperature. Also, it is important to consider that the quantity of heat available is

enough for the distillation itself; thermal storage is required, or another expensive source of heat needs to be considered.

The exothermic methanol synthesis reaction requires maintaining catalyst bed temperatures within a range to prevent deactivation and ensure stable conversion [1]. The minimum stable load for methanol synthesis is between 20 and 30 % for a water-cooled industrial design because the reactor needs that minimum load to sustain its temperature profile. The recycle compressor put extra restrictions on this operational capacity. The standard compressors used for methanol synthesis loops are unable to operate below 50 to 70 percent of design flow unless operators use anti-surge control. So, the limit can be extended by using a recycle loop or variable speed drives, although this will increase energy consumption and CAPEX [41]. Dynamic simulations of the water-cooled fixed-bed reactor show that it can safely follow load changes across the 20–110% range at ramp rates of up to 2.22%/min, or approximately 133%/hr, without causing wrong-way thermal behavior or violating path constraints [42].

The electrolyzer, which can operate flexibly between 20% and 100% load with a ramp rate of 0.2% per second, cannot be integrated directly with the methanol synthesis reactor. Therefore, an intermediate H_2 storage tank is required, which increases both CAPEX and operational complexity. However, this is outside the scope of the present study [43].

2.7.1 Distillation Column Design Options

The H_2 production is not constant, which leads to fluctuations in the methanol synthesis and, consequently, in the flow rate and composition of the crude methanol fed to the distillation columns. The two design options important to consider here are as follows;

1. **High turn-down** distillation columns that operate from 20 to 100 % feed range without any external storage require a very specialized internal (like structured packing with multiple passes), careful hydraulic design, and, in our case, advanced vacuum control. The turn-down constraint is due to column hydraulics. For instance, sieve trays can only work effectively between 50 and 60% of their designed vapor capacity because this leads to flooding and weeping, which results in poor separation [44]. For valve trays, this range is 40 to 50 %, and their efficiency decreases below this limit [44]. The structured packing system can operate efficiently between 20 and 25% of its design capacity, provided with a precisely designed liquid distribution system [45]. The column operating in vacuum conditions is even more difficult to cope with a high turndown ratio because as the vapor load decreases, the column is unable to maintain the pressure set for 100 % capacity, which leads to over-evacuation, foaming (not relevant in the E-methanol case), and liquid carryover problems [36]. Here, strategies like nitrogen bleed systems, mechanical pumps with variable speed drives, or staged ejector bypass systems are required to achieve the desired turndown ratio.

2. Usually, a decrease in feed without dedicated intermediate storage is controlled

by increasing the reflux ratio, since less vapor is generated at lower feed rates and a higher reflux compensates by improving the separation per stage [27]. However, because the trays, packing, condenser, and reflux drum all hold liquid, the column cannot reach a new steady state as soon as the reflux ratio changes. Recent dynamic simulation studies quantify this lag directly: Chen et. [15] report that a 10% change in feed flow rate to an ethanol–water binary column takes approximately 2.5 hours to reach steady state, and [46] report that a 20% feed change in an extractive distillation system requires 3–6 hours before the column re-stabilizes.

These response times set the practical **Ramp Rate** for the distillation column at roughly 5%/h for both the feed mass flow rate and the feed composition, since a change faster than this outpaces the liquid holdup before reflux adjustment alone can bring the column back to steady state. The electrolyzer and synthesis loop, by contrast, can ramp at up to 133%/h [42]– an order of magnitude faster than the column can tolerate. This mismatch is the central operational problem addressed in this thesis: without a decoupling mechanism between the synthesis loop and the distillation section, relying on reflux adjustment alone against a disturbance of this magnitude risks off-specification product during the transition and pushes the column toward flooding or weeping depending on the direction of the swing, reinforcing the need for the buffering strategies developed in this thesis.

Luyben [47] also demonstrates that for products that are not expensive, it becomes more cost-effective to operate in constant-capacity steady columns with buffer storage capacity because this method requires lower expenses than constructing a column that can handle substantial load variations and has a high turn-down ratio.

2.8 Distillation Heat Duty Availability

As the distillation column's reboiler operating temperature is lowered through vacuum distillation, the required heat duty at low temperatures increases. The portion of the cooling-water stream that remains above the minimum approach temperature to the process sink, i.e., the reboiler side, can be used directly. However, the remaining fraction may be too cold to satisfy the duty on its own. In such cases, the established solution is to bridge the temperature gap with a heat pump rather than by importing steam, thereby upgrading the low-grade portion of the stream to the temperature required by the process [48, 49, 50]. Electric boilers or low-pressure steam from another source may also be used as alternatives.

2.8.1 Mechanical Vapour-Compression Heat Pump

The heat pump considered here is a closed-cycle mechanical vapour-compression system. A working fluid circulates in a sealed loop through four stages: it absorbs heat at low pressure and low temperature in an evaporator, is compressed to the condensing pressure, rejects heat at the sink temperature in a condenser, and is subsequently expanded back to evaporator pressure to repeat the cycle. Because the working fluid

remains within the loop, the cycle performance can be described entirely in terms of the condensing and evaporating temperatures and the resulting temperature lift, independent of the specific process to which it is coupled. Figure 8 shows that the evaporator extracts $\dot{Q}_{\mathrm{evap}}$ from the ELY waste-heat stream, the compressor supplies electrical work $\dot{W}$, and the condenser delivers $\dot{Q}_{\mathrm{cond}}$ to the reboiler.

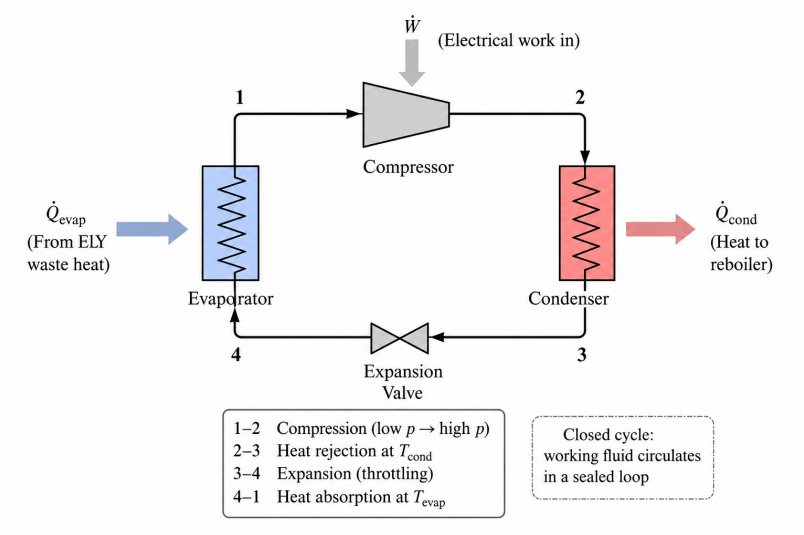

Figure 8: Closed-cycle mechanical vapour-compression heat pump links the electrolyser waste heat stream (evaporator source) to the vacuum-distillation reboiler (condenser sink). Adapted schematically from the standard four-component vapour-compression layout used in the process heat-pump literature [51, 50].

The compressor and expansion valve decouple the evaporator from the condenser, so the source side, governed by the ELY stream, and the sink side, governed by the reboiler, can be treated independently. Because the loop is closed, no process fluid enters the heat pump; the two process streams are connected only through heat transfer.

The condensing and evaporating temperatures are determined by the sink and source temperatures, together with their respective approach temperatures, as given below:

$$T_{\mathrm{cond}} = T_{\mathrm{sink}} + \Delta T_{\mathrm{c}} \tag{16}$$

$$T_{\mathrm{evap}} = T_{\mathrm{src}} - \Delta T_{\mathrm{e}} \tag{17}$$

$$\Delta T_{\mathrm{lift}} = T_{\mathrm{cond}} - T_{\mathrm{evap}} \tag{18}$$

Here, T_{sink} is the reboiler temperature that the condenser must reach, T_{src} is the ELY waste-heat outlet temperature entering the evaporator, ΔT_{c} and ΔT_{e} are the condenser- and evaporator-side approach temperatures, and ΔT_{lift} is the temperature lift that must be provided by the compressor [48].

The theoretical performance ceiling follows from the Carnot limit and is scaled by

a second-law efficiency to obtain a realistic coefficient of performance (COP):

$$\mathrm{COP}_{\mathrm{Carnot}} = \frac{T_{\mathrm{cond}} + 273.15}{\Delta T_{\mathrm{lift}}} \tag{19}$$

$$\mathrm{COP}_{\mathrm{real}} = \eta \cdot \mathrm{COP}_{\mathrm{Carnot}} \tag{20}$$

Here, η is the second-law efficiency of the real machine relative to the ideal cycle [48].

This arrangement combines a vapour-compression heat pump with the fraction of the ELY stream that is sufficiently hot to serve the reboiler directly, thereby reducing the steam demand for distillation.

3 Assumptions

This chapter presents the assumptions adopted across the four main components of the study: the process design, the optimization models, the techno-economic analysis, and the heat pump integration, where applicable.

3.1 Process Simulation

The following assumptions were adopted in the distillation process design:

1. For the simulations, the **crude methanol feed** nominal capacity is assumed to be 32 t/h and consists of approximately 63.4 wt% methanol and 36.0 wt% H_2O. The remainder is assumed to be trace-level impurities, including light gases (CO_2, CO, H_2, N_2, and O_2) at about 3600 ppm; dimethyl ether (DME) and methyl formate at about 1000 ppm; ethanol at 250 ppm; acetone at 12 ppm; and higher alcohols (propanol, butanol, and pentanol) at 250 ppm.

2. The NRTL–Redlich-Kwong (NRTL–RK) property method is used to describe the vapor–liquid equilibrium of the crude e-methanol stream, including trace organics and dissolved light gases, and is assumed to give sufficiently accurate activity coefficients for this system.

3. Column sizing starts with the Fenske–Underwood-Gilliland (FUG) shortcut method, which provides initial estimates of stage count, minimum reflux, and feed-stage location. These estimates are then checked against rate-based RadFrac simulations before the design is finalized.

4. The vacuum-column design is completed using the steady-state rate-based approach, assuming that the MellapakPlus 250Y and 452Y structured packings maintain pressure drops of ≤ 2 mbar/m and ≤ 3 mbar/m [52], respectively, and that these values remain constant down to 60% turndown.

5. Conventional base-case columns instead use sieve trays, for which a 10 mbar per-stage pressure drop and a 60% tray efficiency are assumed, based on vendor's data in the e-methanol sector.

6. Heat exchangers are designed for a 5°C minimum approach temperature (hot water cooling from 85 to 80°C, cooling water heating from 25 to 30–40°C) together with an overall heat transfer coefficient $U = 1000$ W/m^2·K and a constant cooling-water heat capacity of $C_p = 4.180$ kJ/(kg·K).

3.2 Optimization Models

The optimization is inherently dynamic because it links the hourly feed profile, which depends on hydrogen production and electricity availability, to the steady-state distillation process constrained by a ±5%/h ramp rate. The following assumptions were used for the optimization models (see subsection 4.3):

1. The optimization is formulated over a discrete hourly time horizon (T); 1-hour time steps are assumed sufficient to capture the relevant dynamics of feed fluctuations and column response.

2. Within this time horizon, the ramp-rate constraint (±5%/h) as discussed in subsubsection 2.7.1 and the lowest possible turndown limit based on ASPEN PLUS simulations are the only dynamic limitations considered for sizing the buffer systems.

3. The dynamic model demonstrated a maximum stable ramping rate of approximately 133 %/hr (2.22 %/min) for the methanol synthesis reactor subsubsection 2.7.1. To ensure robust operation and avoid running the process at its stability limit, a conservative safety margin of 50 % was applied, giving a design ramp rate of 66.5 %/hr (≈ 1.11 %/min). This provides a buffer against controller lag, model uncertainty, and real-world disturbances not captured in the simulation.

4. Product quality — methanol purity and impurity limits — is assumed to be maintained at all times as long as the feed rate (D_t) stays within its maximum and minimum 60% capacity interval.

5. Available heat for the distillation process from the synthesis loop is assumed to scale linearly with the crude methanol feed rate over the 20–100% capacity range. At 100% nameplate capacity of the methanol synthesis reactor, the synthesis loop provides 8.5 MW of medium-pressure steam and 2.7 MW of low-pressure steam, and the available heat is reduced proportionally as the load decreases to the reactor's minimum allowable operating capacity of 20% subsubsection 2.7.1. These heat availability values are taken from the upstream process design and heat integration network, which are outside the scope of the present study.

6. Reboiler duty, condenser cooling duty, and steam requirements are instead obtained from steady-state simulations of the distillation column at discrete feed rates (100%, 99%, 98%, down to 60% of D_t) and interpolated using a Special Ordered Set of type 2 (SOS2) formulation, which activates only the two neighbouring breakpoints required at any given optimization step.

7. The intermediate tank stores crude methanol that mainly contains water and dissolved CO_2 along with some other trace impurities [53] that evaporate readily, therefore the tank volume is sized at twice the nominal requirement to provide adequate headspace; no minimum storage level is imposed.

8. A fixed handling cost of 0.05 €/t was applied to the fraction of feed supplied from storage or reintroduced through product recycle, while storage boil-off losses were represented by a fixed cost of 0.001 €/t. This handling cost was imposed uniformly across all cases to enable a consistent basis for comparison between the flexibility strategies. The pumping electricity demand of other

distillation process pumps is not included in this term but is instead evaluated separately within the overall balance-of-plant electricity demand, assessed against the hourly electricity prices of the respective region of operation.

9. The methanol feed composition is held constant throughout operation by mixing water into the methanol product ahead of the feed mixing point. The methanol concentration in the wastewater is assumed to be zero, since it was found to be only 205 ppm based on the ASPEN PLUS-based analysis presented in subsection 4.1.

3.3 Techno-Economic Analysis

The following assumptions and cost data were used for the techno-economic comparison (see subsection 4.5) between the Nordic and South American case studies.

1. The RFNBO methanol price is set regionally to reflect the local production cost, which is dominated (≈60–70%) by the cost of green hydrogen production and hence by the local renewable electricity cost and capacity factor [54]. Accordingly, a selling price of 1100 €/t is used for South America, which benefits from its high-capacity-factor solar–wind resource, and 1400 €/t for the Nordics, where predominantly wind-based supply gives a higher production cost [54].

2. The plant life is considered to be 30 years with a discount rate of 6%.

3. CAPEX depreciation is assumed to be 10 years.

4. The CAPEX for distillation process cases is calculated using Aspen Economic Analyzer and then multiplied by 1.5 to account for uncertainties due to additional equipment costs not explicitly included in the estimation.

5. Costs outside the scope of this study include the electrolyzer, synthesis loop, and CO_2 capture CAPEX and OPEX. The CAPEX of all the equipment is considered constant; however, their OPEX varies because of utility cost differences between the two regions, the Nordics and South America.

6. Alkaline electrolyzer restacking is performed every 8th year, and the catalyst for the methanol synthesis reactor is replaced every 3rd year.

7. The plant is assumed to be idle in the first year due to construction, with 50% of CAPEX deployed that year and the remaining 50% deployed in Year 2. Operation ramps up in step with this spending: 50% in Year 2, then full (100%) operation from Year 3 onward. The one exception is years requiring re-stacking and catalyst replacement, when operation is reduced to 90%.

8. Utility cost data were sourced from prominent industrial suppliers for hot utilities, and Intratec [55, 56] is considered to approximate cooling utility cost. The utility costs for both regions are summarized in Table 6.

Table 6: Utility cost comparison between Nordic and South American regions.

Parameter	Nordics	South America
LP Steam	44 €/MWh	9 €/MWh
MP Steam	45 €/MWh	11 €/MWh
Cooling Water	0.085 €/ton	0.05 €/ton

9. A Power Purchase Agreement (PPA) price of €30/MWh is used for South America, reflecting the elevated ACL (free contracting environment for electricity) contract prices driven by ongoing hydropower sector uncertainty [57], and is expected to decline toward €18–22/MWh by 2030 as the market stabilizes [58]. For the Nordics, a PPA price of €45/MWh is used, close to the most recent observed level of €43.38/MWh in 2025 [59], with prices expected to remain broadly stable going forward as wind technology in the region continues to mature. The PPA and electricity transmission costs for both regions are summarized in Table 7.

Table 7: PPA and electricity transmission costs for Nordic and South American regions.

Parameter	Nordics	South America
Renewable PPA	45 €/MWh	30 €/MWh
Transmission Cost	2 €/MWh	0.42 €/MWh

10. For the Nordics, hourly day-ahead electricity prices for the year 2025 are used, obtained from the Nord Pool and ENTSO-E Transparency Platform [60, 61]. For South America, the corresponding hourly market data are sourced from the hourly Difference Settlement Price (*PLD horário*) for 2025, published by the Chamber of Electric Energy Commercialization (CCEE) [62]. The hourly analysis is performed for both markets. Although hourly electricity prices are used in the optimization model, the electricity supply is presented here as a monthly average cost to derive a clear trend. Figure 9 shows the monthly grid electricity price for the corresponding markets, which indicates that the grid electricity price is generally higher in the Nordics than in South America, except for the month of August.

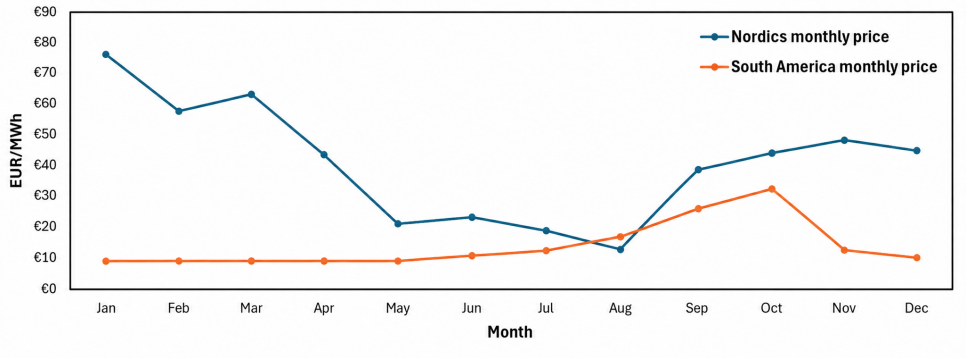

Figure 9: Monthly grid electricity price in MWh.

11. According to Commission Delegated Regulation (EU) 2023/1184 [63], grid electricity may be considered renewable for RFNBO production if the bidding-zone electricity emission intensity is below 18 gCO_2eq/MJ under the specified conditions. Based on this criterion, the share of green versus grey e-methanol is determined and subsequently used to calculate revenue. The share of grey hydrogen converted to grey methanol, which is costed at 400 €/ton in both regions. Since green and grey methanol are sold at different prices, it is necessary to accurately measure their shares in each market. The overall division of e-methanol share across these 2 categories is as follows Table 8:

Table 8: Green versus grey e-methanol share for the Nordic and South American cases.

Parameter	**Nordics**	**South America**
RFNBO methanol	85 %	93 %
Grey methanol	15 %	7 %

Similarly, although the hourly profile is used in the optimization model, the monthly share of PPA electricity, which always qualifies as RFNBO-compliant, together with the grid electricity classified as green or grey, is presented here as an averaged trend in Figure 10.

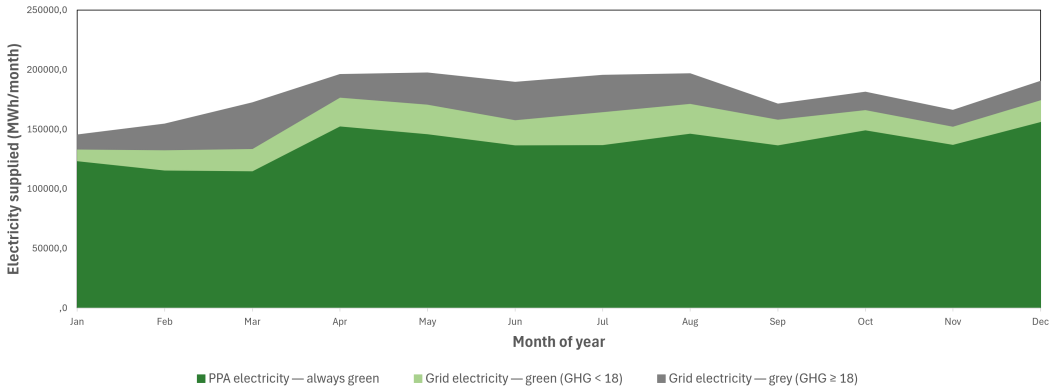

(a) Nordics

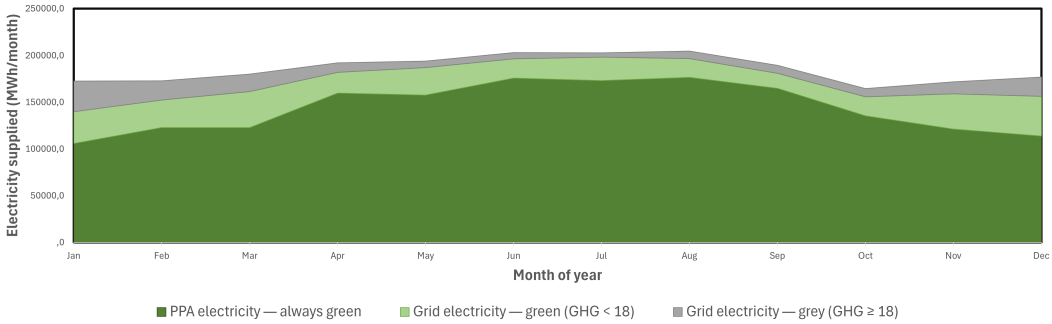

(b) South America

Figure 10: Electricity consumption and the corresponding share of green versus grey e-methanol (including the PPA green mix) for (a) the Nordic market and (b) the South American market.

3.4 Heat Pump Analysis

The following assumptions and cost data were used for the heat pump analysis in the vacuum distillation study.

1. Based on vendor data, a minimum driving force of 5–15 K is typically required across heat pump evaporators and condensers to ensure adequate heat transfer. A value of $\Delta T_{\min} = 10$ K is selected for the heat pump analysis.

2. For the direct heat exchanger between the electrolyzer waste-heat stream and the reboiler, the process water is cooled from 85 to 80 °C to supply heat directly to the reboiler, which operates at 75 °C under isothermal methanol boiling conditions. Because this stream operates closer to the reboiler temperature than the evaporator/condenser loop, a tighter minimum approach temperature of $\Delta T_{\min} = 5$ K is assumed, consistent with the 80 °C outlet and the 75 °C reboiler.

3. A motor efficiency of $\eta_{\text{motor}} = 1$ is assumed, and no separate shaft or drive losses are modeled.

4. A constant $\dot{m}c_p$ is assumed over the electrolyzer cooling range, allowing the available heat to be calculated directly from the temperature difference.

5. Elwardany M. [64] reported that industrial high-temperature heat pumps (HTHPs) typically achieve exergy efficiencies of approximately 0.28–0.39, while Ma X. [65] reported a realistic peak of about 43.3% under favorable operating conditions. Since this case does not assume an ideally tuned design, an efficiency of 0.45 is used for calculations.

6. The heat pump model assumes a fixed temperature lift, with load variation absorbed entirely through adjustment of the source (waste electrolyzer heat) mass flow rate at the evaporator. Under this assumption, the COP remains constant across the full range of electrolyzer loads. This simplification does not reflect actual part-load behavior: compressor isentropic efficiency declines away from its design point, and evaporator/condenser heat-exchanger effectiveness shifts with mass flow, so the real COP would vary with load rather than stay fixed. A constant-COP formulation is adopted here because part-load compressor performance maps specific to the selected unit were not obtained for this study, and the resulting error is treated as a modeling limitation rather than a physical property of the system.

7. The maximum possible coefficient of performance, $\mathrm{COP}_{\mathrm{max}}$, is assumed to be 5. If the calculated $\mathrm{COP}_{\mathrm{real}}$ exceeds 5, it is capped at that value because vendor-quoted equipment cannot deliver a higher COP.

8. CAPEX for the heat pump is assumed to be in the range 150–800 €/kW based on the literature [66, 67]. A value of 500 €/kW is selected as the central estimate for the CAPEX calculations.

4 Methodology

This chapter outlines the methodology used to design and evaluate the e-methanol vacuum distillation process. It covers Aspen Plus simulation results, the integration of intermittent crude methanol feed into the distillation system, the techno-economic analysis, and the design of a heat pump to support the process when waste heat from the alkaline electrolyzer is insufficient to meet the required heat demand.

4.1 Vacuum Distillation: Process Design and Simulation

The first 3 objectives from subsection 1.2 must be fulfilled in the distillation process design presented here. In order to comply with objectives, the main requirements for the design are as follows:

1. At least a 2-column configuration is required because acetone, methyl formate, and dimethyl ether are more volatile than methanol; they must be removed in the topping column. A separate refining column is then required to limit the ethanol concentration in the methanol product to below 35 ppm.

2. To use electrolyzer waste heat as the reboiler heat source, the column bottom temperature must remain below 75 °C. The available hot-water stream enters at about 85 °C and can be cooled only to 80 °C in order to maintain a minimum pinch temperature difference of 5 °C between outlets of the hot and cold streams. This temperature constraint limits the maximum allowable bottom temperature and therefore strongly influences the operating pressure and overall column design.

3. Cooling water is the only cooling utility, so the condenser temperature must remain sufficiently above 25 °C (typically 5–15 °C), leading to a minimum top temperature of about 30-40 °C to ensure sufficient driving force for heat transfer.

4.1.1 Topping Column

The Non-Random Two-Liquid–Redlich–Kwong (NRTL–RK) property method is used for thermodynamic property estimation in the crude methanol distillation system[13, 35, 32]. The Aspen Plus Short-Cut Distillation method based on the Fenske–Underwood–Gilliland (FUG) approach is used for the initial estimation of reflux ratio, distillate-to-feed ratio, number of stages, and feed stage. Then a Radfrac column is used for actual process design.

Without a topping column, all the acetone will end up in the product at a concentration of 18–20 ppm, and the light gases will also remain in the product, making it difficult to achieve IMPCA-specification methanol product quality.

4.1.1.1 Number of Stages and Feed Stage

For the initial analysis, the condenser pressure was set to 1.013 bar(a), and the condenser temperature was fixed at 40 °C, with the distillate-to-feed ratio used as the design specification.

Under these conditions, the optimal column configuration at 100% nominal capacity was found to have 40 stages, with the feed introduced at stage 17. This arrangement gave the acetone concentration less than 5 ppm in the bottom stream while maintaining a relatively low reboiler duty, as shown in Figure 11.

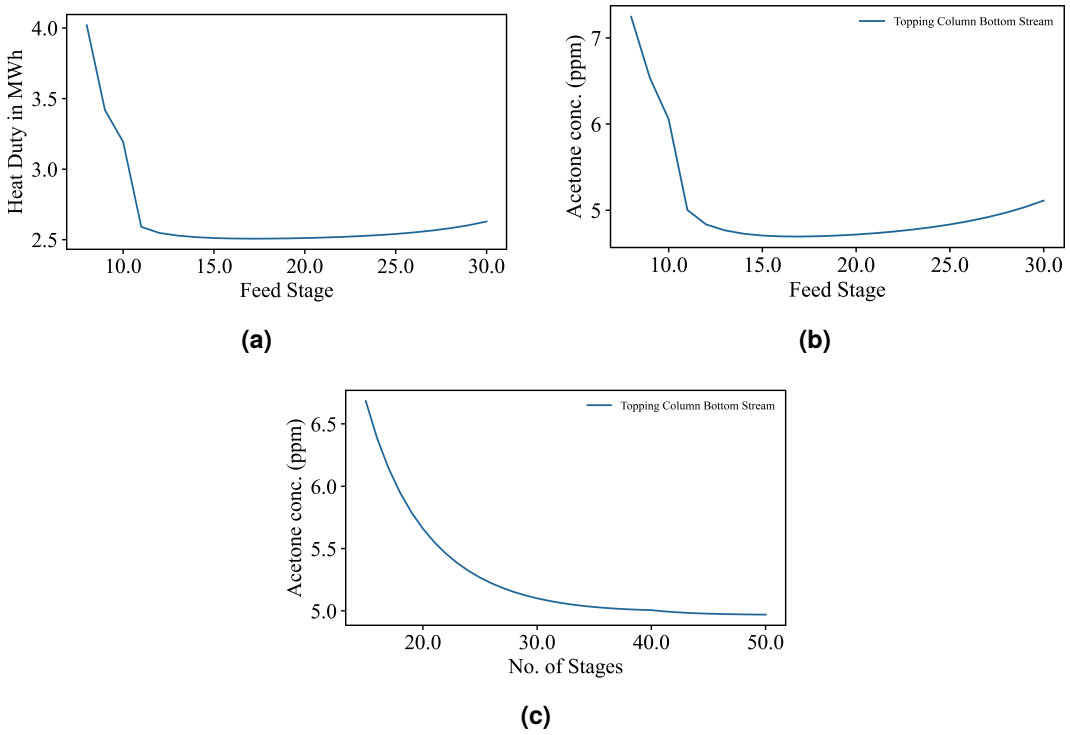

Figure 11: Topping column optimized parameters: (a) Shows effect on reboiler duty as feed stage changes, (b) Shows effect on concentration of acetone in bottom stream as feed stage changes, and (c) Shows effect on concentration of acetone in bottom stream as number of stages increases.

After optimizing the number of stages and the feed stage, the acetone concentration in the bottoms stream of the topping column is limited to 5 ppm by adjusting the reboiler duty per the design specification.

4.1.1.2 Reboiler and Condenser Temperature

The reboiler temperature depends on the condenser pressure and the pressure drop across stages. The reboiler temperatures for the different column internals, with the condenser pressure held constant at 1.013 bar (a), obtained from the rate-based analysis, are presented in Table 9. The mass transfer, heat transfer, and interfacial area equations used for rate-based analysis are presented in *Appendix Table 28*.

Table 9: Column internals with pressure drop and bottom temperature.

Column Internals	Pressure Drop (mbar(a)/m)	Bottom Temp. (°C)
Sieve Tray	12	79.5
Random PALL 15 mm	8.9	76.7
Mellpackplus 250Y	2.2	74.2

The results show that the structured packing gives the lowest pressure drop, which is consistent with the Suzler pressure drop of 2 mbar/m [52]. Analyses were performed on all packings (125X, 250X, 350X, 125Y, 250Y, 252Y, 350Y, 352Y) across various HETP values. The 250Y packing with an HETP of 0.5 m was selected as the most suitable column internal for the next analysis, in which the impact of changing the condenser pressure on the column bottom temperature is investigated while maintaining the condenser temperature at 40 °C, using a design specification for the distillate-to-feed rate.

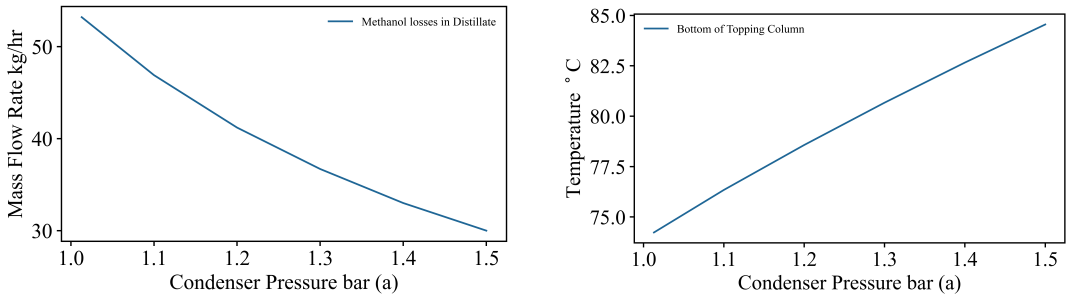

Figure 12: Changing the condenser pressure effects on: (a) Amount of methanol wasted in distillate of topping column and (b) bottom temperature of the topping column *Appendix Table 29*.

Based on Figure 12, a bottom temperature below 75 °C is only achievable at 1.013 bar (a) or under vacuum pressure conditions. Also, decreasing condenser pressure increases methanol loss in the distillate, but the methanol losses in the topping column also depend on the condenser temperature. The impact of varying the condenser temperature, as shown in Figure 13, confirms that the initially selected value of 40 °C, chosen to maintain a 5 °C temperature difference between the cold-side outlet and the hot-side outlet, is appropriate from a technical feasibility perspective.

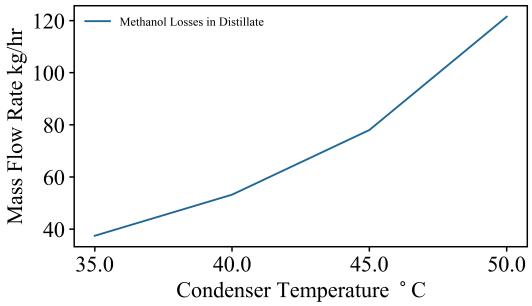

Figure 13: Effect of changing condenser temperature on methanol waste in the distillate of the topping column *Appendix Table 30*.

The economic impact of condenser temperature selection is evaluated in Table 10. For a fixed minimum approach temperature of 5 °C, varying the condenser temperature has a significant effect on OPEX, as higher cooling-water flow rates directly increase operating costs. Furthermore, Table 11 indicates that decreasing the condenser temperature does not significantly increase CAPEX, but it does raise cooling operating costs by approximately 100% due to an almost twofold increase in cooling-water flow rate. Therefore, further lowering the condenser temperature does not significantly enhance methanol recovery and instead leads to higher overall CAPEX and OPEX.

Table 10: Cooling water mass flow rate at different minimum approach temperatures.

Condenser Temperature (°C)	**Hot Stream (°C)**	**Cooling Water (°C)**	**Cooling Water Mass Flow Rate (kg/s)**
35	63.55 → 35	25 → 30	78.4
40	63.55 → 40	25 → 35	38.2

Table 11: Cooling water optimization for condenser duty of 1.6 MW (C_p = 4180 J/kg·K, U = 1000 W/m^{2}K).

Condenser Temperature (°C)	**LMTD (°C)**	**HX Area (m^2)**
35	19.57	81.65
40	20.73	77.3

4.1.1.3 Turn-Down Ratio

Turn-down ratio represents the operational flexibility of the distillation column [68]. It is the minimum fraction of the nominal vapor (or feed) load that the trays or packing can handle without compromising the desired product specifications. Since vapor load depends on the reboiler duty of the column, the minimum stable reboiler duty defines the turndown limit at fixed reflux ratio conditions. For instance, if a column has a turndown ratio of 50%, it can deliver products that meet the desired specifications down to 50% of the nominal feed capacity.

At first, the diameter was kept constant throughout the column to improve structural integrity and avoid mechanical stresses. The column diameter was found to be 1.2 m, ensuring that the approach to flooding remained below 80% based on rate-based analysis. However, the main drawback of using a constant diameter is that even a 5% decrease in feed is required to increase the reflux ratio, and only a slight decrease in reboiler duty is observed to maintain the hydraulics of the column.

The limiting factor is the rectifying section, the section above the feed stages, where vapor flow and its velocity decrease, and the reflux ratio is not enough for proper wetting of packings. In order to achieve the desired vapor-liquid fraction throughout the column at lower loads, the section above the feed diameter is optimized and decreased to 0,9 m. By decreasing the diameter of the rectifying section, a turndown ratio of 67,5% was achieved as shown in Figure 14 and *Appendix Table 31*.

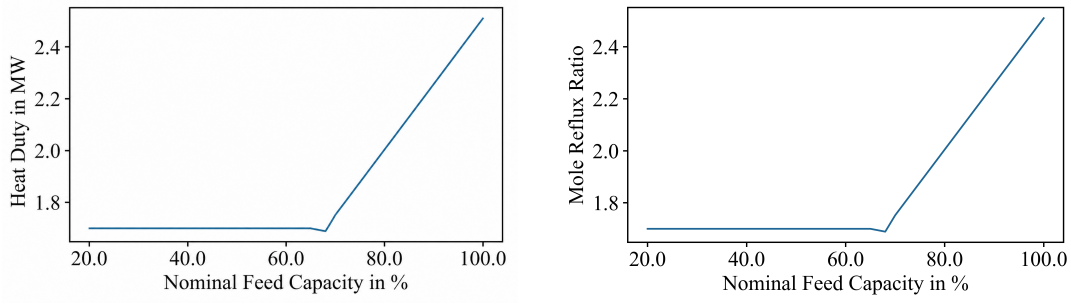

Figure 14: Topping Column with changing nominal feed capacity: (a) Reboiler duty in MW and (b) Mole reflux ratio of the column *Appendix Table 31*.

In this column design, the column can be operated down to 67.5% of the nominal feed capacity with an almost constant reflux ratio while achieving the minimum reboiler duty of 1.7 MW. Below this feed capacity, the reboiler duty is fixed at 1.7 MW, and the product quality is controlled by adjusting the reflux ratio through a design specification. As the feed rate decreases, the reflux ratio is increased to maintain appropriate column hydraulics and vapor–liquid equilibrium.

4.1.2 Refining Column

The main purpose of this column is to produce clean methanol with an ethanol concentration below 35 ppm and the lowest possible turndown ratio.

Conventional methanol refining uses 2 to 3 columns: a medium-pressure column followed by a low-pressure (atmospheric) refining column [13, 69]. However, the available electrolyzer waste heat temperature is insufficient to provide reboiler duty to the medium-pressure column operating at 9 bar (a). Therefore, a single distillation column operating under vacuum conditions is required to utilize the available waste heat.

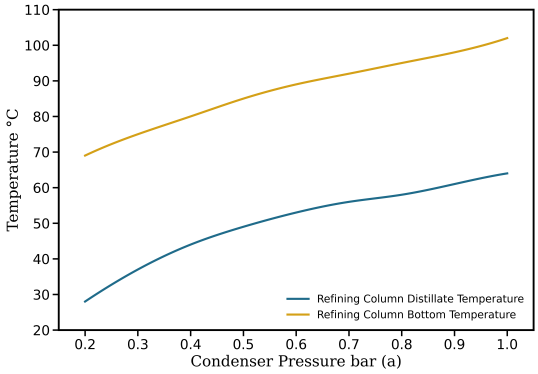

Figure 15: Distillate and bottom temperature versus changing condenser pressure.

Based on shortcut distillation calculations, assuming a total column pressure drop of 100 mbar, cooling water temperatures of 25–30 °C, and electrolyzer waste heat cooling from 85 °C to 80 °C, a minimum temperature approach of 5 °C at both ends results in a condenser pressure of approximately 0.30–0.35 bar(a), as shown in Figure 15.

4.1.2.1 Number of Stages and Feed Stage

Based on the shortcut distillation calculation, approximately 29 theoretical stages are required at a condenser pressure of 0.3 bar(a) to produce methanol with a mass fraction of 0.9999. Using a RADFRAC distillation column and considering 100%stage efficiency and including two additional stages for the condenser and reboiler, the total number of stages required to achieve this methanol purity is estimated to be 48.

However, the main objective of the design is not only to obtain high-purity methanol but also to limit the ethanol concentration in the product to below 35 ppm. Therefore, the subsequent parameter analysis in Figure 16 was carried out using a 60-stage column configuration under the assumption of 100% stage efficiency to evaluate the effect of the number of stages and operating conditions on the ethanol specification. Figure 16b was generated using the mole reflux ratio of 2.

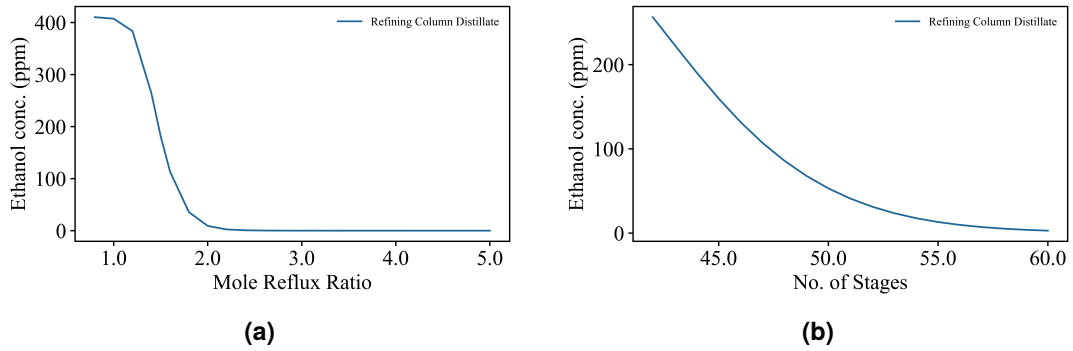

Figure 16: For 100% stage efficiency, the concentration of ethanol in distillate vs: (a) Mole Reflux Ratio, and (b) Number of stages required.

Figure 16 shows that at least 52 stages and a reflux ratio of 1,9 is required to achieve an ethanol concentration below 35 ppm in the distillate. However, when the stage efficiency decreases to 60%, the ethanol concentration no longer meets the target specification included in the *Appendix* Figure 42, and the ethanol concentration in the distillate exceeds 200 ppm, so it is required to either increase the number of stages or the reflux ratio.

For further analysis, the number of stages was increased to 80, and the performance of the column was evaluated at four reflux ratios. As shown in Figure 17, increasing the reflux ratio only provides a marginal improvement in ethanol concentration profiles and does not significantly reduce the required number of stages. However, a higher reflux ratio increases both condenser and reboiler duties. Since the condenser is already operating with a minimum temperature approach of 5°C, a higher reflux ratio would require a much larger heat-transfer area and higher cooling water flow rates.

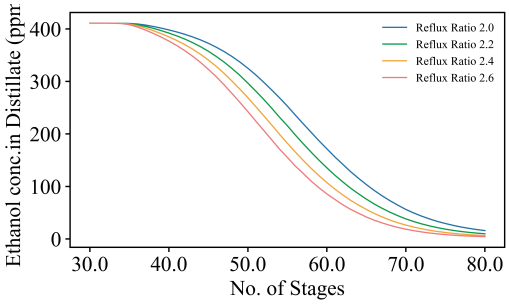

Figure 17: Effect of mole reflux ratio on ethanol concentration in the refining column distillate (ppm).

Table 12 also suggests that the required number of stages does not decrease significantly as the reflux ratio increases. Therefore, a reflux ratio of 2.2 and 72 stages, based on 60% stage efficiency, were selected as the optimal design. The feed stage for this configuration was then also optimized and found to be the 26th stage, as shown in Figure 18.

Table 12: Total number of stages required and ethanol concentration in distillate at varying reflux ratios.

Reflux Ratio	No. of Stages Required	Ethanol Conc. in Distillate (ppm)
2.0	75	29.32
2.2	71	33.04
2.4	69	30.72
2.6	67	30.38

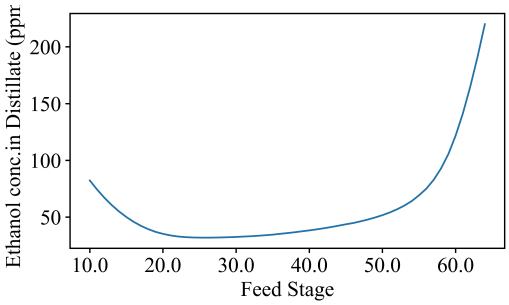

Figure 18: Feed stage vs concentration of ethanol in the distillate of the refining column

4.1.2.2 Reboiler and Condenser Temperature

Because 72 stages represent a relatively high stage count and the total pressure drop must be kept as low as possible to limit the bottom temperature, only structured packings were considered suitable for the refining column. A rate-based analysis was conducted for four different packing types, and MellapakPlus 452 Y was found to provide the best performance while also resulting in the lowest pressure drop, as presented in Table 13 and Table 14.

Table 13: Packing geometry and product purity at condenser pressure of 0.30 bar(a).

Packing	Height (m)	Dia (m)	MeOH Mass Frac	EtOH (ppm)
452 Y	30.5	3.5	0.99996	32.82
352 Y	38.0	3.4	0.99995	34.16
350 Y	38.5	3.5	0.99996	32.81
252 Y	46.5	3.2	0.99996	32.30

Table 14: Pressure drop and column temperatures for different packings at condenser pressure of 0.30 bar(a).

Packing	ΔP (mbar)	T_{cond} (°C)	T_{bottom} (°C)
452 Y	93.09	36.53	75.00
352 Y	94.65	36.53	75.78
350 Y	98.69	36.53	76.80
252 Y	99.94	36.53	75.69

The HETP (Height Equivalent to a Theoretical Plate, i.e., the height of packing that achieves the same separation as one ideal equilibrium stage) values for each packing in Table 13 were determined using rate-based analysis in Aspen Plus. In addition, component-based stage efficiencies were evaluated for ethanol and methanol, as these are the key components governing the separation performance. Based on these efficiencies, the effective HETP was calculated as:

$$\text{Effective HETP} = \frac{\sum \text{Packing HETP}}{\sum \text{Component Efficiency}}$$

The effective HETP was calculated separately for ethanol and methanol for each theoretical stage, and the larger value was used for design purposes. Table 15 suggests ethanol is controlling HETP values. Also, the pressure drop was estimated to be 1.33 mbar/stage, corresponding to 3 mbar/m, which is consistent with [52].

Table 15: Effective HETP values for the refining column.

Column Section	Effective HETP for Ethanol (m)	Effective HETP for Methanol (m)
Rectifying	0.45	0.41
Stripping	0.42	0.42

Using the ethanol-based HETP values, the total packing height for 452 Y was calculated to be 10,5 m for the rectifying section and 20 m for the stripping section.

4.1.2.3 Fusel Oils Side stream

The concentration of higher alcohol impurities in the feed is relatively low, accounting for only about 0.05% of the total feed. Nevertheless, a side stream is required to prevent these components from accumulating in the column over time, as summarized in Table 16. The mass fraction of the impurities in the feed stream is included in *Appendix* Table 33.

Table 16: Impurities in the feed stream.

Impurity	Mass Flow Rate (kg/hr)
Ethanol	8.339
Propanol	4.604
n-Butanol	2.705
s-Butanol	0.397
Pentanol	0.636
Total	**16.681**

To determine the optimal side stream location, the cumulative liquid-phase mass fraction of the higher alcohol impurities was evaluated across the column stages. The stage with the highest combined impurity concentration was selected as the side stream withdrawal point, which was found to be stage 62 from the top, as shown in Figure 19.

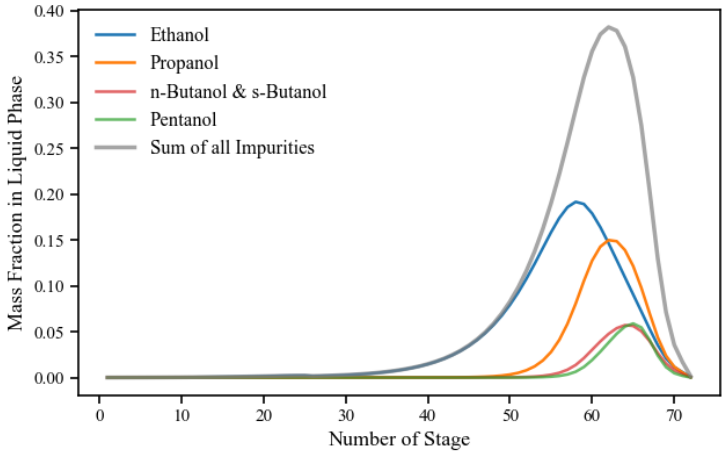

Figure 19: Number of stages vs mass fraction of impurities in liquid phase

The side stream flow rate was then optimized based on impurity removal and methanol loss. A sidestream flow rate of 100 kg/h was selected, as further increases did not result in any significant additional reduction in impurities, as presented in Table 17. At this flow rate, approximately 93% of the impurities were removed, while limiting the loss of valuable methanol.

Table 17: Side stream effect on fusel oil impurities and methanol production.

Side stream (kg/hr)	Impurity Removed (kg/hr)	Impurities Left (%)	MeOH Prod. (kg/hr)
50	13.589	19	20340.06
100	15.450	6.5	20337.75
150	15.717	6	20334.96
200	15.809	5	20332.52
250	15.854	4.8	20330.51

4.1.2.4 Turn-Down Ratio

The refining column has a turndown ratio of 57.5% and can operate down to that point by reducing the reboiler duty at a constant reflux ratio. Beyond this point, as shown in Figure 20, the reboiler duty is fixed, and the reflux ratio must be increased to maintain column hydraulics.

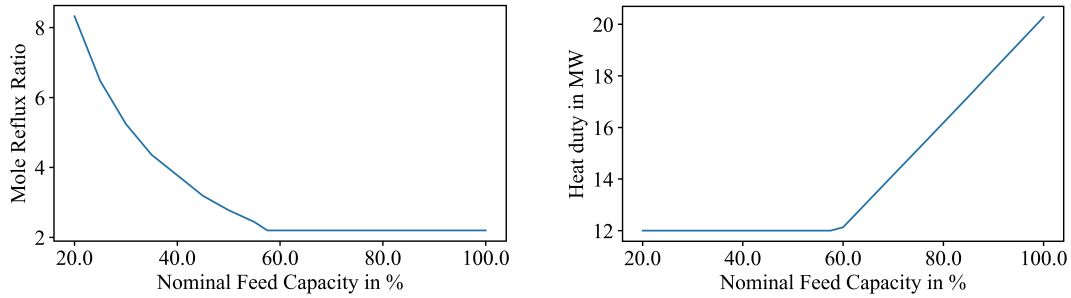

Figure 20: Variable feed capacity effects on (a) Mole reflux ratio and (b) Reboiler duty of the refining column Table 32.

The vacuum distillation process flow diagram, along with the stream data, is included in the *Appendix Figure 43 and Table 33*.

4.2 Base Case: Conventional Distillation

To address the fourth objective in subsection 1.2, conventional distillation is used as the base case for comparing the economic performance of vacuum distillation. E-methanol is conventionally purified using a three-column distillation configuration [13, 69]. There are 2 different configurations for a conventional distillation, depending on the position of the high-pressure column. But in both configurations, the first distillation column is a topping column that removes light gases and volatile impurities.

4.2.1 Base Case 1: Process Design and Simulation

Base case 1 refers to a configuration in which the medium- to high-pressure rectifying column is placed in the middle. In this configuration, the rectifying column recovers approximately 20-30% of the methanol product while simultaneously enriching the feed stream before it is introduced to the final refining column. The refining column is thermally integrated with the rectifying column to improve the overall thermal efficiency of the distillation process, as shown in Figure 21. The detailed process flow diagram is included in the *Appendix* Figure 44.

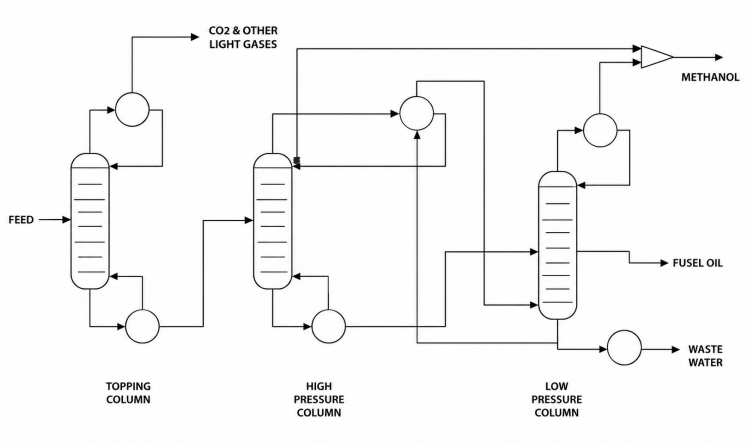

Figure 21: Three-Column Conventional distillation (Base case 01)

Base case 1 was modeled and simulated in Aspen Plus, considering 60% stage efficiency, and the key process parameters and design specifications are presented in Table 18. The heating and cooling duties for the columns for 100% nominal feed capacity are included in Table 19.

Table 18: Specifications of distillation columns.

Column	Condenser Pressure bar(a)	No. of stages	Diameter (m)	Height (m)
Topping	1.5	40	1.2	28
Rectifying	9	62	1.8	44
Refining	1.013	84	2.5	60

Table 19: Condenser and reboiler duties for distillation columns.

Column	Condenser Duty (MW)	Reboiler Duty (MW)
Topping Column	1.99	2.70
Rectifying Column	12.33	13.50
Refining Column	13.73	12.33

4.2.2 Base Case 2: Process Design and Simulation

Base case 2 places the high-pressure column after the low-pressure column, as shown in Figure 22. The high-pressure column is thermally integrated with the middle low-pressure column, which makes this configuration roughly 20% more thermally efficient than Base Case 1 [13]. The gain comes down to how the product draw is split. Here, 60–70% of the methanol product is withdrawn from the middle low-pressure column, so only the remainder passes to the downstream high-pressure column. With less material to process, vapor and liquid loading in the high-pressure column drop, and its reboiler duty falls accordingly. This smaller stream also means

the high-pressure column no longer needs as high an operating pressure to reach a condensing temperature suitable for thermal integration with the low-pressure column. The lower pressure in turn, improves relative volatility, easing the separation while further reducing the heat duty [14].

This configuration is also referred to as backward integration, and the detailed process flow diagram is attached in Appendix Figure 45.

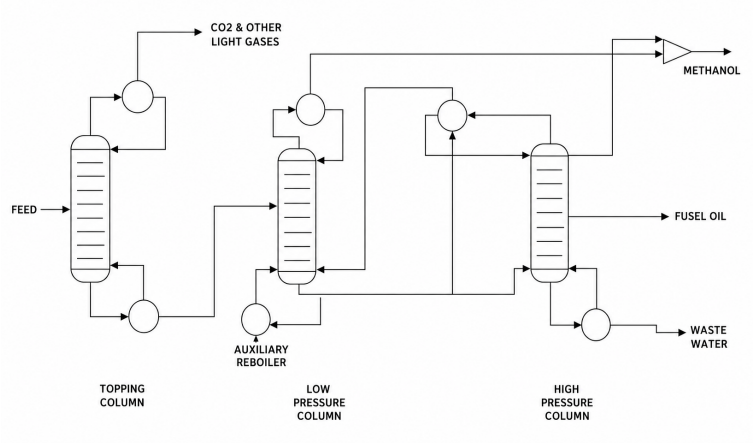

Figure 22: Three-Column Conventional distillation (Base case 02)

Similarly, base case 2 was also designed, and the key process parameters and design specifications are presented in Table 20. The heating and cooling duties for the columns for 100% nominal feed capacity are included in Table 21.

Table 20: Specifications of distillation columns.

Column	Condenser Pressure bar(a)	No. of stages	Diameter (m)	Height (m)
Topping	1.5	40	1.2	28
Low Pressure	1.013	72	2.5	51
High Pressure	9	62	1.8	44

Table 21: Condenser and reboiler duties for distillation columns.

Column	Condenser Duty (MW)	Reboiler Duty (MW)
Topping Column	1.99	2.70
Low Pressure	11.10	11.15
High Pressure	8.43	8.5

4.2.3 Turn-Down Ratio

Both the reference Base Case distillation processes are designed for a turndown ratio of 60% of the nominal feed capacity, as shown in Figure 23. As the nominal feed

capacity decreases from 100% to 60%, the reboiler heat duty for both base cases decreases approximately linearly, and below 60% of nominal capacity, the hydraulics of the columns fail, and in order to maintain stable operation, internal recirculation must be increased by increasing the reflux ratio, while keeping the reboiler duty constant at the 60% nominal load level. This operating strategy ensures continued separation performance under part-load conditions, despite reduced feed throughput.

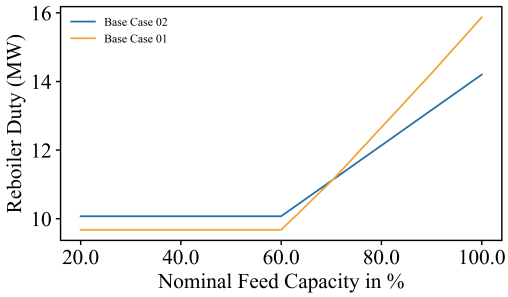

Figure 23: Variable feed-capacity effects on Base case 01 and 02 steam cumulative heat-duty (Low pressure and medium pressure) consumption.

4.3 Crude Methanol Feed Variability

The production of crude e-methanol depends on intermittent renewable electricity supplied through wind- and solar-based power purchase agreements (PPAs). Because these contracts do not guarantee a constant electricity supply, the crude methanol flow rate to the downstream distillation process fluctuates over time. The corresponding 2025 data for two separate markets, South America and the Nordics, are presented in Figure 24.

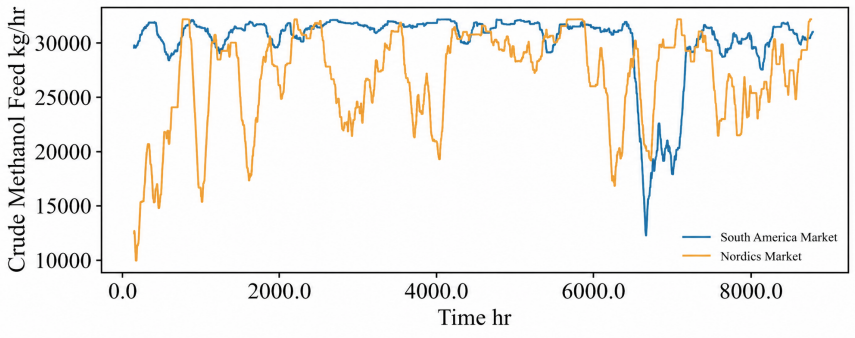

Figure 24: Feed fluctuation comparison for South American and Nordic electricity markets for the year 2025 (Weekly moving average).

The South American electricity market is relatively stable, resulting in a consistently high crude methanol supply, whereas the more variable Nordic electricity market leads to greater feed fluctuations, with the crude methanol supply exceeding 80% of nominal capacity for only 73% of the operating time, as shown in Table 22.

Table 22: Available nominal feed capacity per hour for the Nordics and South America.

Nominal Feed Available in %	Nordics (hr)	South America (hr)
100 – 90	6223	7633
90 – 80	188	230
80 – 70	190	118
70 – 60	344	282
Less than 60	1815	521

4.3.1 Problem Statement

The distillation column has a minimum stable turndown of 60% of nameplate capacity and can handle only a 5% change in feed mass flow rate per hour without changing internal vapor-liquid traffic or product quality. In contrast, the electrolyzer and synthesis loop can ramp up or down by 66.5% of capacity per hour subsection 3.2.

For example, if the upstream feed drops from 100% to 60% in one hour, the column needs approximately eight hours to reach 60% because of the 5% per hour ramp-rate limitation. This mismatch between rapid upstream changes and the slower response of the distillation column creates the need for an intermediate buffer to absorb the difference during transient operation.

To maintain stable operation and product quality under variable feed conditions, three buffering strategies are evaluated: intermediate storage, product recycling, and a hybrid combination of both. These are the three alternatives considered in the optimization framework presented in the thesis.

Because the required buffering depends not only on the magnitude of the feed fluctuations but also on their duration and sequence over time, a dynamic optimization model is required. The model uses hourly crude methanol production data over the full annual operating horizon (8,760 h) together with discrete Aspen Plus performance data for the distillation system, as shown in Figure 25.

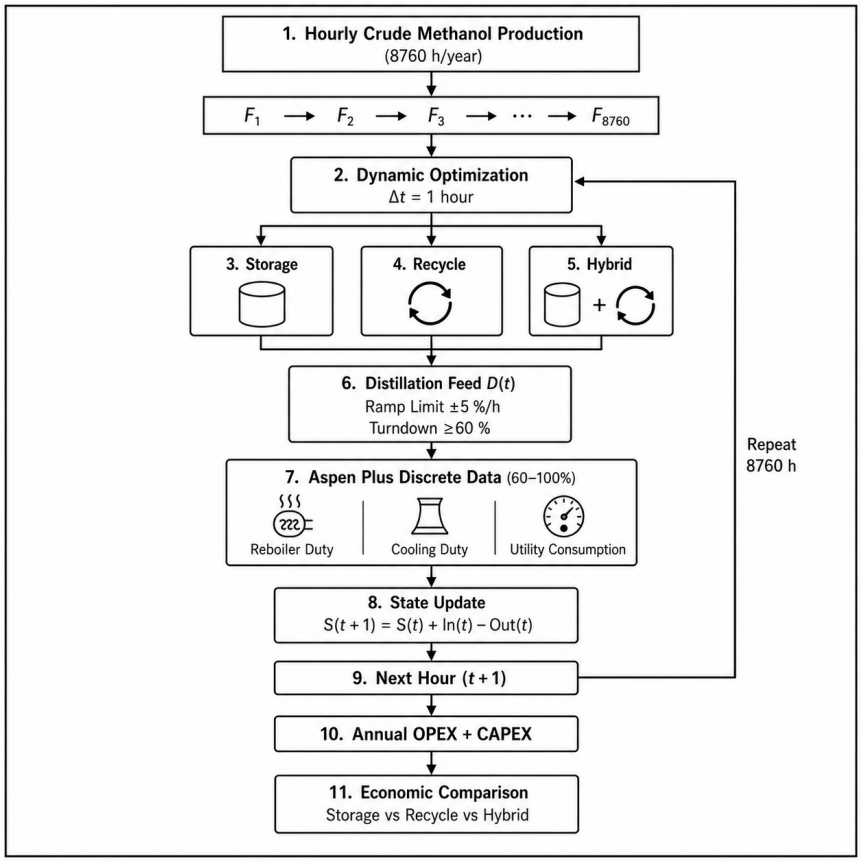

Figure 25: Dynamic optimization framework for evaluating storage, recycle, and hybrid buffering strategies under hourly crude methanol production variability

At each hourly time step, as illustrated by Figure 25, the model determines the distillation throughput, storage inventory, recycle flow, and corresponding utility consumption while satisfying mass-balance, ramp-rate, turndown, storage-capacity, and utility-availability constraints. The state of the buffering system is carried forward from one hour to the next, thereby linking consecutive operating periods and capturing the effect of upstream variability on downstream distillation operation.

Finally, the hourly utility consumption and operating requirements are aggregated to determine the annual OPEX, while the required buffering capacity is used to determine the annualized CAPEX. The total annualized cost therefore provides a common economic basis for comparing the storage-only, product-recycling, and hybrid buffering strategies. The methodology for each individual buffering strategy is discussed in detail in the following section.

4.3.2 Optimization Modeling Approach

The three buffering strategies in the following sections are each formulated as a mathematical optimization problem, implemented in Python using PuLP [70] with the open-source CBC (COIN-OR Branch-and-Cut) solver. All three are solved to deliver the same total methanol production over the one-year horizon — that's what keeps

them comparable. Any cost difference you see is down to the buffering mechanism, not throughput. Capital cost of any installed equipment, particularly storage tanks, is annualized using the capital recovery factor (CRF), allowing CAPEX-intensive and OPEX-intensive solutions to be compared on an equivalent annual basis.

The optimization framework was selected because the governing mass-balance, ramp-rate, storage-capacity, and utility constraints can be expressed as linear equations and inequalities. Furthermore, the utility demand and steam availability data obtained from Aspen Plus are either linear or nearly convex over the operating range considered. Consequently, the problem is well suited to a Linear Programming (LPro) formulation. The remaining non-linear utility relationships are represented using SOS2 piecewise-linear interpolation, providing an accurate approximation while preserving the linear structure of the model. This enables the use of the CBC solver, which guarantees globally optimal solutions for LP and MILP formulations and remains computationally efficient for the full 8760-hour optimization horizon. Alternative nonlinear formulations (NLP/MINLP) were not adopted because they would increase computational complexity without providing significant accuracy improvements for the nearly convex datasets considered in this study. The optimization terminologies used throughout the analysis are described as follows:

- **Linear Programming (LPro)**: It minimizes or maximizes a linear objective function subject to linear equality and inequality constraints, with all decision variables treated as continuous. The intermediate storage and product recycling models have mostly continuous and linear decision variables (distillation rate, storage inventory, recycle flow, and purchased steam). All the non-linear terms are linearized exactly through pairs of inequalities, so the problems remain fully linear.

- **Mixed-Integer Linear Programming (MILP)**: It is an LPro that additionally contains integer (here binary, $\{0, 1\}$) decision variables, which allow the model to make discrete yes/no design choices. The hybrid model is a MILP because it uses the binaries z_{storage} and z_{recycle} to decide whether a storage tank and/or a recycle line is installed at all; CBC then solves the problem by branch-and-cut over these binaries.

- **Piecewise-linear Interpolation (SOS2)**: Reboiler duty, condenser duty, and steam availability from Aspen Plus vary non-linearly with throughput. Over the operating range, they're mildly curved but nearly convex. To fit these curves into a linear model, they're represented as a piecewise-linear interpolation using a Special Ordered Set of type 2 (SOS2): non-negative weights, at most two non-zero, and if two are non-zero, they have to be adjacent. Requiring the weights to sum to one and reconstruct D_t puts the throughput on the straight segment between two neighboring breakpoints, and every duty gets interpolated on that same segment. Since the underlying data are close to convex, this reproduces the tabulated curves faithfully while keeping the models solvable as LPs and MILPs.

- **Alternative solution approaches**: The same optimization problem could instead be handled in a couple of other ways. One is fitting a single regression trend-line to each utility curve and passing its coefficients directly to the model — the simplest option, and exact where a curve is genuinely linear, but it smooths over any real curvature. The other is formulating the problem as a nonlinear program (NLP) or mixed-integer nonlinear program (MINLP) that carries the curved functions explicitly, at the cost of possible local optima in non-convex regions and the need for more specialized solvers.

Given that the present data are almost convex, the LP/MILP formulation with SOS2 interpolation was chosen because it guarantees a global optimum, solves quickly for the full 8760-hour horizon, and runs on an open-source CBC solver.

4.3.3 Intermediate Storage Tank Model

The first strategy considered for decoupling the distillation column from upstream feed fluctuations is the use of an intermediate storage tank, as illustrated in Figure 26. The storage tank acts as a buffer by allowing the distillation feed rate, D_t, to differ from and accommodate variations in the incoming feed flow rate, F_t, at each time step through changes in the tank inventory, S_t. The blue line in Figure 26 indicates that the crude methanol feed can bypass the storage tank when no buffering is required, which will avoid additional pumping costs to withdraw that same feed from storage.

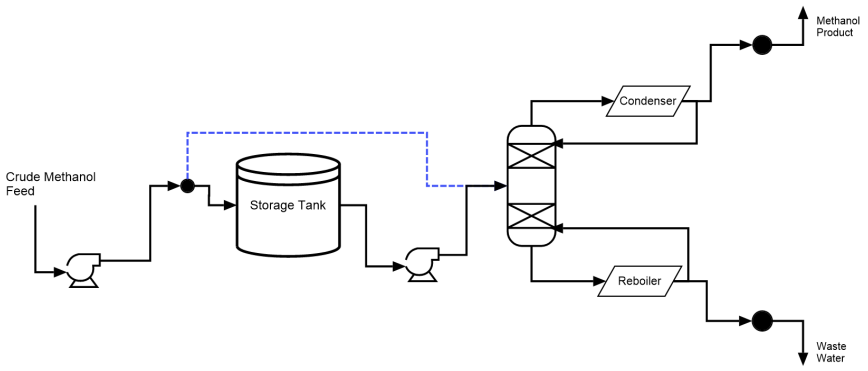

Figure 26: Conceptual Schematic of the Intermediate Storage Tank.

The workflow starts from the 2025 crude methanol feed profile, (F_t), which serves as the primary input to a linear programming model of the storage tank. This model is constrained by mass balance, distillation ramp-rate limits, and the column turndown ratio. Solving it provides the optimal distillation feed profile, (D_t), along with the required initial storage inventory, (S_i). The resulting distillation feed profile is then combined, in a post-processing step, with the distillation heat demand obtained from Aspen Plus (over the 60–100% capacity range) and the synthesis loop heat availability (over the 20–100% capacity range). Piecewise interpolation is used to calculate the corresponding utility demands and any shortfall that must be covered by purchased

steam. The outcome of this post-processing step is the minimum annual cost of distillation.

As introduced in subsubsection 4.3.2, the storage model is solved as a linear program first, and utility costs are interpolated only afterward. This ordering matters because the storage tank has to be sized before its operating cost can even be evaluated — in the initial hours, the tank is accumulating crude methanol to build up the inventory that will buffer later feed swings. The linear program finds this initial capacity together with the smoothed distillation feed profile, which tracks the incoming feed within the 5% per hour ramp limit.

With that feed profile fixed, the per-hour distillation rate is just matched to the corresponding utilities to get the operating cost. No accuracy is lost by doing it this way rather than solving the interpolation inside the optimization itself, since the utility curves are almost convex.

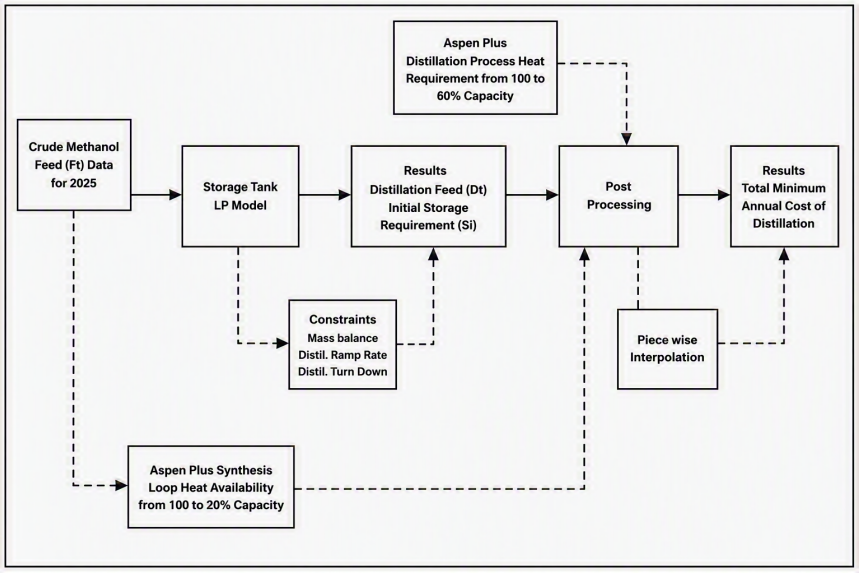

Figure 27: Workflow of the Intermediate Storage Tank Optimization Model. The model is attached in *Appendix* subsubsection 7.2.1 and subsubsection 7.2.2

The storage system is formulated as an optimization problem Equation (21), where the objective is to minimize the total annual cost of operating the storage system over the optimization horizon (T). The objective function consists of two components: (i) the operating cost, which includes the storage cost $c_s S_t$ and the pumping cost $c_p P_t$, summed over all time steps, and (ii) the capital cost of the storage tank.

The mass balance constraints are applied to the storage level from hour to hour as a function of the incoming feed and the outgoing distillation feed, with the initial inventory level given by S_{init} for the first hour or the storage level of the previous hour $S_{\text{t}-1}$ at each hour S_{t}. The tank level is constrained not to exceed the maximum storage capacity $S_{\max}$, which is a decision variable and is calculated by the model as the minimum tank size required to buffer the anticipated feed fluctuations at minimum total cost.

The distillation feed mass flow rate, D_{t}, is bounded between a minimum turndown level,$D_{\min}$, and the maximum nominal feed capacity, $D_{\max}$. Also, the rate of change in D_{t} between two consecutive hours is constrained to the maximum ramp rate of 5% of $D_{\max}$ per hour. This ramp-rate constraint directly couples the storage model to the column's dynamic limits: even with very large storage capacity, the column cannot change its throughput faster than this bound, so the tank must be sized to absorb feed fluctuations over the entire duration required for the column to ramp between operating points. Pumping cost P_{t} is the cost for anything being pumped into or out of the storage tank, and that is given by the absolute change in tank inventory between consecutive hours. All the constraints are collectively represented in Equation (21).

$$
\begin{aligned}
\min \quad & \sum_{t=0}^{T-1} (c_s S_t + c_p P_t) + \frac{2c_{\mathrm{cap}}}{\rho} S_{\max} \\
\text{s.t.} \quad & \begin{cases}
S_0 = S_{\mathrm{init}} + F_0 - D_0, & \\
S_t = S_{t-1} + F_t - D_t, & t = 1, \ldots, T-1, \\
S_t \le S_{\max}, & \forall t, \\
D_t \le F_t + S_t, & \forall t, \\
|D_t - D_{t-1}| \le R_{\max}, & t = 1, \ldots, T-1, \\
P_t \ge |S_t - S_{t-1}|, & t = 1, \ldots, T-1, \\
P_0 = 0, & \\
D_{\min} \le D_t \le D_{\max}, & \forall t, \\
S_t,\ P_t,\ S_{\max} \ge 0. &
\end{cases}
\end{aligned}
\tag{21}
$$

Here, D_t — Distillation rate (kg/h), F_t — Crude methanol Feed rate (kg/h), S_t — Storage inventory (kg), P_t — Pumping Cost (kg/h), $S_{\max}$ — Maximum storage capacity (kg), S_{init} — Initial storage inventory, T — Number of hours, $R_{\max}$ — Maximum ramp rate ($0.05D_{\max}$), $D_{\max}$ — Maximum distillation rate ($\max(F_t)$), $D_{\min}$ — Minimum distillation rate, c_s — Storage cost, c_p — Pumping cost, c_{cap} — Tank capital cost, and ρ — crude methanol liquid density.

Afterward, **post-processing** is performed as shown in figure (27), since the reboiler duty and condenser cooling duty depend on, and are functions of, D_t; these duties are then evaluated over the full year and represented by Equations (22), (23), and (24). At the same time, the steam generated in the synthesis loop, which is used in the distillation process and is a function of F_t which is represented by Equations (25) and (26), is accounted for at each hour by calculating the amount of steam that must be purchased as the difference between the required steam and the steam available from the synthesis loop which is represented by Equations (27) and (28).

$$C_t^{\text{cool}} = f_{\text{cool}}(D_t), \tag{22}$$
$$LP_t^{\text{req}} = f_{\text{LP}}(D_t), \tag{23}$$
$$MP_t^{\text{req}} = f_{\text{MP}}(D_t), \tag{24}$$
$$LP_t^{\text{avail}} = f_{\text{LP}}(F_t), \tag{25}$$
$$MP_t^{\text{avail}} = f_{\text{MP}}(F_t), \tag{26}$$
$$LP_t^{\text{buy}} = \max\left(LP_t^{\text{req}} - LP_t^{\text{avail}}, 0\right), \tag{27}$$
$$MP_t^{\text{buy}} = \max\left(MP_t^{\text{req}} - MP_t^{\text{avail}}, 0\right). \tag{28}$$

Here, C_t^{cool} — Cooling cost, LP_t^{req} — LP steam requirement, MP_t^{req} — MP steam requirement, LP_t^{avail} — Available LP steam, MP_t^{avail} — Available MP steam, LP_t^{buy} — Purchased LP steam, MP_t^{buy} — Purchased MP steam, $f_{\text{cool}}(\cdot)$ — Cooling cost interpolation, $f_{\text{LP}}(\cdot)$ — LP steam requirement interpolation, $f_{\text{MP}}(\cdot)$ — MP steam requirement interpolation, $f_{\text{LP}}(\cdot)$ — LP steam availability interpolation, $f_{\text{MP}}(\cdot)$ — MP steam availability interpolation, i — Interest rate, n — Project lifetime, and CRF — Capital recovery factor.

Finally, all costs are added to obtain the overall cost of the distillation system with a storage tank represented by Equation (29); here c_{LP} is the cost of low-pressure steam, and c_{MP} is the cost of medium-pressure steam. Capital investment c_{cap} is converted into an annualized cost using the capital recovery factor (CRF), allowing direct comparison with the annual costs of other models, which do not have such high CAPEX. This provides a consistent techno-economic basis for determining the optimal annual storage cost in comparison with other buffering options.

$$C_{\text{annual}} = c_s \sum_{t=0}^{T-1} S_t + c_p \sum_{t=0}^{T-1} P_t + \sum_{t=0}^{T-1} C_t^{\text{cool}} + c_{\text{LP}} \sum_{t=0}^{T-1} LP_t^{\text{buy}} + c_{\text{MP}} \sum_{t=0}^{T-1} MP_t^{\text{buy}} + \text{CRF}(\text{CAPEX}_{\text{Storage}}). \tag{29}$$

4.3.4 Product Recycling Model

An alternative strategy for handling feed fluctuations is shown in Figure 28. It decouples upstream feed fluctuations by mixing the variable feed with the recycled stream, which contains a portion of product and wastewater, before the distillation column. The technical reasoning for this alternate design is included in subsubsection 2.7.1. By adjusting the recycle flow rates, the crude methanol feed variations are absorbed while ensuring that the column operates within its ramp rate and turndown constraints.

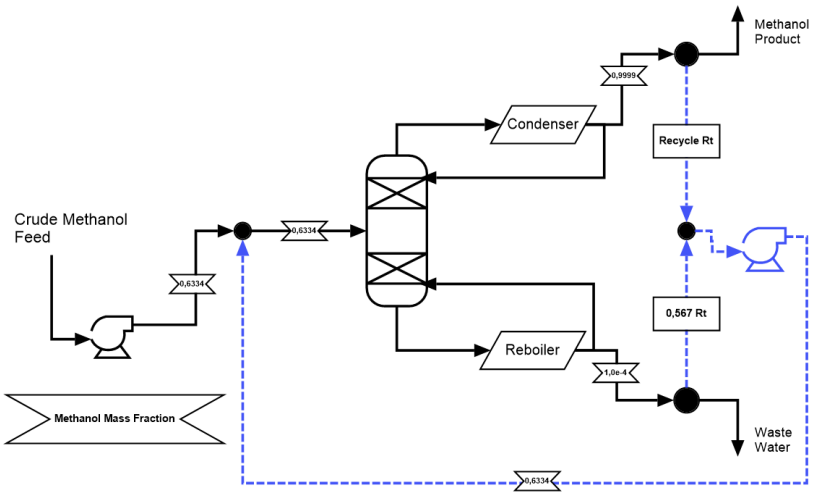

Figure 28: Conceptual Schematic of the product recycling Model.

The influence of feed composition changes on column behavior is complex, and a detailed dynamic analysis is beyond the scope of this thesis. Research [15] indicates that a 10% change in feed composition typically requires approximately 4–6 hours for the column to return to steady state and the same product purity. For simplicity, in this work, the composition of the feed in the recycling model is maintained using the rate at which wastewater is mixed with the methanol product. The amount at which wastewater is added to the methanol product to maintain the composition of the outgoing stream equal to the feed composition is calculated to be 0.578 times the recycle methanol product at any given time t. Mass and component balance for methanol is given by (30), and (31)

$$D_t = F_t + R_t + \alpha_t \tag{30}$$

$$x_D D_t = x_F F_t + x_R R_t + x_W \alpha_t. \tag{31}$$

Putting methanol mass fraction values in Equation (31) from Figure 28. The term $x_W \alpha_t$ is eliminated since x_W is 0.

$$0.6334\, D_t = 0.6334\, F_t + 0.99995\, R_t. \tag{32}$$

Putting Equation (30) into Equation (32). The term α_t, which is the amount of water that needs to be added to the methanol product at any time t is calculated.

$$0.6334\,(F_t + R_t + \alpha_t) = 0.6334\, F_t + 0.99995\, R_t. \tag{33}$$

$$\alpha_t = \frac{0.99995 - 0.6334}{0.6334} R_t = 0.57\, R_t. \tag{34}$$

In this model, the total distillation rate, D_t, is defined as the sum of the actual feed rate, F_t, and the recycle stream, R_t, adjusted by a factor $(1 + \alpha)$ to account for the water content introduced by the recycle stream, where α represents the recycle water-to-methanol ratio found out in Equation (34). Similarly, this model uses the same turn-down ratio and ramp rate constraints as in the storage model, since the

physical hydraulic and thermal limitations of the column remain unchanged regardless of whether the additional throughput originates from storage or recycle.

Unlike the storage model, the recycling model needs no initial inventory buildup — feed variability gets absorbed instantaneously by the recycle stream instead of accumulating over time. Utility relationships are interpolated directly inside the optimization, using the SOS2 piecewise-linear formulation from subsubsection 4.3.2.

The objective function minimizes the sum of the recycle pumping cost, $c_R(1-\alpha)R_t$, together with other utilities computed in a similar way as in the storage model. Because recycling avoids the need for a storage tank, this model does not have a CAPEX term included in the objective function; however, it introduces an operating cost penalty associated with redistilling the product that has already been purified by the column once. Therefore, the comparison between this strategy and the intermediate storage depends on the trade-off between avoided CAPEX and increased OPEX due to increased utility usage.

The objective function, along with all the constraints, is represented in Equation (35).

$$
\begin{aligned}
\min \quad & \sum_{t=0}^{T-1} \left(c_R(1-\alpha)R_t + C_t^{\text{cool}} + c_{\text{LP}} L_t^{\text{buy}} + c_{\text{MP}} M_t^{\text{buy}} \right) \\
\text{s.t.} \quad & \begin{cases}
D_t = F_t + (1+\alpha)R_t, & \forall t, \\
D_{\min} \le D_t \le D_{\max}, & \forall t, \\
|D_t - D_{t-1}| \le R_{\max}, & t = 1, \ldots, T-1, \\
C_t^{\text{cool}} = f_{\text{cool}}(D_t), & \forall t, \\
LP_t^{\text{req}} = f_{\text{LP}}(D_t), & \forall t, \\
MP_t^{\text{req}} = f_{\text{MP}}(D_t), & \forall t, \\
LP_t^{\text{avail}} = f_{\text{LP}}(F_t), & \forall t, \\
MP_t^{\text{avail}} = f_{\text{MP}}(F_t), & \forall t, \\
LP_t^{\text{buy}} \ge LP_t^{\text{req}} - LP_t^{\text{avail}}, & \forall t, \\
MP_t^{\text{buy}} \ge MP_t^{\text{req}} - MP_t^{\text{avail}}, & \forall t, \\
R_t,\ LP_t^{\text{buy}},\ MP_t^{\text{buy}} \ge 0.
\end{cases}
\end{aligned}
\tag{35}
$$

Here, R_t is the recycled methanol flow rate (kg/h), α is the recycle water-to-methanol ratio, and c_R is the recycle pumping cost. The model is attached in *Appendix* subsubsection 7.2.3.

4.3.5 Hybrid Model

The final model combines both intermediate storage and product recycling into a single hybrid model, as shown in Figure Figure 29, allowing the optimization to provide the optimal size of the storage tank together with product recycling in a way that reduces the overall cost of the distillation operation for the whole year.

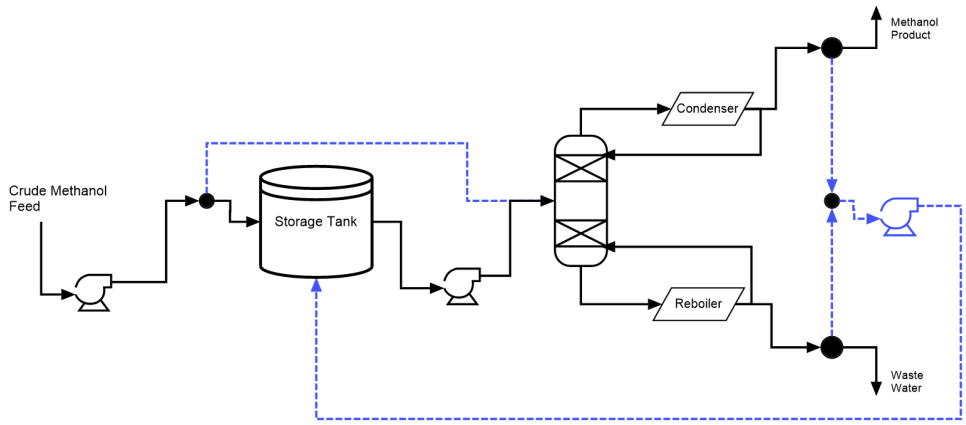

Figure 29: Conceptual Schematic of the Hybrid (Storage + Recycling) Model.

The optimization model flowchart, as shown in Figure 30, takes the 2025 crude methanol feed profile, synthesis loop heat availability, distillation utility requirements across the operating range, and the relevant cost parameters as inputs. It uses mixed-integer optimization to minimize the total annual distillation cost. At the same time, it decides whether to activate recycling and/or storage using binary variables, along with a set of continuous decision variables like the distillation mass flow rate, recycle flow, storage inventory, and purchased steam utilities, which are further constrained by mass balance, ramp rate, and turndown ratio.

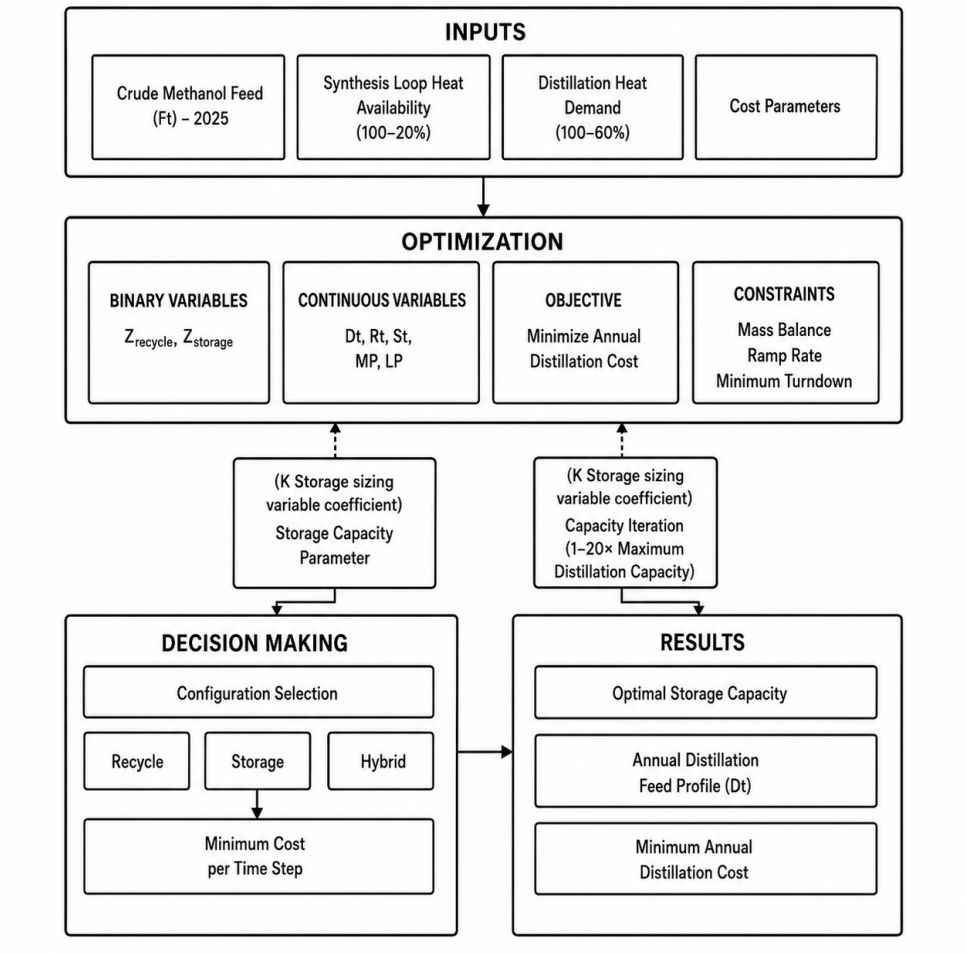

Figure 30: Workflow of the Hybrid Optimization Model.

Storage tank size is governed by a variable coefficient, K, which scales the storage capacity used in each simulation run. Each unit of K corresponds to a fixed capacity step ($K = 1$ corresponds to 32 tons), so storage size scales linearly with K. The simulation varies K from 1 to 30 in discrete steps, rerunning the full system model for each value.

At each K, the total cost is calculated as the sum of three components: the heating and cooling duty required for distillation, the annualized capital cost of the storage tank, and the pumping cost associated with the buffering strategy. As K increases, this cost is tracked to identify the point of diminishing returns. Beyond a certain tank size, additional capacity no longer reduces operating cost enough to offset its added capital and pumping expense. This lets the simulation size the optimal storage tank, based on a cost trade-off between storage investment and operational savings, rather than fixing or assuming a storage capacity in advance.

The mass balance in the hybrid model considers both storage and recycle stream $(1 + \alpha)R_t$ formulation as an additional inflow to the tank alongside the feed, F_t, and outflow, D_t. This reflects a configuration in which recycled product can be put back into the storage tank rather than directly into the column feed, providing additional

operational flexibility. Similarly, like previous models, the hybrid model has the same ramp rate and turn-down ratio constraints, along with other feasibility constraints,

To determine whether storage, recycling, or both should be installed, and to switch any of them on or off at any given time t, the model introduces two binary decision variables, z_{storage} and z_{recycle}. The recycle flow, R_t, is constrained to zero unless $z_{\text{recycle}} = 1$, and similarly the storage outflow, S_t, is forced to zero unless $z_{\text{storage}} = 1$, enforced via the K, variable coefficient. The constraint $z_{\text{recirc}} + z_{\text{storage}} \geq 1$ ensures that at least one of the two strategies must be selected, since some mechanism for absorbing feed variability is required; the optimization is otherwise free to select either strategy individually or both in combination, whichever yields the lowest total annualized cost. The objective function therefore combines the annualized CAPEX of storage, the OPEX of both storage (holding and pumping) and recycling (pumping and reprocessing), and the associated utility costs, providing a unified techno-economic framework for identifying the optimal feed-fluctuation mitigation strategy.

As in the recycling model, the utility curves are interpolated inside the optimization through the SOS2 piecewise-linear formulation of subsubsection 4.3.2 here as well, and the two binary variables make the hybrid model a mixed-integer linear program rather than a pure LP.

The objective function, along with all the constraints for the hybrid model, is included in Equation (36).

$$
\begin{aligned}
\min \quad & \sum_{t=0}^{T-1} \left(c_R(1+\alpha)R_t + c_p P_t + c_s S_t + C_t^{\text{cool}} + c_{\text{LP}} LP_t^{\text{buy}} + c_{\text{MP}} MP_t^{\text{buy}} \right) + \text{CRF} \frac{2c_{\text{cap}}}{\rho} S_{\max} \\
\text{s.t.} \quad & \begin{cases}
S_0 = S_{\text{init}} + F_0 - D_0 + (1+\alpha)R_0, & \\
S_t = S_{t-1} + F_t - D_t + (1+\alpha)R_t, & t = 1, \ldots, T-1, \\
D_{\min} \le D_t \le D_{\max}, & \forall t, \\
|D_t - D_{t-1}| \le R_{\max}, & t = 1, \ldots, T-1, \\
S_t \le S_{\max}, & \forall t, \\
R_t \le z_{\text{recyclr}}, & \forall t, \\
S_{\max} \le K z_{\text{storage}}, & \\
z_{\text{recirc}} + z_{\text{storage}} \ge 1, & \\
P_t \ge S_t - S_{t-1}, & t = 1, \ldots, T-1, \\
P_t \ge S_{t-1} - S_t, & t = 1, \ldots, T-1, \\
P_0 = 0, & \\
C_t^{\text{cool}} = f_{\text{cool}}(D_t), & \forall t, \\
LP_t^{\text{req}} = f_{\text{LP}}(D_t), & \forall t, \\
MP_t^{\text{req}} = f_{\text{MP}}(D_t), & \forall t, \\
LP_t^{\text{avail}} = f_{\text{LP}}(F_t), & \forall t, \\
MP_t^{\text{avail}} = f_{\text{MP}}(F_t), & \forall t, \\
LP_t^{\text{buy}} \ge LP_t^{\text{req}} - LP_t^{\text{avail}}, & \forall t, \\
MP_t^{\text{buy}} \ge MP_t^{\text{req}} - MP_t^{\text{avail}}, & \forall t, \\
R_t,\ P_t,\ S_t,\ LP_t^{\text{buy}},\ MP_t^{\text{buy}} \ge 0, & \\
z_{\text{recycle}},\ z_{\text{storage}} \in \{0, 1\}. &
\end{cases}
\end{aligned}
\tag{36}
$$

Here, K is a variable coefficient for the storage tank size, z_{recycle} is the binary symbol of product recycling, and z_{storage} is the binary symbol of storage. The model is attached in *Appendix* subsubsection 7.2.4.

4.4 Heat Pump Modeling

The crude methanol leaving the synthesis reactor is purified in a two-column sequence: an atmospheric column at 1.013 bar(a) removes the light gases, and a vacuum column operating at 0.3 bar(a) produces the final methanol product at 99.99 wt% purity, as shown in Figure 31. Waste heat from the alkaline electrolyzer is available as hot water at 85 °C and 480 kg/s, corresponding to a maximum recoverable duty of 72–74 MW, and is returned to the electrolyzer loop at 50 °C. Since the reboiler duty is limited by the source temperature rather than the available heat quantity, the electrolyzer waste heat can cover only 10 MW of the total 22.5 MW duty at 100% nameplate capacity.

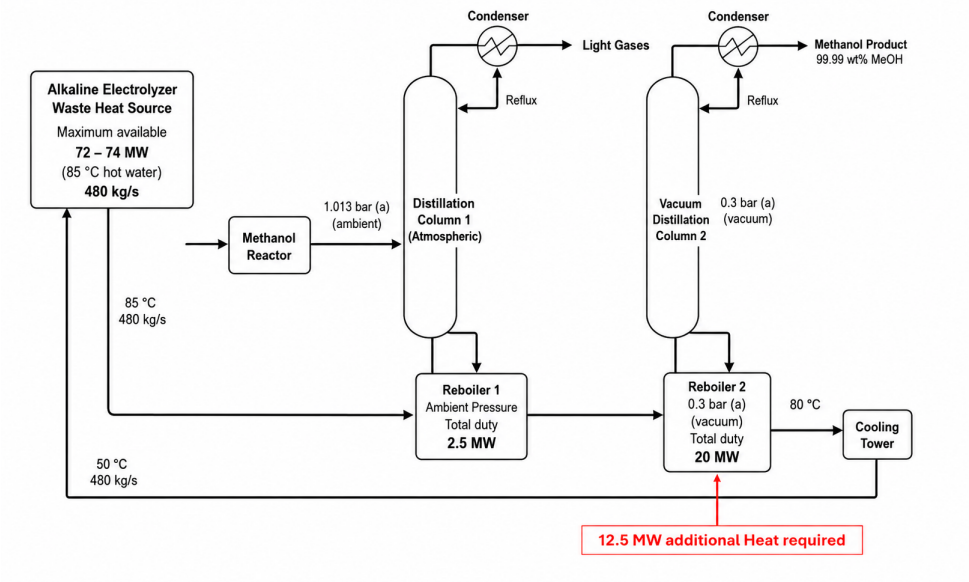

Figure 31: Schematic of the vacuum distillation reboiler duty requirement.

The remaining 12.5 MW reboiler duty in Figure 31 is supplied by a closed-loop compression heat pump that upgrades the electrolyzer cooling water to the temperature required by the vacuum-column reboiler. The cooling water leaves the electrolyzer at 85 °C and first passes through a heat exchanger, where it transfers heat to the isothermal reboiler at 75 °C with a minimum approach of 5 K, cooling to 80 °C. The remaining sensible heat between 80 °C and 61.5 °C (see subsubsection 4.4.1) serves as the heat-pump source. As shown in Figure 32, refrigerant evaporates at 50 °C and 23.39 bar(a) with a 10 K approach, is compressed to 44.56 bar(a), and condenses at 85 °C to supply the reboiler; the condensate is then expanded back to the evaporation pressure to close the loop. The evaporator outlet is trimmed to 50 °C in a cooling-water exchanger before returning to the electrolyzer, maintaining a constant return temperature independent of heat-pump load. The 10 K approach on both heat exchangers gives a 35 K temperature lift, which determines the compressor duty and the COP.

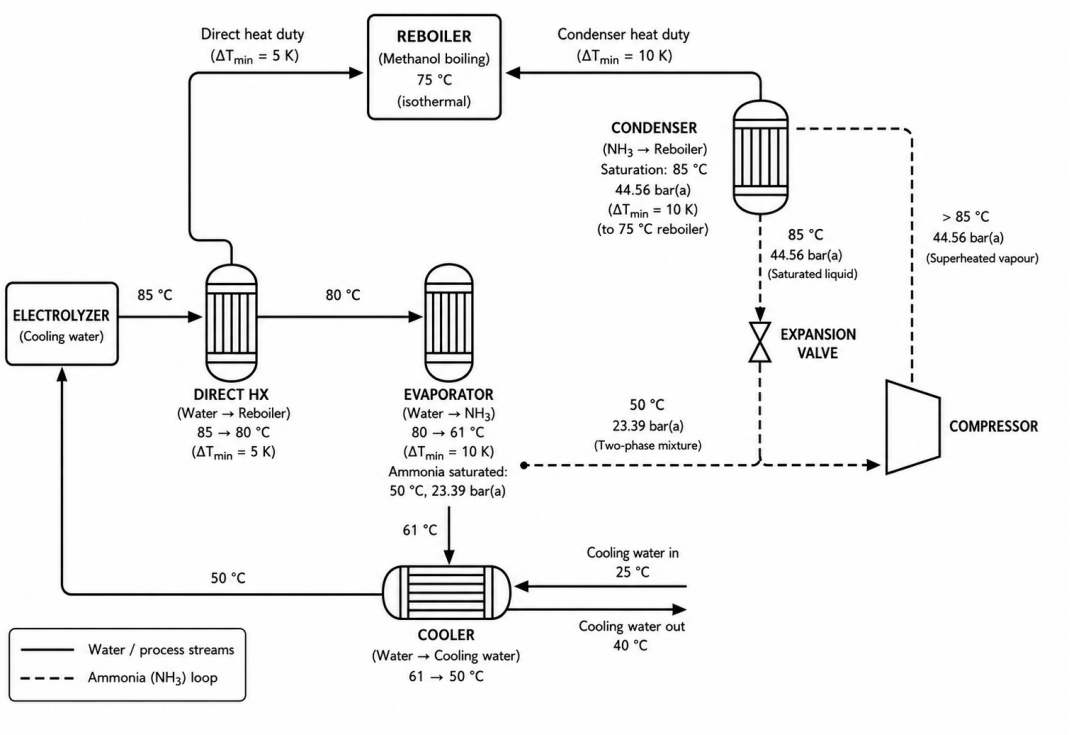

Figure 32: Schematic of the ammonia (R717) closed-loop compression heat pump used to upgrade low-grade electrolyzer waste heat to the temperature level required by the vacuum column reboiler

Here, ammonia was selected as the working fluid after comparison with R1233zd(E), R1336mzz(Z), and R1224yd(Z). Its critical temperature of 132.4 °C provides a comfortable margin above the 85 °C condensing temperature, and its zero global warming potential (GWP), zero ozone depletion potential (ODP), and favorable COP make it the most suitable candidate [71]. Although ammonia is classified as B2L (mildly toxic, low-flammability refrigerant), it is acceptable for the present industrial setting.

4.4.1 Electrolyzer Waste Heat Variability

The electrolyzer waste heat is not a constant source. Because hydrogen production follows hourly electricity prices and renewable availability, the electrolyzer operates over its full 100%–20% load range, and the recoverable waste heat varies accordingly between 71MW (483 kg/s) and 17 MW (116 kg/s). The heat pump must therefore be designed for this variation rather than for the nominal point alone. Since the water leaving the electrolyzer has a constant temperature of 85 °C, the reduction in available heat appears entirely as a reduction in mass flow. The temperature levels of the cycle are therefore preserved at all loads, and the operating envelope is defined by how the available water is split between the two streams shown in Figure 33 and Figure 34.

Figure 33 shows the mass and energy balance at 100% capacity. Of the 483 kg/s leaving the electrolyzer, the direct heat exchanger delivers 10.14 MW to the reboiler. The remaining 12.5 MW is supplied by the heat pump, which requires 9.85 MW at the

heat pump evaporator and 2.51 MW of compressor work. This evaporator duty is met by sensible cooling of the waste electrolyzer stream from 80 °C to 61.5 °C. However, only 126.7 kg/s is needed for this branch, so the remaining 356.3 kg/s bypasses the heat pump and is rejected as 44.89 MW of heat in the cooler parallel to the heat pump stream.

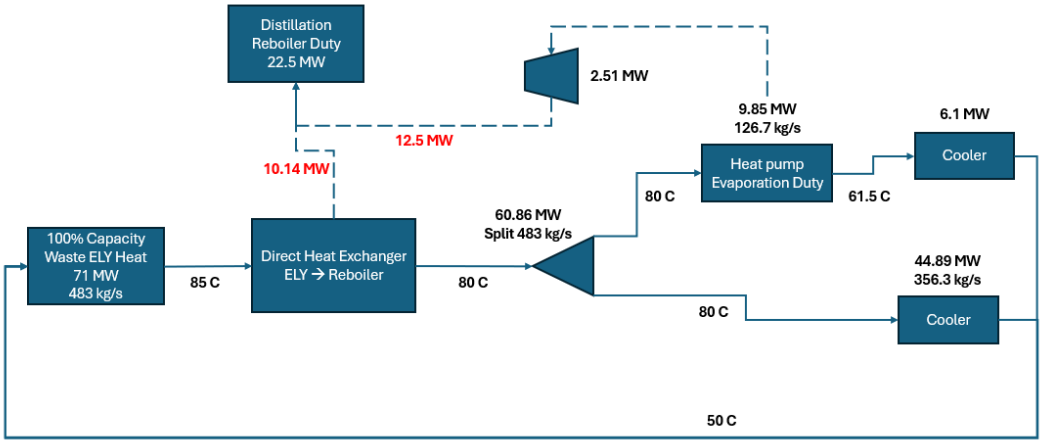

Figure 33: Mass and energy balance of the waste-heat recovery system at 100% electrolyzer capacity (71 MW, 483 kg/s), showing the direct heat-exchanger duty, the heat-pump branch, and the surplus flow rejected through the parallel cooler.

Figure 34 shows the same balance at the minimum electrolyzer load. With only 17 MW available at 116 kg/s, the direct heat exchanger delivers 2.4 MW, and the required reboiler duty falls to 13.7 MW, leaving 11.3 MW to be supplied by the heat pump at 9 MW evaporator duty and 2.3 MW of compressor work. At this operating point, the complete 116 kg/s electrolyzer cooling-water stream is required to meet the heat-pump evaporator duty over the 80 °C to 61.5 °C temperature range. This condition, therefore, defines the design limit of the integration. Above this point, the heat pump evaporator branch is fully utilized, and no flow goes through the other branch. Any further reduction in electrolyzer load would leave insufficient heat available to sustain the required evaporator duty, and the resulting shortfall would have to be covered by imported low-pressure steam.

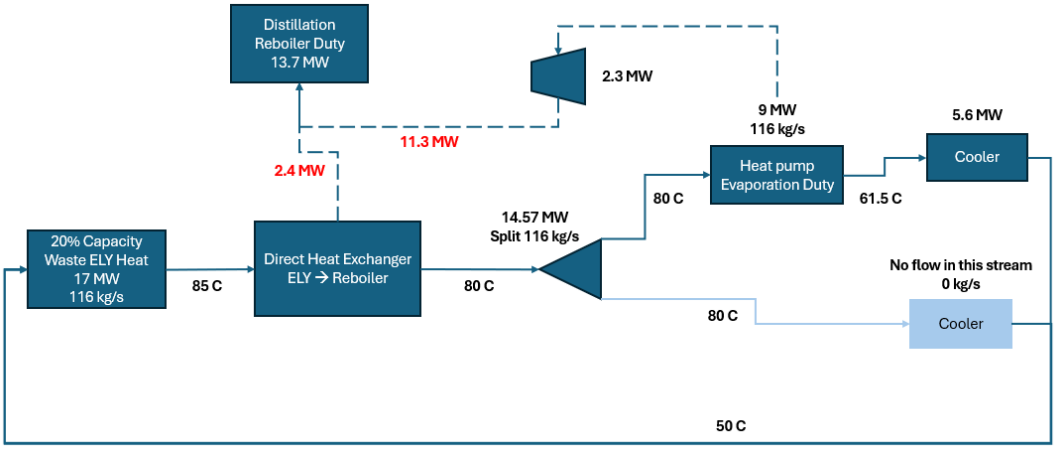

Figure 34: Mass and energy balance at the minimum electrolyzer load (17 MW, 116 kg/s), where the entire cooling-water stream is required by the heat-pump branch, and the bypass carries zero flow, defining the design limit of the integration.

Two design considerations are concluded from this analysis. First, the compressor is sized for the maximum heat-pump duty at full electrolyzer load, delivering 12.5 MW of heat with 2.51 MW of shaft work.

Second, the flow split is adjusted according to the electrolyzer load. By maintaining the evaporator outlet at 61.5 °C, the evaporating temperature and temperature lift remain constant. Consequently, the COP remains unchanged, allowing a single COP value to be applied throughout the hourly model.

4.4.2 Annual Dynamic Performance of the Heat Pump

The heat pump is evaluated on an hourly basis over a full year ($h = 1, \ldots, 8784$). The cycle parameters, including the condensing temperature, evaporating temperature, and temperature lift, are calculated using the relations given in subsubsection 2.8.1. These parameters are calculated once from the fixed process temperatures and held constant throughout the year. The applied COP is taken as the lower of the following two values:

$$\mathrm{COP} = \min\left(\eta\,\mathrm{COP}_{\mathrm{Carnot}},\ \mathrm{COP}_{\max}\right), \qquad \mathrm{COP}_{\mathrm{Carnot}} = \frac{T_{\mathrm{cond}}}{T_{\mathrm{cond}} - T_{\mathrm{evap}}} \tag{37}$$

Here η is the second-law (Carnot) efficiency and $\mathrm{COP}_{\max} = 5$ is the commercial ceiling (subsection 3.4). In practice, the ceiling does not bind: the derated Carnot value is 4.81, so the applied COP is thermodynamically determined, and the ceiling acts only as a dormant guard.

The electrolyzer duty in each hour is floored at a minimum fraction of its nominal capacity so that unrealistic shutdown states are not propagated into the economic analysis:

$$\dot{Q}_{\mathrm{ELY},h} = \max\left(\dot{Q}^{\mathrm{raw}}_{\mathrm{ELY},h},\ \dot{Q}_{\mathrm{fl}}\right), \qquad \dot{Q}_{\mathrm{fl}} = \phi\,\dot{Q}_{\mathrm{nom}} \tag{38}$$

Here $\dot{Q}_{\mathrm{ELY},h}$ is the hourly electrolyzer waste-heat duty after applying the minimum-load constraint, $\dot{Q}^{\mathrm{raw}}_{\mathrm{ELY},h}$ is the raw hourly waste-heat duty, $\dot{Q}_{\mathrm{fl}}$ is the minimum allowable heat duty, $\dot{Q}_{\mathrm{nom}}$ is the maximum hourly electrolyzer heat duty over the year, and ϕ is the minimum-load fraction, assumed to be 20% (see subsection 3.2).

Assuming constant $\dot{m}c_p$ over the cooling range, the fraction of the available electrolyzer heat above the direct-heat-exchanger cutoff temperature, T_{lim}, is transferred directly to the reboiler. The remaining reboiler duty is supplied by the heat pump:

$$\dot{Q}_{\mathrm{dir},h} = \min\left[\dot{Q}_{\mathrm{reb},h},\ \max\left(0,\ \dot{Q}_{\mathrm{ELY},h}\frac{T_{\mathrm{in}} - T_{\mathrm{lim}}}{T_{\mathrm{in}} - T_{\mathrm{out}}}\right)\right] \tag{39}$$

$$\dot{Q}_{\mathrm{HP},h} = \dot{Q}_{\mathrm{reb},h} - \dot{Q}_{\mathrm{dir},h} \tag{40}$$

Here $\dot{Q}_{\mathrm{reb},h}$ is the reboiler heat requirement in hour h, $\dot{Q}_{\mathrm{dir},h}$ is the heat supplied directly from the electrolyzer cooling stream, and $\dot{Q}_{\mathrm{HP},h}$ is the heat supplied by the heat-pump condenser. Here, T_{in} is the inlet temperature of the electrolyzer cooling stream, T_{out} is its target outlet temperature after heat recovery, and T_{lim} is the temperature at which direct heat recovery is terminated. The cutoff temperature is defined as

$$T_{\mathrm{lim}} = T_{\mathrm{reb}} + \Delta T_{\mathrm{d}} \tag{41}$$

where T_{reb} is the reboiler operating temperature and ΔT_{d} is the minimum temperature approach required in the direct heat exchanger.

The heat-pump duty is converted to electrical compressor work using the COP, while the evaporator duty is obtained from the first-law energy balance:

$$\dot{W}_h = \frac{\dot{Q}_{\mathrm{HP},h}}{\mathrm{COP}} \tag{42}$$

$$\dot{Q}_{\mathrm{evap},h} = \dot{Q}_{\mathrm{HP},h} - \dot{W}_h \tag{43}$$

where $\dot{W}_h$ is the compressor electrical power requirement and $\dot{Q}_{\mathrm{evap},h}$ is the heat absorbed by the heat-pump evaporator. Thus, the condenser supplies $\dot{Q}_{\mathrm{HP},h}$ to the reboiler, while the evaporator supplies the remaining heat required by the cycle. $\dot{Q}_{\mathrm{reb},h}$ is determined by rounding the available electrolyzer heat to the nearest integer MW and selecting the corresponding value from the discrete reboiler-duty table created using ASPEN PLUS simulations.

Since the evaporator draws heat from the T_{lim} to T_{src} section of the same electrolyzer cooling stream, the available heat is evaluated on an hourly basis:

$$\dot{Q}_{\mathrm{avail},h} = \dot{Q}_{\mathrm{ELY},h}\frac{T_{\mathrm{lim}} - T_{\mathrm{src}}}{T_{\mathrm{in}} - T_{\mathrm{out}}} \tag{44}$$

Here, $\dot{Q}_{\mathrm{avail},h}$ is the maximum heat that the evaporator can extract from this temperature range, and T_{src} is the minimum source-stream temperature considered for the recovery of the evaporator heat. The feasibility condition is expressed as

$$\mathrm{flag}_h = \begin{cases} \text{feasible}, & \dot{Q}_{\mathrm{evap},h} \le \dot{Q}_{\mathrm{avail},h} + \varepsilon \\ \text{infeasible}, & \dot{Q}_{\mathrm{evap},h} > \dot{Q}_{\mathrm{avail},h} + \varepsilon \end{cases} \tag{45}$$

where $\varepsilon = 10^{-3}$ is a numerical tolerance used to avoid false violations caused by rounding.

The hourly economics compare the electricity cost of operating the compressor with the value of the low-pressure steam displaced by the heat pump:

$$C_{\mathrm{el},h} = \dot{W}_h \, p_h \tag{46}$$

$$C_{\mathrm{st},h} = \dot{Q}_{\mathrm{HP},h} \, c_{\mathrm{st}} \tag{47}$$

$$S_h = C_{\mathrm{st},h} - C_{\mathrm{el},h} \tag{48}$$

where $C_{\mathrm{el},h}$ is the hourly compressor electricity cost, p_h is the hourly electricity price, $C_{\mathrm{st},h}$ is the avoided steam cost, c_{st} is the unit cost of displaced steam, and S_h is the resulting hourly saving. Only the heat-pump duty is credited with steam displacement because the heat supplied by the direct exchanger is available in both the baseline and heat-pump cases and therefore does not affect the comparison.

Finally, the hourly results are aggregated to annual values, the heat-pump equipment is sized according to the peak hourly duty, its CAPEX is estimated, and the annual operating cost with the heat pump is compared against the annual cost of supplying the same duty with steam:

$$E_{\mathrm{HP}} = \sum_h \dot{Q}_{\mathrm{HP},h}, \qquad W_{\mathrm{el}} = \sum_h \dot{W}_h \tag{49}$$

$$\dot{Q}_{\mathrm{peak}} = \max_h \dot{Q}_{\mathrm{HP},h} \tag{50}$$

$$\mathrm{CAPEX} = c_{\mathrm{spec}} \cdot 1000 \, (1 + m) \, \dot{Q}_{\mathrm{peak}} + A_{\mathrm{HX}} \tag{51}$$

$$\mathrm{OPEX}_{\mathrm{HP}} = \sum_h C_{\mathrm{el},h} = \sum_h \dot{W}_h \, p_h \tag{52}$$

$$\mathrm{OPEX}_{\mathrm{st}} = \sum_h C_{\mathrm{st},h} = \sum_h \dot{Q}_{\mathrm{HP},h} \, c_{\mathrm{st}} \tag{53}$$

$$S_{\mathrm{annual}} = \mathrm{OPEX}_{\mathrm{st}} - \mathrm{OPEX}_{\mathrm{HP}} \tag{54}$$

where E_{HP} is the annual heat supplied by the heat pump, W_{el} is the annual compressor electricity consumption, and $\dot{Q}_{\mathrm{peak}}$ is the maximum hourly heat-pump duty used to size the equipment. The parameter c_{spec} is the specific equipment cost, $m = 10\%$ is a design margin applied to the peak duty, and A_{HX} represents the heat-exchanger cost, together giving the heat pump CAPEX. $\mathrm{OPEX}_{\mathrm{HP}}$ is the annual electricity cost of operating the compressor, $\mathrm{OPEX}_{\mathrm{st}}$ is the annual cost of supplying the same heat duty with steam instead, and S_{annual} is the resulting annual operating-cost saving from using the heat pump.

Since each model row represents one hour, summation over the hourly heat duties and costs directly gives annual energy and cost values, provided that the hourly quantities are expressed consistently in MW and €/h, respectively. Detailed calculations for one hour are shown in *Appendix* subsection 7.3.

4.5 Techno-Economic Analysis

Vacuum distillation is compared with conventional distillation based on net present value (NPV), investment rate of return (IRR), and the levelized cost per ton of methanol produced (LCO-MeOH). The techno-economic analysis (TEA) depends on five key aspects: capital cost, operating cost, fixed operating cost, revenue, and methanol production, following the framework shown in Figure 35. The assumptions for TEA are listed in subsection 3.3.

Other than methanol distillation, the process includes an electrolyzer, a methanol synthesis loop producing approximately 20 tons of methanol per hour, CO_2 capture, and the necessary safety systems. These upstream units and safety systems are part of the CAPEX: a flare system for safe burning of excess vent gas, a fire system for detection and suppression of fires (due to highly flammable hydrogen and methanol), and a nitrogen system for inerting and purging during maintenance, shutdown, and start-up, as well as for blanketing the crude methanol storage tank. The costs of these units are outside the scope of this study, but their total cost, including installation, is treated as a constant fixed value for comparison.

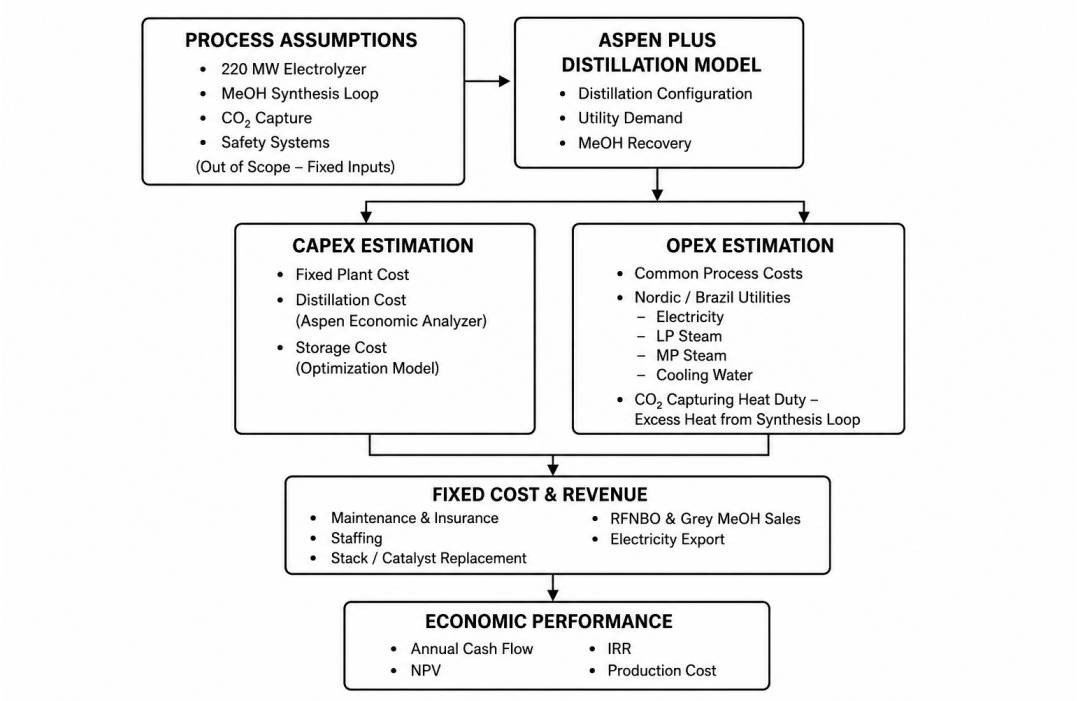

Figure 35: Framework for techno-economic analysis.

The capital cost for the methanol distillation process varies for each case and is computed using Aspen Economic Analyzer. A factor of 1.5 was applied to the calculated value to account for uncertainties and additional equipment costs not explicitly included in the estimation. The capital cost of storage is also included and depends on the optimization model discussed in subsection 4.3. The CAPEX and OPEX of the heat pump are also considered in the vacuum distillation case.

The TEA considers two markets, Nordic and South America, so the OPEX of the synthesis loop is different for both regions. The electrolyzer requires electricity, whose price depends on the region; therefore, electricity and transmission prices are treated separately for each market. In addition, the costs of CO_2 capture, distillation using low- or medium-pressure steam, and cooling water are individually evaluated. Thus, the OPEX is determined by combining the common process costs for both markets with the region-specific electricity, steam, and cooling costs, as illustrated in Figure 35. In the case of vacuum distillation, where the excess heat from the synthesis loop is not utilized in distillation, it is subtracted from the heat demand of the CO_2 capture system.

Total revenue is generated from RFNBO methanol, grey methanol, and surplus electricity sold to the grid. The annual fixed cost covers maintenance, insurance, personnel, replacement of the electrolyzer stack, and replacement of the methanol catalyst. In all cases, methanol production is obtained from Aspen simulations. Since the crude methanol availability differs between the two regions, methanol production is simulated for each region over the full year to determine the total annual production.

The CAPEX, OPEX, fixed costs, revenue, and methanol production terms are then used to analyze the economic performance in terms of NPV, IRR, and LCO-MEOH.

5 Results and Discussion

This section presents the simulation and techno-economic results for the two case-study locations, South America and the Nordics. For each site, the reboiler heat duty and heat-recovery performance of the conventional and vacuum distillation configurations are compared, the economics of heat-pump retrofit are evaluated against the local cost of steam, and the impact of three feed variability flexibility strategies (storage, product recycling, and a hybrid model) on operating cost is assessed. The two case studies are then compared directly to establish how local energy pricing shapes the relative attractiveness of heat-pump integration and vacuum operation.

5.1 Conventional Distillation

To evaluate how vacuum distillation performs economically compared to conventional distillation, it is first necessary to establish a fair basis for comparison against the best available conventional alternative on the market. Two base cases were therefore examined to determine which conventional configuration performs better economically. Both configurations consist of the same three columns, and since the capital expenditure (CAPEX) calculated using Aspen Process Economic Analyzer is identical for both, the comparison comes down to operating cost alone. The two cases differ only in column sequencing: Base Case 1 follows the order topping column, medium-pressure column, and low-pressure column, while Base Case 2 follows the order topping column, low-pressure column, and medium-pressure column.

As shown in Table 23, Base Case 2 achieves a lower operating cost, reducing total steam consumption by 27.2% in South America and 12.2% in the Nordics relative to Base Case 1. Since CAPEX is identical between the two configurations, this reduction in steam consumption translates directly into a lower operating expenditure (OPEX) for Base Case 2.

For this reason, Base Case 2 was chosen as the benchmark for comparison with the vacuum distillation system. This ensures that the vacuum distillation process is evaluated against the best available conventional alternative, thereby yielding a conservative and robust economic assessment.

Table 23: Annual steam consumption comparison: Base Case 1 vs Base Case 2.

	South America		**Nordics**	
Steam Type	**Base Case 1**	**Base Case 2**	**Base Case 1**	**Base Case 2**
LP Steam (MWh/yr)	569	27,663	1,698	27,056
HP Steam (MWh/yr)	40,266	2,070	35,919	5,979
Total (MWh/yr)	**40,835**	**29,733**	**37,616**	**33,035**

5.2 Case Study: South America

This section presents the corresponding results for the South America site.

5.2.1 Vacuum Distillation

Figure 36a presents the reboiler duty required for the vacuum distillation column, alongside the heat recovered from the electrolyzer waste heat stream, while Figure 36b shows the resulting additional heat demand. The required reboiler duty remains remarkably stable across the annual operating horizon, fluctuating within a narrow band of approximately 21–23 MW for the majority of the year. Within this demand, the recovered electrolyzer (ELY) waste heat makes a consistent contribution of 9–10 MW, covering close to half of the total reboiler duty.

The remaining heat demand, shown in Figure 36b, must be met either through steam purchased from an external source or via a heat pump that upgrades the low-temperature waste heat to a temperature level suitable for the distillation column reboiler.

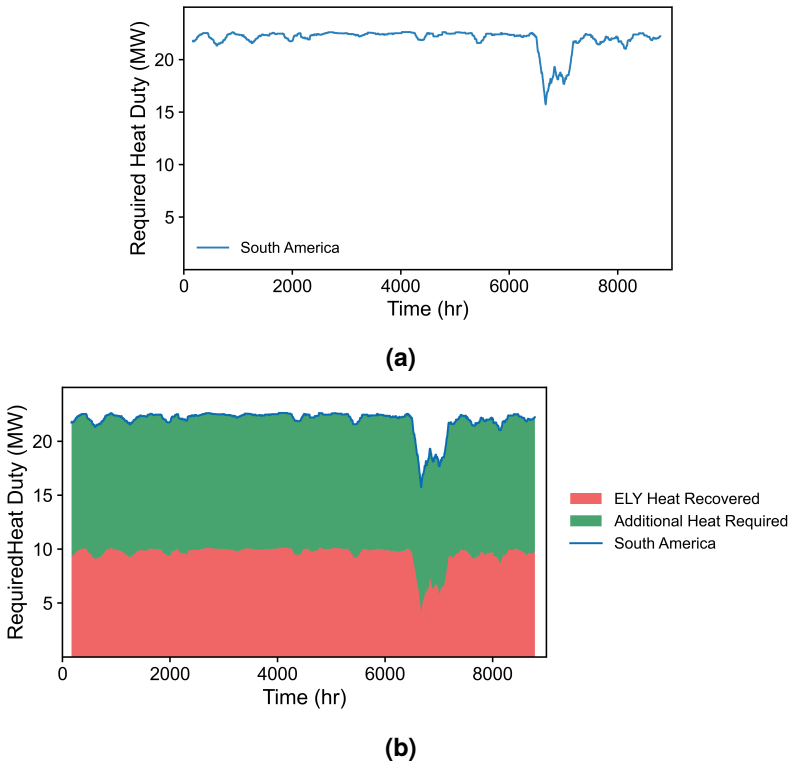

Figure 36: Reboiler heat duty for the South American vacuum distillation: (a) presents the overall heat duty required, and (b) presents the amount of heat recovered from waste electrolyzer heat and additional heat required.

Figure 37 presents the relative economics of heat-pump-supplied versus steam-supplied reboiler heat for the South American site. Because low-pressure (LP) steam is generated on-site from a comparatively inexpensive fuel source, its cost remains near-constant throughout the year, at approximately 110–115 €/hr. Heat-pump-delivered heat, by contrast, tracks the volatility of the local electricity price. For roughly the first 6,000 operating hours, the electricity cost of running the heat pump stays consistently and substantially below the cost of steam, typically under 30 €/hr, before rising

sharply during a high-price period between approximately 6,000 and 7,500 hours, during which it twice exceeds the steam cost and peaks at over 220 €/hr. Outside this window, the heat pump offers a clear operating-cost advantage over steam generation.

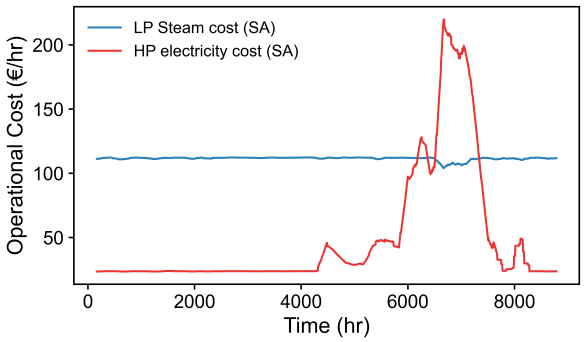

Figure 37: Comparison of hourly operational cost for LP steam generation versus heat-pump electricity consumption, South America.

Despite this favorable operating-cost profile for most of the year, the overall economic case for a heat-pump retrofit in South America is unfavorable once capital costs are considered (Table 24). While the heat pump generates a meaningful annual saving on electricity versus avoided steam cost before Operation and Maintenance (O&M), the capital cost of the installation is high enough to erode most of this saving once annualized, giving a simple payback of 17 years and a negative NPV of −1.20 M€ over a 30-year horizon at a 6% discount rate. Under these conditions, continuing to use steam remains the more economical option for supplying reboiler heat to the distillation column, and a heat-pump retrofit is not justified.

Table 24: Heat-pump economic performance: South America (500 €/kW_{th}, 6% discount rate).

Parameter	Value
Heat delivered by heat pump	108 851 MWh/yr
Electricity consumed by HP	22 626 MWh/yr
Steam cost avoided	979 660 €/yr
HP electricity cost	429 324 €/yr
Net saving before O&M	550 336 €/yr
Installed CAPEX (500 €/kW)	6 878 292 €
O&M (2% of CAPEX)	137 566 €/yr
Net saving after O&M	412 770 €/yr
Simple payback	17 yr
NPV over 30 years	−1 196 581 €

5.2.2 Process Optimization: Distillation Feed Mass Flowrate

Feed mass flow rate optimisation for the South American site, based on the overall distillation cost including the annualised CAPEX and OPEX of the buffering technology

used, is shown in Figure 38. The results show a consistent ranking between the vacuum and base-case configurations, with the vacuum case operating at a substantially higher absolute cost level (approximately 200–450 €/hr versus 60–110 €/hr for the base case) due to the added energy penalty of vacuum operation. In both configurations, the hybrid model delivers the lowest overall cost, consistently outperforming the storage and product-recycling models throughout the entire operating horizon, including during the high-price excursion between 6,000 and 7,500 operating hours.

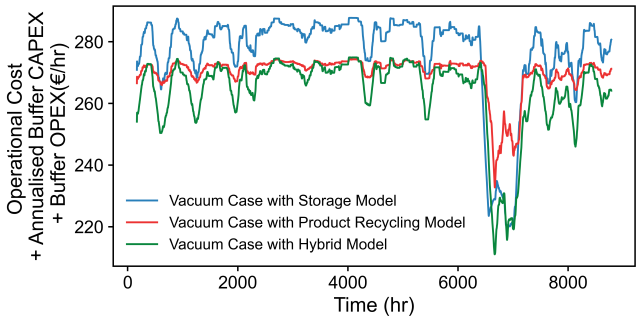

(a) Vacuum Case

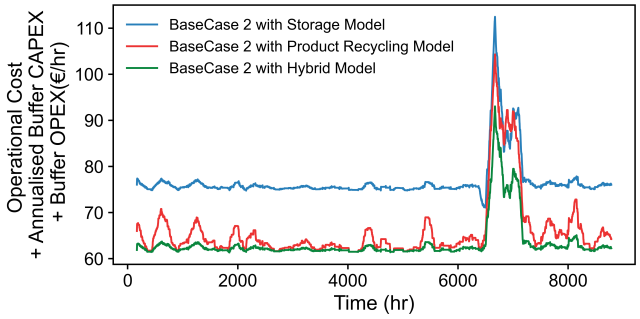

(b) Base Case 2

Figure 38: Comparison of operational cost (including annualised buffer CAPEX and buffer OPEX) across the storage, product-recycling, and hybrid flexibility strategies for the South American: (a) vacuum case and (b) Base Case 2.

Beyond its cost advantage, the hybrid model's ability to combine product recycling with storage substantially reduces the reliance on large buffer inventories to maintain stable operation during low-demand periods. As a result, the required storage tank size drops from 1,200 tons under the storage-only model to just 80 tons, confirming the hybrid model as the best-performing strategy both in terms of operating cost and capital efficiency.

5.2.3 Techno-economic Analysis

Since Base Case 2 was selected as the benchmark for its higher efficiency, steam (rather than the heat pump) is used for the vacuum case based on the returns analysis, and the hybrid model is adopted for its lower overall distillation cost. The full techno-economic comparison between Base Case 2 and the vacuum-distillation alternative for South

America, evaluated at the whole-plant level, is summarized in Table 25. Base Case 2 achieves a substantially higher NPV (50.4 M€ versus 36.7 M€) and a marginally higher IRR (6.6% versus 6.5%) than the vacuum case, with a correspondingly lower levelised cost of methanol (1008.9 €/t versus 1017.0 €/t).

Table 25: Techno-economic Analysis: Base Case 2 vs Vacuum Case (South America).

Parameter	Base Case 2	Vacuum Case
NPV (M€)	50.4	36.7
IRR (%)	6.6	6.5
LCO-Methanol (€/t)	1008.9	1017.0

This outcome reflects several factors specific to the South American site. First, the reduction in steam demand achieved through vacuum operation is limited, as the electrolyzer can supply only approximately half of the required low-temperature heat. Second, vacuum operation requires higher capital investment than the conventional configuration. In addition, the vacuum case has substantially higher cooling-water costs. Owing to the increased condensation duty and the low cooling-water temperature rise of only about 5,°C, the required cooling-water mass flow rate is approximately five times higher than in the base case (see *Appendices* Table 34 & Table 35). Given a cooling-water cost of 0.05 €/t, this significantly increases annual operating expenses. Collectively, the limited utility savings, higher equipment costs, and higher cooling-water consumption make the conventional distillation configuration the economically preferable option for the South American case.

5.3 Case Study: Nordics

This section presents the corresponding results for the Nordic site, where higher steam costs and greater variability in renewable electricity supply lead to a different economic outcome than observed in South America.

5.3.1 Vacuum Distillation

Figure 39a presents the reboiler duty required for the vacuum distillation column, alongside the heat recovered from the electrolyser waste-heat stream, while Figure 39b shows the resulting additional heat demand. Unlike the South American case, the Nordic reboiler duty does not settle into a narrow steady-state band but instead varies between roughly 15 and 22.5 MW over the year. This variability reflects the stronger seasonal and hourly fluctuations in both the availability of crude methanol and the renewable electricity supply that characterize the Nordic operating environment. Recovered electrolyser waste heat covers a smaller share of the reboiler duty than in South America, so a larger fraction of the load must be met by supplementary heating throughout the year.

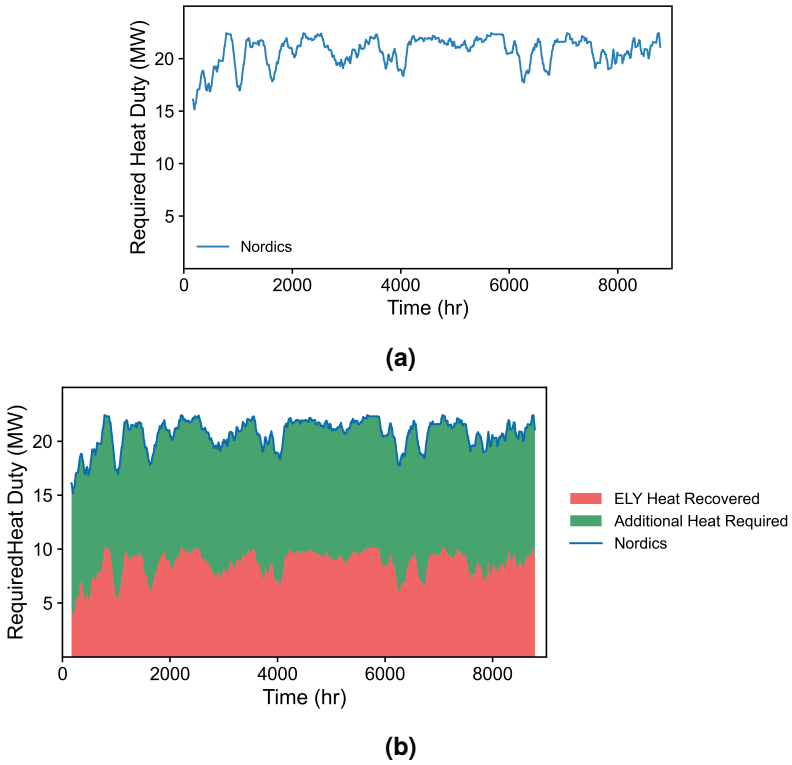

Figure 39: Reboiler heat duty for the Nordic's vacuum distillation: (a) presents the overall heat duty required, and (b) presents the amount of heat recovered from waste electrolyzer heat and additional heat required.

The cost comparison between heat-pump and steam-supplied heat for the Nordics (Figure 40) reveals a different picture from South America. LP steam cost is an order of magnitude higher, holding steady at approximately 510–540 €/hr throughout the year. The heat-pump electricity cost briefly exceeds this during a short initial transient (peaking near 595 €/hr), but then drops and stays well below the steam cost for the rest of the year, typically 50–200 €/hr, with brief peaks near 290 €/hr. The heat pump thus offers a consistent, substantial cost advantage over steam for almost the entire year.

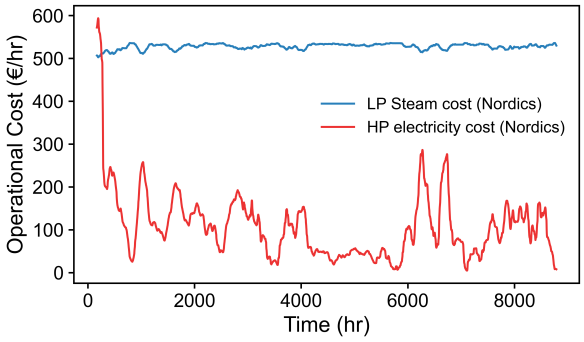

Figure 40: Comparison of hourly operational cost for LP steam generation versus heat-pump electricity consumption, Nordics.

Following the same economic evaluation approach as for South America, Table 26 summarises the heat-pump retrofit case for the Nordics. With similar heat delivered (105, 382 MWh/yr) and electricity consumed (21, 905 MWh/yr) as in South America, the much higher avoided steam cost of 4, 636, 805 €/yr (nearly five times that of South America) against an electricity cost of 972, 166 €/yr gives a net saving before O&M of 3, 664, 639 €/yr. After CAPEX (6.72 M€ at 500 €/kW$_{th}$) and O&M (134, 423 €/yr), the net saving is 3, 530, 216 €/yr. Because of the high local steam cost, the payback is just 2 years, with a strongly positive NPV of 41.87 M€ over 30 years, making the heat pump an economically feasible choice for the Nordics.

Table 26: Heat-pump economic performance — Nordics (500 €/kW$_{th}$, 6% discount rate).

Parameter	Value
Heat delivered by heat pump	105 382 MWh/yr
Electricity consumed by HP	21 905 MWh/yr
Steam cost avoided	4 636 805 €/yr
HP electricity cost	972 166 €/yr
Net saving before O&M	3 664 639 €/yr
Installed CAPEX (500 €/kW)	6 721 149 €
O&M (2% of CAPEX)	134 423 €/yr
Net saving after O&M	3 530 216 €/yr
Simple payback	2 yr
NPV over 30 years	41 871 681 €

5.3.2 Process Optimization: Distillation Feed Mass Flowrate

Feed mass flow rate optimisation for the Nordic site, based on the overall distillation cost including the annualised CAPEX and OPEX of the buffering technology used, is shown in Figure 41. As in South America, the Nordic site shows the vacuum case operating at a substantially higher absolute cost level than Base Case 2, reflecting the added energy penalty of vacuum operation. In both configurations, the hybrid model again delivers the lowest overall cost, outperforming the storage and product-recycling models, which confirms the hybrid model as the preferred flexibility strategy for the Nordic site as well.

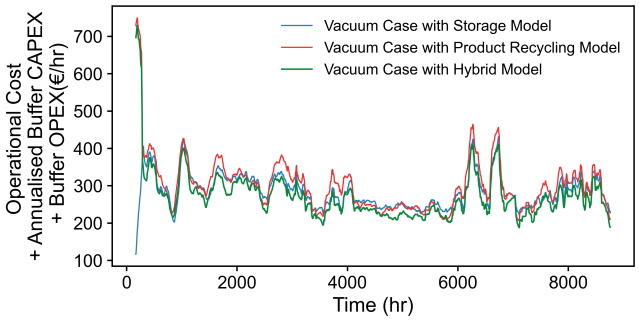

(a) Vacuum Case

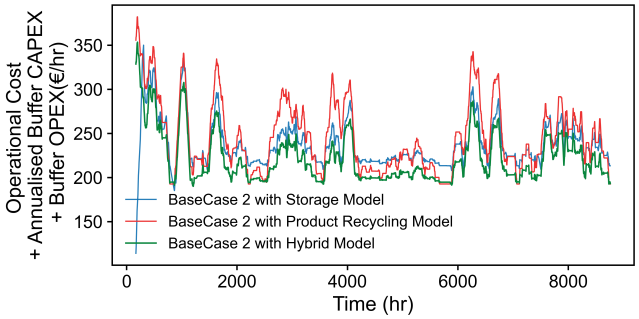

(b) Base Case 2

Figure 41: Comparison of operational cost (including annualised buffer CAPEX and buffer OPEX) across the storage, product-recycling, and hybrid flexibility strategies for the Nordic: (a) vacuum case and (b) Base Case 2.

5.3.3 Techno-economic Analysis

The techno-economic comparison for the Nordic site (Table 27) presents a very different overall investment picture from South America: both configurations return a negative NPV over the project lifetime, reflecting the generally less favorable economics of methanol production at this location. However, in contrast to the South American result, the vacuum case is here the preferable configuration on every metric considered. The vacuum distillation case achieves a less negative NPV (−46.1 M€ versus −64.9 M€), a higher IRR (5.4% versus 5.2%), and a lower LCO-Methanol (1457.4 €/t versus 1470.1 €/t) relative to Base Case 2.

The opposite outcome for Nordics relative to South America is driven by the heat-pump retrofit: being electrically driven, it displaces the distillation steam demand and frees the synthesis-loop steam for carbon capture. The resulting reduction in overall steam consumption is more valuable in the Nordics, where steam costs are high, so the lower reboiler duty under vacuum operation yields an operating-cost saving that outweighs the incremental capital cost.

Table 27: Economic comparison — Base Case 2 vs Vacuum Case (Nordics).

Parameter	Base Case 2	Vacuum Case
NPV (M€)	−64.9	−46.1
IRR (%)	5.2	5.4
LCO-Methanol (€/t)	1470.1	1457.4

A sensitivity analysis on the renewable power purchase agreement (PPA) price, holding all other costs constant, reinforces this conclusion. The vacuum case reaches NPV = 0 at a renewable PPA price of 41.6 €/MWh, compared with 40.6 €/MWh for Base Case 2. Because the vacuum configuration can tolerate a higher electricity price before the project economics turn unfavorable.

6 Conclusion

This thesis set out to answer whether electrolyzer waste heat at 85 °C could replace utility steam entirely in e-methanol distillation, and whether a vacuum-operated process could be justified economically against conventional alternatives.

A two-column vacuum configuration, comprising a structured-packing topping column removing light gases and acetone followed by a vacuum refining column, was shown to operate with a bottom temperature of 75 °C, low enough for the 85 °C cooling-water stream (returning at 80 °C) to supply the reboiler directly. At full electrolyzer capacity, this direct exchange covers only around 45% of the required reboiler duty; the balance must be met by either purchased steam or the ammonia heat-pump retrofit developed in subsubsection 4.4.1. Waste heat can therefore anchor, but not by itself fully replace, the distillation heat demand.

The selected design (MellapakPlus 250Y topping column, 40 stages; MellapakPlus 452Y refining column, 72 stages at 60% stage efficiency, reflux ratio 2.2, based on a steady-state rate-based RadFrac process design in Aspen Plus) achieves 99.9954 wt% methanol, with 35 ppm ethanol and under 5 ppm acetone in the topping-column bottoms, comfortably within the IMPCA limits of 50 and 20 ppm, respectively, even after accounting for the additional over-design margin specified for the study.

By narrowing the column diameter above the feed stage, the topping column achieves a turndown ratio of 67.5% of nominal feed, while the refining column achieves 57.5%. Both columns satisfy the hydraulic and product-quality constraints at these operating limits. Although the topping column diameter initially limits its turndown to 67.5%, it accounts for only around 10% of the overall reboiler duty. Therefore, at lower loads, its reflux ratio can be increased to maintain the reboiler duty at approximately the 67.5% level and preserve hydraulic performance without significantly affecting the overall energy demand. This adjustment allows the topping column to operate at 60% turndown. Since both columns must operate simultaneously, the overall process turndown is ultimately governed by the topping column, resulting in a minimum operating capacity of 60% of nominal feed.

The 8,760-hour hybrid buffering model, which integrates intermediate storage with product recycling within a mixed-integer linear programming framework, outperformed either strategy applied independently in both markets. A key advantage of the combined configuration is the substantial reduction in required storage capacity. In South America, the storage requirement decreased from approximately 1,200 tons in the intermediate storage-alone model to about 80 tons when recycling was introduced, while in the Nordics it decreased from approximately 2,195 tons to 250 tons. These results indicate that decoupling the distillation system from upstream hydrogen supply fluctuations does not necessarily require a large dedicated storage vessel when product recycling is used in combination with intermediate storage.

The techno-economic comparison shows that the preferred configuration between vacuum and conventional distillation depends strongly on the market context. In South America, where LP/MP steam costs are relatively low at 9–11 €/MWh and hydrogen supply is comparatively stable, Base Case 2 delivers the more favourable

economic performance across all evaluated indicators, with an NPV of 50.4 M€ compared with 36.7 M€, an IRR of 6.6% compared with 6.5%, and an LCO-MeOH of 1008.9 €/t compared with 1017.0 €/t for the vacuum configuration. By contrast, the vacuum configuration performs better in the Nordic market, where steam costs are substantially higher at 44–45 €/MWh. There, the vacuum case achieves an NPV of −46.1 M€ compared with −64.9 M€ for Base Case 2, an IRR of 5.4% compared with 5.2%, and an LCO-MeOH of 1457.4 €/t compared with 1470.1 €/t. This advantage is primarily driven by the value of the steam displaced by the heat-pump-assisted vacuum configuration. Consequently, the heat-pump retrofit becomes economically attractive when the cost of steam is sufficiently high relative to the required electricity input, as in the Nordic case.

Overall, the results demonstrate that the relative economic performance of vacuum and conventional distillation is determined primarily by the local steam-to-electricity price ratio rather than by an inherent technical advantage of vacuum operation. Integrating vacuum distillation with electrolyzer waste heat can provide an economic benefit in regions characterized by high steam costs and favorable electricity prices.

However, the observed improvement is not substantial enough to justify replacing established conventional distillation as a general industrial practice. Vacuum distillation should therefore be regarded as a market-specific optimisation option for e-methanol purification rather than a universally preferable process configuration.

6.1 Limitations

The thermodynamic and composition analysis assumes the reactor feedstock remains constant throughout operation. In practice, catalyst degradation occurs over the three-year replacement cycle, which could shift the feed composition. While the thesis accounts for this through scheduled catalyst replacement, no Aspen-based sensitivity analysis was conducted to quantify composition drift over the cycle interval or its corresponding effect on column performance. This represents a gap between the constant-feed assumption used in the optimization framework and the actual operational reality of catalyst aging.

The assumed 5% per minute ramp rate for distillation column adjustments is grounded in established practice from comparable industrial systems. However, this rate has not been dynamically validated against the specific pressure and thermal constraints of this vacuum design, particularly the narrow operating margins required at low absolute pressure. Whether the column can reliably achieve this ramp rate without exceeding hydraulic or thermal safety limits remains an open question.

A third constraint concerns pressure drop estimation and safety margins across the two columns. The topping column operates at 2 mbar/meter with an additional 50% safety buffer. The refining column, by contrast, operates at 3.05 mbar/meter with no supplementary margin. If the actual pressure drop in the refining column exceeds this baseline, whether due to fouling, flow distribution, or other operability factors, the resulting pressure increase would raise the bottom temperature while simultaneously narrowing the already small temperature difference between sections. This compounding effect would compress the operating window and potentially

constrain achievable throughput. The asymmetric treatment of safety margins between the two columns reflects this difference in risk tolerance but represents a practical vulnerability that warrants closer monitoring during commissioning.

A limitation of the present heat-pump model is that the temperature lift and COP were assumed to remain constant across the operating range, while variations in heat demand were accommodated by adjusting the heat-source mass flow rate. This simplified approach does not fully represent off-design operation, where source and sink temperatures, and consequently the temperature lift and COP, may vary with operating conditions. An alternative control strategy could adjust the temperature lift in response to heat-demand variations, potentially achieving a higher COP under favourable conditions. Therefore, a detailed off-design heat-pump model with a variable COP should be considered in future work.

References

[1] Giulia Bozzano and Flavio Manenti. "Efficient methanol synthesis: Perspectives, technologies and optimization strategies". In: *Progress in Energy and Combustion Science* 56 (Sept. 2016), pp. 71–105. ISSN: 03601285. DOI: 10.1016/j.pecs.2016.06.001.

[2] Yacine Rezgui and Yves Gagnon. "Methanol fundamentals, applications, and market overview". In: *Methanol Biofuel in Combustion Engines*. Elsevier, 2026, pp. 1–44. DOI: 10.1016/B978-0-443-31504-6.00008-2.

[3] Matthew J. Palys and Prodromos Daoutidis. "Power-to-X: A review and perspective". In: *Computers and Chemical Engineering* 165 (Sept. 2022). ISSN: 00981354. DOI: 10.1016/j.compchemeng.2022.107948.

[4] Matteo Genovese et al. *Power-to-hydrogen and hydrogen-to-X energy systems for the industry of the future in Europe*. May 2023. DOI: 10.1016/j.ijhydene.2023.01.194.

[5] D.T. Pio et al. "Decarbonizing the aviation sector with Electro Sustainable Aviation Fuel (eSAF) from biogenic CO2 captured at pulp mills". In: *Chemical Engineering Journal* 463 (May 2023), p. 142317. ISSN: 13858947. DOI: 10.1016/j.cej.2023.142317.

[6] Ottmar Edenhofer. *Climate Change 2014: mitigation of climate change*. Vol. 3. Cambridge University Press, 2015.

[7] *International Energy Agency (2021), Electricity Market Report – July 2021. Paris: IEA*. URL: https://www.iea.org/data-and-statistics/charts/total-final-energy-consumption-and-avoided-energy-demand-in-the-stated-policies-scenario-versus-the-net-zero-scenario-2020-to-2050.

[8] Anna Ingwersen et al. "Prospective life cycle assessment of cost-effective pathways for achieving the FuelEU Maritime Regulation targets". In: *Science of The Total Environment* 958 (Jan. 2025), p. 177880. ISSN: 00489697. DOI: 10.1016/j.scitotenv.2024.177880.

[9] David S Sholl and Ryan P Lively. "Seven chemical separations to change the world". In: *Nature* 532 (2016).

[10] L. Collins. *"World's first large-scale green methanol plant officially inaugurated," Hydrogen Insight. Accessed: March. 18, 2026. [Online]. Available: https://www.hydrogeninsight.com/innovation.*

[11] Selma Brynolf et al. "Electrofuels for the transport sector: A review of production costs". In: *Renewable and Sustainable Energy Reviews* 81 (Jan. 2018), pp. 1887–1905. ISSN: 13640321. DOI: 10.1016/j.rser.2017.05.288.

[12] ANDRITZ Group. *"Integrated EPC solutions for e-methanol production," ANDRITZ Power-to-X Offering. Accessed: March. 17, 2026. [Online]. Available: https://igit.me/PLHEl.*

[13] Juntao Zhang, Shengrong Liang, and Xiao Feng. “A novel multi-effect methanol distillation process”. In: *Chemical Engineering and Processing: Process Intensification* 49.10 (Oct. 2010), pp. 1031–1037. ISSN: 02552701. DOI: 10.1016/j.cep.2010.07.003.

[14] Xiaodong Zhang et al. “Energy-efficient and sustainable methanol distillation: Exploring diluted alcohol strategies, multi-effect heat integration, and heat pump-based electrification for carbon reduction”. In: *Separation and Purification Technology* 363 (Aug. 2025). ISSN: 18733794. DOI: 10.1016/j.seppur.2025.132042.

[15] Yu Ying Chen et al. “Sustainable distillation under feed variability: Embedding flexibility index in early-stage process design”. In: *Process Safety and Environmental Protection* 205 (Jan. 2026). ISSN: 09575820. DOI: 10.1016/j.psep.2025.108200.

[16] S. Skogestad. “’Dynamics and Control of Distillation Columns: A Tutorial Introduction,’ Chem. Eng. Res. Des., 75, 539-562, 1997.” In: ().

[17] S. Skogestad & M. Morari. “The Dominant Time Constant for Distillation Columns,’ Comput. Chem. Eng., 11(6), 607-617, 1987; and I&EC Res. 27, 1848, 1988.” In: ().

[18] Jörg Ott et al. “Methanol”. In: *Ullmann’s Encyclopedia of Industrial Chemistry*. Wiley, Oct. 2012. DOI: 10.1002/14356007.a16{_}465.pub3.

[19] *National Institute of Standards and Technology. (n.d.). NIST Chemistry WebBook, NIST Standard Reference Database Number 69. U.S. Department of Commerce. Retrieved March 19, 2026, from https://webbook.nist.gov/chemistry/.*

[20] *National Center for Biotechnology Information (2026). PubChem Compound Summary for CID 887, Methanol.*

[21] A. Goeppert G. A. Olah and G. K. S. Prakash. *“Production of Methanol from Still Available Fossil-Fuel Resources,” in Beyond Oil and Gas: The Methanol Economy, 3rd ed., John Wiley & Sons, Incorporated, 2018, ch. 12.*

[22] *IRENA and Methanol Institute, “Innovation Outlook: Renewable Methanol,” International Renewable Energy Agency, Abu Dhabi, 2021. Accessed: March 18, 2026. [Online]. Available: www.irena.org*.

[23] “Valmet, “White Paper: Methanol, from waste byproduct to valuable fuel,” 2018. ” In: ().

[24] Cenxi Li, Shi You, and Xiaoti Cui. *From concept to deployment: A review of carbon-to-methanol pathways for e-methanol*. Apr. 2026. DOI: 10.1016/j.apenergy.2026.127429.

[25] L. H. Horsley. “‘Azeotropic Data III’, in Advances in Chemistry Series, vol. 116, American Chemical Society, Washington, D. C., 1973, pp. 74–83.” In: ().

[26] Kiran D Patil and Tanvi Bhatia. *Distillation Operations: Methods, Operational and Design Issues Design of Three Phase separator View project PREHEAT NETWORK RECONFIGURATION OF A KERO HYDRO DESULPHURIZATION UNIT" View project*. Tech. rep. 2009. URL: https://www.researchgate.net/publication/263352060.

[27] Dr Andrzej Gorak. *Distillation: Fundamentals and Principles, Chapter 2*. Elsevier, 2014.

[28] William L. Luyben. *Distillation Design and Control Using Aspen ™ Simulation, Chapter 1 & 2*. WILEY's, 2013.

[29] Qing Li, Ana Somoza-Tornos, and Anton A. Kiss. "A systematic selection and decision matrix for energy-efficient intensified distillation technologies". In: *Chemical Product and Process Modeling* 20.2 (May 2025), pp. 293–307. ISSN: 1934-2659. DOI: 10.1515/cppm-2024-0035.

[30] Chengtian Cui et al. "Efficient heat integration within discretely heat integrated distillation columns using liquid injection". In: *AIChE Journal* 71.8 (Aug. 2025). ISSN: 15475905. DOI: 10.1002/aic.18861.

[31] *Texas Tech University. (2025). Simple and fractional distillations of a mixture: Water & methanol [Unpublished laboratory report]. Department of Chemistry & Biochemistry, Texas Tech University*. Tech. rep.

[32] Zauziah Pramiswari Putri, Cucuk Evi Lusiani, and Zhang Zhishan. "STUDY ON DOUBLE-EFFECT DISTILLATION PROCESS FOR SEPARATING METHANOL-WATER USING ASPEN PLUS V10". In: 2022.2 (), pp. 418–430. ISSN: 2714-7649. URL: http://distilat.polinema.ac.id.

[33] A. P. Douglas and A. F.A. Hoadley. "A process integration approach to the design of the two- and three-column methanol distillation schemes". In: *Applied Thermal Engineering* 26.4 (Mar. 2006), pp. 338–349. ISSN: 13594311. DOI: 10.1016/j.applthermaleng.2005.07.001.

[34] Jinsheng Sun et al. "Energy and exergy analysis of a five-column methanol distillation scheme". In: *Energy* 45.1 (2012), pp. 696–703. ISSN: 03605442. DOI: 10.1016/j.energy.2012.07.022.

[35] Sohail Rasool, Lone Mushtaq, and Ahmad Rather. "Modeling and Simulation of a Distillation Column using ASPEN PLUS for separating methanol/water mixture". In: *International Journal of Scientific & Engineering Research* 6.3 (2015). ISSN: 2229-5518.

[36] William L. Luyben. "Optimum vacuum distillation pressure". In: *Chemical Engineering and Processing - Process Intensification* 171 (Jan. 2022), p. 108630. ISSN: 02552701. DOI: 10.1016/j.cep.2021.108630.

[37] Weiwei Li et al. "Modelling of vacuum distillation in a rotating packed bed by Aspen". In: *Applied Thermal Engineering* 117 (2017), pp. 322–329. ISSN: 13594311. DOI: 10.1016/j.applthermaleng.2017.01.046.

[38] Alexander Buttler and Hartmut Spliethoff. “Current status of water electrolysis for energy storage, grid balancing and sector coupling via power-to-gas and power-to-liquids: A review”. In: *Renewable and Sustainable Energy Reviews* 82 (Feb. 2018), pp. 2440–2454. ISSN: 13640321. DOI: 10.1016/j.rser.2017.09.003.

[39] Nikita Taranin et al. “On the Ramp-Rate Limitation of Electrolysis Plants: Modeling Fundamentals and System-Level Impact Analysis”. In: *IEEE Transactions on Sustainable Energy* 17.2 (Apr. 2026), pp. 1238–1249. ISSN: 1949-3029. DOI: 10.1109/TSTE.2025.3611711.

[40] Ajitanshu Vedrtnam, Kishor Kalauni, and Rahul Pahwa. “A review of water electrolysis technologies with insights into optimization and numerical simulations”. In: *International Journal of Hydrogen Energy* 140 (June 2025), pp. 694–727. ISSN: 03603199. DOI: 10.1016/j.ijhydene.2025.05.295.

[41] T. Giampaolo. “Compressor Handbook: Principles and Practice. Fairmont Press.” In: (2006).

[42] Siphesihle Mbatha et al. “Detailed assessment of dynamic startup, shutdown, and flexibility of the adiabatic, gas-and water-cooled methanol fixed bed reactor: Comparison for power to methanol application”. In: *Chemical Engineering Science* 319 (Jan. 2026), p. 122280. ISSN: 00092509. DOI: 10.1016/j.ces.2025.122280.

[43] Chao Chen and Aidong Yang. “Power-to-methanol: The role of process flexibility in the integration of variable renewable energy into chemical production”. In: *Energy Conversion and Management* 228 (Jan. 2021), p. 113673. ISSN: 01968904. DOI: 10.1016/j.enconman.2020.113673.

[44] H.Z. Kister. *Distillation Design. McGraw-Hill.* 1992. URL: https://www.accessengineeringlibrary.com/content/book/9780070349094.

[45] Ž. Olujić et al. “Equipment improvement trends in distillation”. In: *Chemical Engineering and Processing: Process Intensification* 48.6 (June 2009), pp. 1089–1104. ISSN: 02552701. DOI: 10.1016/j.cep.2009.03.004.

[46] Zeng Li et al. “Design of robust control system of four-column dual-extractant extractive distillation for the separation of xylene isomers”. In: *Chemical Engineering and Processing - Process Intensification* 223 (May 2026), p. 110776. ISSN: 02552701. DOI: 10.1016/j.cep.2026.110776.

[47] William Luyben. “Distillation Design and Control Using Aspen™ Simulation, Chapter 5”. In: 2006.

[48] B. Linnhoff and E. Hindmarsh. *“The pinch design method for heat exchanger networks,” Chemical Engineering Science, vol. 38, no. 5, pp. 745–763, 1983.*

[49] *I. C. Kemp, Pinch Analysis and Process Integration: A User Guide on Process Integration for the Efficient Use of Energy, 2nd ed. Oxford: Butterworth-Heinemann, 2007.*

[50] Nishant Modi et al. “Techno-economic analysis of vapour compression heat pump integration for decarbonizing the dairy processing industry in India”. In: *Energy Conversion and Management* 356 (May 2026), p. 121379. ISSN: 01968904. DOI: 10.1016/j.enconman.2026.121379.

[51] K. Malleswararao et al. “Innovative approaches to waste heat recovery: Coupling high temperature vapour compression heat pumps with salt hydrate thermochemical systems”. In: *Applied Energy* 405 (Feb. 2026), p. 127229. ISSN: 03062619. DOI: 10.1016/j.apenergy.2025.127229.

[52] Suzler. *250 Y Mellapak Structured Packing*. URL: https://www.sulzer.com/en/shared/products/mellapak-and-mellapakplus.

[53] Dana S. Marlin, Emeric Sarron, and Ómar Sigurbjörnsson. “Process Advantages of Direct CO2 to Methanol Synthesis”. In: *Frontiers in Chemistry* 6 (Sept. 2018). ISSN: 2296-2646. DOI: 10.3389/fchem.2018.00446.

[54] Mahdi Fasihi and Christian Breyer. “Global production potential of green methanol based on variable renewable electricity”. In: *Energy & Environmental Science* 17.10 (2024), pp. 3503–3522. ISSN: 1754-5692. DOI: 10.1039/D3EE02951D.

[55] *Cooling Water costs are part of the Industry Economics & Competitiveness in Brazil report | Updated on July 6th, 2026*. URL: https://www.intratec.us/solutions/industry-economics-competitiveness/cooling-water-cost/brazil.

[56] *Cooling Water costs are part of the Industry Economics & Competitiveness in Finland report | Updated on July 6th, 2026*. URL: https://www.intratec.us/solutions/industry-economics-competitiveness/cooling-water-cost/finland.

[57] Wagner Freire. “New energy price dynamics open space for generation expansion.” In: (). URL: https://canalsolar.com.br/en/new-energy-price-dynamics-open-space-for-expansion-of-generation/?language_edit=1#respond.

[58] Poliana Souto. *Reduction in PPA prices opens space for the domestic market for green hydrogen.* URL: https://megawhat.uol.com.br/hidrogenio/reducao-dos-precos-de-ppas-abre-espaco-para-mercado-interno-de-hidrogenio-verde-afirma-relatorio-do-itau-bba/.

[59] *Finland’s PPA prices 2024 - 2025*. URL: https://aeeolica.org/en/levelten-energy-indice-de-precios-de-ppa-del-q4-2025-en-europa-los-precios-de-la-energia-solar-siguen-bajando-mientras-el-mercado-eolico-tambien-cae/.

[60] *Nord Pool – Day-ahead prices*. URL: https://data.nordpoolgroup.com/auction/day-ahead/prices?deliveryDate=latest&currency=EUR&aggregation=DeliveryPeriod&deliveryAreas=AT.

[61] *ENTSO-E Transparency Platform: Hourly day-ahead prices, EUR/MWh, archive from 2015–present; open data under EU Reg. 543/2013*. URL: https://entsoemcp.com/day-ahead/finland.

[62] *CCEE – PLD Horário: Hourly Difference Settlement Price (PLD) per submarket; open data (CC-BY-4.0), calculated hourly via the DESSEM model since 2021*. URL: https://dadosabertos.ccee.org.br/dataset/pld_horario.

[63] European Commission. "Commission Delegated Regulation (EU) 2023/1184". In: *Official Journal of the European Union* L157 (June 2023), pp. 11–19. URL: http://data.europa.eu/eli/reg_del/2023/1184/oj.

[64] Mohamed Elwardany et al. "High-temperature heat pumps for industrial decarbonization: Technologies, integration strategies, and future perspectives". In: *Chemical Engineering and Processing - Process Intensification* 225 (July 2026), p. 110806. ISSN: 02552701. DOI: 10.1016/j.cep.2026.110806.

[65] Xudong Ma et al. "Energy, exergy, economic, and environmental analysis of a high-temperature heat pump steam system". In: *International Journal of Refrigeration* 160 (Apr. 2024), pp. 423–436. ISSN: 01407007. DOI: 10.1016/j.ijrefrig.2024.01.020.

[66] George Kosmadakis et al. "Techno-economic analysis of high-temperature heat pumps with low-global warming potential refrigerants for upgrading waste heat up to 150 °C". In: *Energy Conversion and Management* 226 (Dec. 2020), p. 113488. ISSN: 01968904. DOI: 10.1016/j.enconman.2020.113488.

[67] Hussam Jouhara et al. "High-temperature heat pumps: Fundamentals, modelling approaches and applications". In: *Energy* 303 (Sept. 2024), p. 131882. ISSN: 03605442. DOI: 10.1016/j.energy.2024.131882.

[68] Phillip C. Wankat. "Decreasing costs of distillation columns with vapor feeds". In: *Chemical Engineering Science* 137 (Dec. 2015), pp. 955–963. ISSN: 00092509. DOI: 10.1016/j.ces.2015.07.047.

[69] Xiaodong Zhang et al. "Energy-efficient and sustainable methanol distillation: Exploring diluted alcohol strategies, multi-effect heat integration, and heat pump-based electrification for carbon reduction". In: *Separation and Purification Technology* 363 (Aug. 2025). ISSN: 18733794. DOI: 10.1016/j.seppur.2025.132042.

[70] Stuart Mitchell and Contributors. *PuLP: A Linear and Mixed-Integer Programming Modeler for Python*. URL: https://pypi.org/project/PuLP/.

[71] *Ammonia (R717) Properties*. URL: https://fluidtool.com/tools/fluid/ammonia.

7 Appendix

7.1 Vacuum Case Appendix

Table 28: Column internals and the corresponding model equations used paragraph 4.1.1.2.

Column Internals	Equations Used
Sieve Tray	Mass transfer: Chen and Chuang (1993); Heat transfer: Chilton and Colburn (1934); Interfacial area: Zuiderweg (1982).
Random PALL 1 inch	Mass transfer: Billet and Schultes (1993); Heat transfer: Chilton and Colburn (1934); Interfacial area: Billet and Schultes (1993).
Mellpackplus 252Y	Mass transfer: Bravo, Rocha, and Fair (1992); Heat transfer: Chilton and Colburn (1934); Interfacial area: Bravo, Rocha, and Fair (1992).

Table 29: Methanol loss with light gases as a function of condenser pressure and bottom temperature Figure 12.

Condenser Pressure bar(a)	Bottom Temperature (°C)	Methanol wasted (kg/hr)
1.500	84.55	30
1.400	82.66	33
1.300	80.67	36.7
1.200	78.57	41.2
1.100	76.34	46.9
1.013	74.23	53.2

Table 30: Methanol loss with light gases as a function of condenser temperature Figure 13.

Condenser Temperature (°C)	Methanol wasted with Light gases (kg/hr)
50	121.5
45	78.02
40	53.21
35	37.43

Table 31: Topping column performance at varying feed rates (distillate temperature constant at 40°C *Figure 14*

Feed	Mass Flow Rate (kg/h)	Mole-RR	Reboiler Duty (MW)	Flooding CS1	Flooding CS2	Acetone in Bottom (ppm)
100%	32166.47	25.27	2.51	75.00	81.00	5.0
95%	30558.14	25.27	2.38	71.92	78.35	5.0
90%	28949.82	25.27	2.26	68.12	74.23	5.0
85%	27341.50	25.27	2.13	64.33	70.10	5.0
80%	25733.18	25.27	2.00	60.55	65.98	5.0
75%	24124.85	25.27	1.88	56.77	61.86	5.0
70%	22516.53	25.27	1.75	52.98	57.74	5.0
68%	21712.37	25.27	1.70	51.09	55.68	5.0
65%	20908.21	28.50	1.70	52.28	55.29	3.0
60%	19299.88	30.56	1.70	53.36	54.30	3.0
55%	17691.56	40.36	1.70	58.18	54.16	0.0
50%	16083.24	45.39	1.70	59.26	53.53	0.0
45%	14474.91	51.42	1.70	60.23	52.62	0.0
40%	12866.59	58.96	1.70	61.43	52.32	0.0
35%	11258.27	68.65	1.70	62.51	51.74	0.0
30%	9649.95	81.57	1.70	63.21	51.04	0.0
25%	8041.62	99.67	1.70	64.55	51.00	0.0
20%	6433.30	141.36	1.70	65.79	50.21	0.0

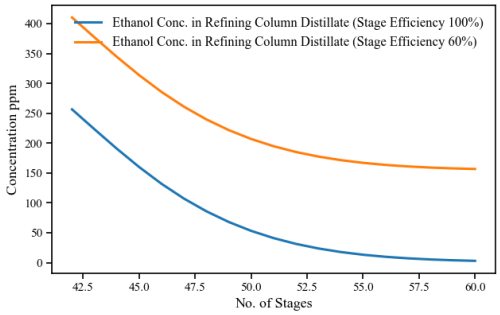

Figure 42: Comparison between 100% and 60% stage efficiency based on the concentration of ethanol in the distillate of the refining column paragraph 4.1.2.1.

Table 32: Refining column performance at varying feed rates (distillate temperature constant at 36.53 °C, Figure 20).

Feed	Mass Flow (kg/h)	MeOH Mass Frac	EtOH (ppm)	Mole-RR	Reboiler Duty (MW)	Flooding CS1 (%)	Flooding CS2 (%)	Distillate Flow (kg/h)
100%	32166.467	0.999954	3.50e-5	2.2000	20.282	75.121	74.810	20341.000
95%	30558.144	0.999955	3.50e-5	2.2000	19.256	71.372	71.346	19290.645
90%	28949.821	0.999956	3.50e-5	2.2000	18.233	67.622	67.824	18275.401
85%	27341.498	0.999957	3.50e-5	2.2000	17.199	64.083	64.704	17260.156
80%	25733.175	0.999958	3.50e-5	2.2000	16.182	60.876	60.876	16244.912
75%	24124.852	0.999958	3.50e-5	2.2000	15.167	57.671	58.476	15229.668
70%	22516.529	0.999958	3.50e-5	2.2000	14.160	52.618	53.336	14214.424
65%	20908.206	0.999959	3.50e-5	2.2000	13.144	48.865	49.762	13199.179
60%	19299.883	0.999959	3.50e-5	2.2000	12.130	45.112	46.173	12183.935
58%	18656.551	0.999959	3.50e-5	2.2000	12.000	43.610	44.725	11777.836
55%	17691.560	0.999960	3.50e-5	2.4409	12.000	44.213	45.379	11168.691
50%	16083.237	0.999960	3.50e-5	2.7772	12.000	45.162	46.169	10153.447
45%	14474.914	0.999962	3.50e-5	3.1881	12.000	45.449	46.492	9138.203
40%	12866.591	0.999961	3.50e-5	3.7770	12.000	45.641	46.806	8122.958
35%	11258.268	0.999963	3.50e-5	4.3622	12.000	46.009	47.067	7107.714
30%	9649.945	0.999962	3.50e-5	5.2428	12.000	46.282	47.349	6092.470
25%	8041.622	0.999963	3.50e-5	6.4756	12.000	46.551	47.651	5077.226
20%	6433.299	0.999964	3.50e-5	8.3248	12.000	46.816	48.000	4061.981

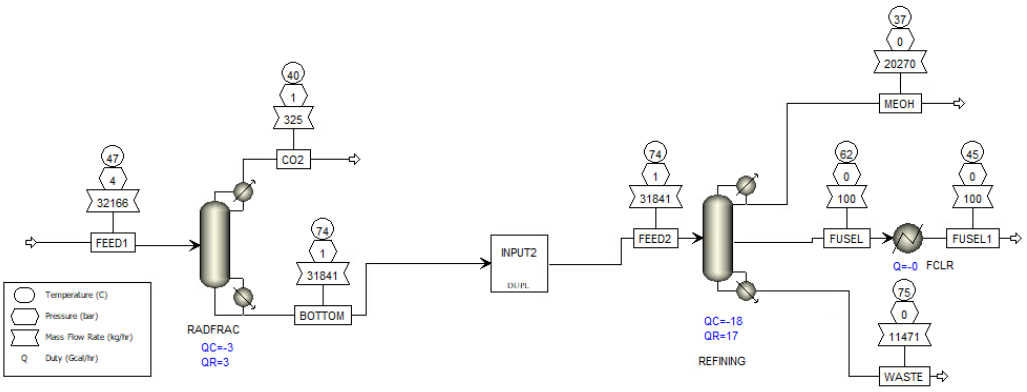

Figure 43: Vacuum distillation process flow diagram paragraph 4.1.2.4.

Table 33: Stream summary for the refining column paragraph 4.1.2.4.

	FEED1	CO2	BOTTOM	FEED2	FUSEL	FUSEL1	WASTE	MEOH
Phase	Mixed	Vapor	Liquid	Liquid	Liquid	Liquid	Liquid	Liquid
Temp. (°C)	47.000	40.000	73.615	73.615	62.738	45.000	75.459	36.530
Pressure (bar a)	4.490	1.013	1.025	1.025	0.386	0.350	0.393	0.300
Mass Vap. Frac.	3.82e-6	1	0	0	0	0	0	0
Mass Liq. Frac.	0.999996	0	1	1	1	1	1	1
Mass flow (kg/h)	32166.467	200.694	31965.773	31965.773	100.000	100.000	11524.566	20341.207
Mass Fractions								
CO2	0.003565	0.571382	1.46e-19	1.46e-19	0	0	0	0
H2	1.20e-6	0.000193	3.49e-25	3.49e-25	0	0	0	0
CO	7.90e-7	0.000127	1.34e-23	1.34e-23	0	0	0	0
WATER	0.360401	0.000110	0.362663	0.362663	0.709908	0.709908	0.999755	3.24e-6
METHANOL	0.634532	0.265188	0.636851	0.636851	0.147909	0.147909	0.000205	0.999954
N2	6.18e-7	9.91e-5	1.20e-18	1.20e-18	0	0	0	0
DIMET-01	0.000244	0.039102	2.45e-18	2.45e-18	0	0	0	0
METHY-01	0	0	0	0	0	0	0	0
ACETONE	1.15e-5	0.001044	5.00e-6	5.00e-6	5.35e-18	5.35e-18	3.33e-23	7.86e-6
METHY-02	0.000764	0.122439	7.29e-11	7.29e-11	3.81e-19	3.81e-19	1.94e-24	1.15e-10
ETHANOL	0.000255	6.91e-6	0.000257	0.000257	0.071585	0.071585	2.89e-5	3.50e-5
PROPANOL	0.000143	2.97e-8	0.000145	0.000145	0.045361	0.045361	5.92e-6	4.31e-10
BUTANOL	0.000137	4.34e-9	0.000138	0.000138	0.042729	0.042729	1.10e-5	5.46e-12
2-BUT-01	1.36e-5	1.56e-9	1.37e-5	1.37e-5	0.004365	0.004365	1.42e-7	5.70e-12
PENTANOL	7.32e-5	2.30e-10	7.36e-5	7.36e-5	0.023505	0.023505	2.83e-7	2.30e-13
O2	1.93e-6	0.000309	5.74e-18	5.74e-18	0	0	0	0

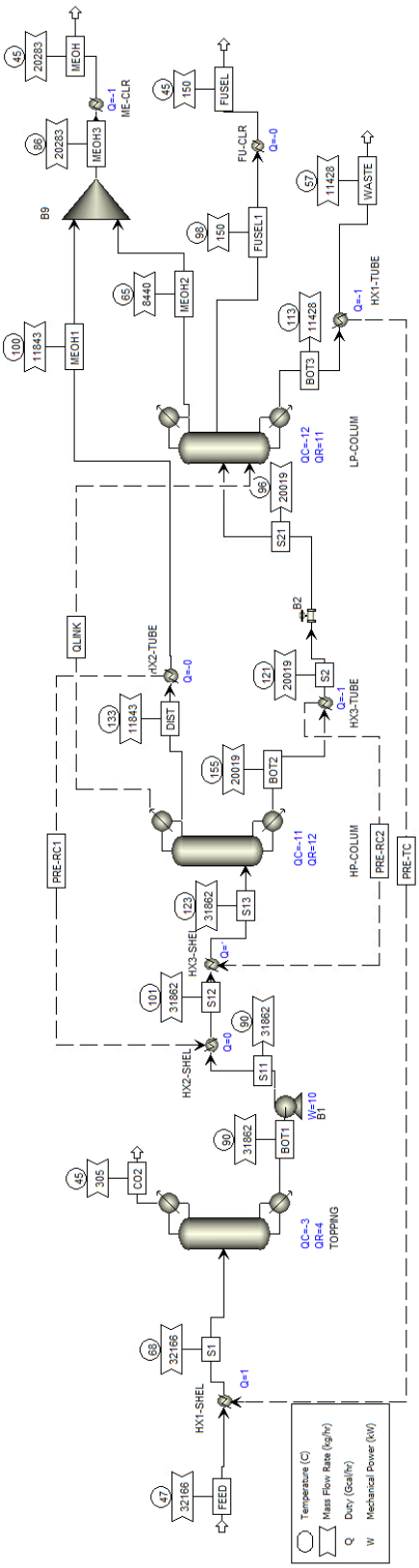

Figure 44: Three-Column Conventional distillation (Base case 01). subsection 4.2

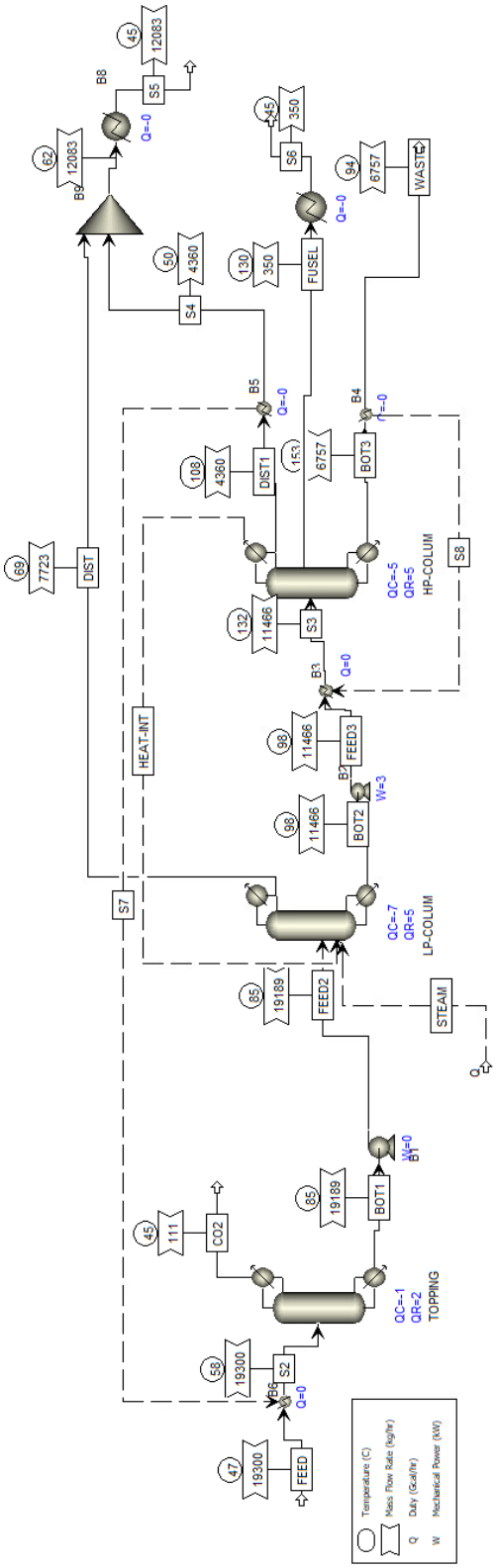

Figure 45: Three-Column Conventional distillation (Base case 02). subsubsection 4.2.2

Table 34: Condenser cooling requirements and cost for Base Case 1 (heat-integrated TC/RC) at varying feed loads (South America).

Feed Load (%)	Condenser Duty (MW)	CW Flow (kg/s)	Effective ΔT (K)	Cooling Cost (€/h)
100	13.4400	232.61563	15	41.8708134
95	12.9270	223.02233	15	40.1440191
90	12.5161	216.01515	15	38.8827273
85	12.0355	207.41599	15	37.3348780
80	11.5548	198.81683	15	35.7870287
75	11.0742	190.21766	15	34.2391794
70	10.5936	181.61850	15	32.6913301
65	10.1130	173.01934	15	31.1434809
60	9.6323	164.42018	15	29.5956316
55	9.6173	164.06132	15	29.5310383
50	9.6023	163.70247	15	29.4664450
45	9.5873	163.34362	15	29.4018517
40	9.5723	162.98477	15	29.3372584
35	9.5573	162.62592	15	29.2726651
30	9.5423	162.26707	15	29.2080718
25	9.5273	161.90821	15	29.1434785
20	9.5123	161.54936	15	29.0788852

Table 35: Condenser cooling requirements and total cooling cost for the Vacuum Case at varying feed loads. Cooling duty of the topping column for vacuum distillation is not included here, which has a temperature difference of 10 K and only imposes a 6-3 €/hr additional cost of cooling water (South America).

Feed Load (%)	Condenser Duty (MW)	CW Flow (kg/s)	Effective ΔT (K)	Total Cost (€/h)
100	20.7644	993.51196	5	178.8321531
95	19.7263	943.84023	5	169.8912422
90	17.7767	850.56211	5	153.1011792
85	16.7688	802.33696	5	144.4206528
80	15.7778	754.91952	5	135.8855137
75	14.7879	707.55298	5	127.3595370
70	13.8056	660.55668	5	118.9002025
65	12.8158	613.19663	5	110.3753937
60	11.8268	565.87321	5	101.8571770
55	11.7000	559.80861	5	100.7655502
50	11.7000	559.80861	5	100.7655502
45	11.7000	559.80861	5	100.7655502
40	11.7000	559.80861	5	100.7655502
35	11.7000	559.80861	5	100.7655502
30	11.7000	559.80861	5	100.7655502
25	11.7000	559.80861	5	100.7655502
20	11.7000	559.80861	5	100.7655502

7.2 Optimization Model Appendix

7.2.1 Storage Initial Inventory Estimator

The following Python script implements the linear programming model used to estimate the minimum initial storage inventory required for stable operation of the distillation system. subsubsection 4.3.3

Listing 1: Linear programming model for estimating the required initial storage inventory

```python
import pandas as pd
import pulp

# Load data
df = pd.read_excel(
    "Crude Methanol yearly Profile.xlsx",
    sheet_name="Nordics or South America"
)

F = df["Ft"].tolist()
T = len(F)

# Parameters
Dmax = max(F)
Dmin = 0.6 * Dmax
ramp = 0.05 * Dmax

# Model
model = pulp.LpProblem(
    "Initial_Storage_Estimator",
    pulp.LpMinimize
)

# Decision variables
D = pulp.LpVariable.dicts(
    "D",
    range(T),
    lowBound=Dmin,
    upBound=Dmax
)

S = pulp.LpVariable.dicts(
    "S",
    range(T),
    lowBound=0
)

S0 = pulp.LpVariable(
    "S0",
    lowBound=0
)

# Objective: minimise initial storage inventory
model += S0

# Constraints
for t in range(T):

    # Inventory balance
    if t == 0:
        model += (
            S[t] == S0 + F[t] - D[t]
        )
```

```
    else:
        model += (
            S[t] == S[t - 1] + F[t] - D[t]
        )

        # Distillation ramp-rate limits
        model += (
            D[t] - D[t - 1] <= ramp
        )
        model += (
            D[t - 1] - D[t] <= ramp
        )

    # Storage cannot exceed the initialised capacity
    model += S[t] <= S0

    # Distillation cannot exceed feed plus available storage
    model += D[t] <= F[t] + S[t]

# Solve
solver = pulp.PULP_CBC_CMD(msg=True)
model.solve(solver)

# Results
D_values = [
    pulp.value(D[t])
    for t in range(T)
]

S_values = [
    pulp.value(S[t])
    for t in range(T)
]

S0_value = pulp.value(S0)

# Output
out = df.copy()
out["Distillation"] = D_values
out["Storage"] = S_values
out["Status"] = pulp.LpStatus[
    model.status
]

out.to_excel(
    "Storage_Initial_Inventory.xlsx",
    index=False
)

print("Status:", pulp.LpStatus[model.status])
print("Required Initial Inventory (S0):", S0_value)
print("Maximum Storage Level:", max(S_values))
```

7.2.2 Storage Optimization

The initial storage inventory is fixed here, which was previously calculated. Also, the simulation starts at the hour after the storage is filled to its initial capacity. subsubsection 4.3.3

Listing 2: Python implementation of the South America base-case storage optimisation

```
import pandas as pd
import pulp
import numpy as np

# ============================================================
# Starting row (manual control)
# ============================================================
start_row = 3  # 3 for South America, 120 for Nordics

# ============================================================
# Data
# ============================================================
df_full = pd.read_excel(
    "Crude Methanol yearly Profile.xlsx",
    sheet_name="Nordics or South America"
)

# Apply starting row
df = df_full.iloc[start_row:].reset_index(drop=True)

F = df["Ft"].tolist()
T = len(F)


# ============================================================
# Utility mapping data
# ============================================================
map_df = pd.read_excel(
    "Distillation Feed ASPEN Data.xlsx",
    sheet_name="Vacuum or Base Case"
).sort_values("Percentage")

pct_breakpoints = map_df["Percentage"].to_numpy()

cooling_break = map_df["CoolingCost"].to_numpy()
lp_req_break = map_df["LP_req"].to_numpy()
mp_req_break = map_df["MP_req"].to_numpy()

lp_avail_break = map_df["LP_avail"].to_numpy()
mp_avail_break = map_df["MP_avail"].to_numpy()

max_capacity = 32166.467
x_break = pct_breakpoints * max_capacity

# ============================================================
# FT-dependent utility availability
```

```
# ============================================================
def interpolate_ft_dependent(ft):

    pct = np.clip(
        ft / max_capacity,
        0.20,
        1.00
    )

    lp_avail = np.interp(
        pct,
        pct_breakpoints,
        lp_avail_break
    )

    mp_avail = np.interp(
        pct,
        pct_breakpoints,
        mp_avail_break
    )

    return lp_avail, mp_avail

LP_avail_values = []
MP_avail_values = []

for ft in F:

    lp_avail, mp_avail = interpolate_ft_dependent(ft)
    LP_avail_values.append(lp_avail)
    MP_avail_values.append(mp_avail)

# ============================================================
# Parameters
# ============================================================
Dmax = max(F)
Dmin = 0.6 * Dmax

# 5% limit on distillation-rate changes
distillation_ramp_limit = 0.05 * Dmax

c_store = 0.00001
c_pumping = 0.0005

lp_price = 9    # 9 for South America, 44 for Nordics
mp_price = 11   # 11 for South America, 45 for Nordics

S0 = 41950  # 41950 for South America, 1870000 for Nordics

rho = 894.9
capex_eur_per_m3 = 600.0

# ============================================================
# Annualisation (Capital Recovery Factor)
```

```
# ============================================================
i = 0.06
n = 30

CRF = (
    i * (1 + i)**n
    / ((1 + i)**n - 1)
)

# ============================================================
# Optimisation model
# ============================================================
model = pulp.LpProblem(
    "Tank_Model_Corrected",
    pulp.LpMinimize
)

# ============================================================
# Decision variables
# ============================================================
D = pulp.LpVariable.dicts(
    "D",
    range(T),
    lowBound=Dmin,
    upBound=Dmax
)

S = pulp.LpVariable.dicts(
    "S",
    range(T),
    lowBound=0
)

# Pumping variable based on storage change
Pumping = pulp.LpVariable.dicts(
    "Pumping",
    range(T),
    lowBound=0
)

Smax = pulp.LpVariable(
    "Smax",
    lowBound=0
)

# ============================================================
# Storage CAPEX
# ============================================================
storage_capex_expr = (
    (Smax / rho)
    * 2
    * capex_eur_per_m3
)

```

```
annualised_capex_expr = (
    CRF * storage_capex_expr
)

# ============================================================
# Objective function
# ============================================================
opex_expr = pulp.lpSum(
    c_store * S[t]
    + c_pumping * Pumping[t]
    for t in range(T)
)

model += (
    opex_expr
    + annualised_capex_expr
)

# ============================================================
# Constraints
# ============================================================
for t in range(T):

    # Inventory balance
    if t == 0:

        model += (
            S[t]
            == S0 + F[t] - D[t]
        )

    else:

        model += (
            S[t]
            == S[t - 1] + F[t] - D[t]
        )

        # Distillation ramp-rate constraint
        model += (
            D[t] - D[t - 1]
            <= distillation_ramp_limit
        )

        model += (
            D[t - 1] - D[t]
            <= distillation_ramp_limit
        )

    # Maximum storage capacity
    model += S[t] <= Smax

    # Distillation cannot exceed feed
    # plus material available in storage
```

```
    model += D[t] <= F[t] + S[t]

    # Pumping cost based on absolute
    # change in storage level
    if t > 0:

        # Filling storage
        model += (
            Pumping[t]
            >= S[t] - S[t - 1]
        )

        # Emptying storage
        model += (
            Pumping[t]
            >= S[t - 1] - S[t]
        )

    else:

        # No pumping at the initial time step
        model += Pumping[t] == 0

# ============================================================
# Solve
# ============================================================
solver = pulp.PULP_CBC_CMD(msg=True)

model.solve(solver)

# ============================================================
# Results
# ============================================================
D_values = [
    pulp.value(D[t])
    for t in range(T)
]

S_values = [
    pulp.value(S[t])
    for t in range(T)
]

Pumping_values = [
    pulp.value(Pumping[t])
    for t in range(T)
]

# ============================================================
# D-based utility demand
# ============================================================
cooling_values = np.interp(
    D_values,
    x_break,
```

```
    cooling_break
)

lp_req_values = np.interp(
    D_values,
    x_break,
    lp_req_break
)

mp_req_values = np.interp(
    D_values,
    x_break,
    mp_req_break
)

# ============================================================
# Utility balances
# ============================================================
lp_purchase_values = np.maximum(
    np.array(lp_req_values)
    - np.array(LP_avail_values),
    0
)

mp_purchase_values = np.maximum(
    np.array(mp_req_values)
    - np.array(MP_avail_values),
    0
)

# ============================================================
# Cost calculations
# ============================================================
storage_opex = pulp.value(opex_expr)

storage_capex = pulp.value(
    storage_capex_expr
)

annualised_capex = pulp.value(
    annualised_capex_expr
)

total_cooling = np.sum(
    cooling_values
)

lp_cost = (
    np.sum(lp_purchase_values)
    * lp_price
)

mp_cost = (
    np.sum(mp_purchase_values)
```

```
    * mp_price
)

overall_opex = (
    storage_opex
    + total_cooling
    + lp_cost
    + mp_cost
)

total_annual_cost = (
    overall_opex
    + annualised_capex
)


# Pumping penalty reported separately
pumping_penalty = sum(
    c_pumping * v
    for v in Pumping_values
)

# ============================================================
# Print results
# ============================================================
print(
    "STATUS:",
    pulp.LpStatus[model.status]
)

print("\n----- COSTS -----")
print("Storage OPEX:", storage_opex)
print("Pumping Penalty:", pumping_penalty)
print("Cooling Cost:", total_cooling)
print("LP Cost:", lp_cost)
print("MP Cost:", mp_cost)
print("Overall OPEX:", overall_opex)
print("\nStorage CAPEX:", storage_capex)
print("Annualised CAPEX:", annualised_capex)

print(
    "\nTOTAL ANNUAL COST:",
    total_annual_cost
)
```

7.2.3 Product Recycling

This appendix presents the Python implementation used to optimise direct product recycling without intermediate storage. The simulation started at hour 3, since it was the first hour with 100% crude methanol production capacity that is required to have enough product recycled back to the distillation feed during the deficient period. subsubsection 4.3.4

Listing 3: Python implementation of the product recycling optimisation model

```
import pandas as pd
import pulp
import numpy as np


# ============================================================
# 1. LOAD DATA
# ============================================================
df0 = pd.read_excel(
    "Crude Methanol yearly Profile.xlsx",
    sheet_name="Nordics or South America"
)

map_df = pd.read_excel(
    "Distillation Feed ASPEN DATA.xlsx",
    sheet_name="Vacuum vs Base Case"
).sort_values("Percentage")

F_full = df0["Ft"].to_numpy()

pct_breakpoints = map_df["Percentage"].to_numpy()

cooling_break = map_df["CoolingCost"].to_numpy()
lp_req_break = map_df["LP_req"].to_numpy()
mp_req_break = map_df["MP_req"].to_numpy()

lp_avail_break = map_df["LP_avail"].to_numpy()
mp_avail_break = map_df["MP_avail"].to_numpy()

max_capacity = 32166.467
x_break = pct_breakpoints * max_capacity

# ============================================================
# 2. FT-DEPENDENT AVAILABILITY
# ============================================================
def interpolate_ft_dependent(ft):
    pct = np.clip(
        ft / max_capacity,
        0.20,
        1.00
    )
    lp_avail = np.interp(
        pct,
        pct_breakpoints,
```

```
        lp_avail_break
    )
    mp_avail = np.interp(
        pct,
        pct_breakpoints,
        mp_avail_break
    )
    return lp_avail, mp_avail

LP_avail_full, MP_avail_full = zip(
    *(
        interpolate_ft_dependent(ft)
        for ft in F_full
    )
)
LP_avail_full = list(LP_avail_full)
MP_avail_full = list(MP_avail_full)

# ============================================================
# 3. START ROW
# ============================================================
START_ROW = 3  # 3 for both Nordics and South America
df = df0.iloc[
    START_ROW:
].reset_index(drop=True)
F = F_full[START_ROW:]
LP_avail_hr = LP_avail_full[
    START_ROW:
]
MP_avail_hr = MP_avail_full[
    START_ROW:
]
T = len(F)

# ============================================================
# 4. PARAMETERS
# ============================================================
x = 0.6334
x_rec = 0.99995

alpha = (
    (x_rec - x) / x
)
Dmax = float(np.max(F))
Dmin = 0.60 * Dmax
# 5% limit on distillation-rate changes
ramp = 0.05 * Dmax
c_R = 0.0005
lp_price = 9    # 9 for South America, 44 for Nordics
mp_price = 11   # 11 for South America, 45 for Nordics

# ============================================================
# 5. OPTIMISATION MODEL
# ============================================================
```

```
model = pulp.LpProblem(
    "Recirculation_Model",
    pulp.LpMinimize
)

# ============================================================
# Decision variables
# ============================================================
D = pulp.LpVariable.dicts(
    "D",
    range(T),
    lowBound=Dmin,
    upBound=Dmax
)
R = pulp.LpVariable.dicts(
    "R",
    range(T),
    lowBound=0
)
LP = pulp.LpVariable.dicts(
    "LP",
    range(T),
    lowBound=0
)
MP = pulp.LpVariable.dicts(
    "MP",
    range(T),
    lowBound=0
)

# ============================================================
# Interpolation variables
# ============================================================
lambda_cont = {
    (t, k): pulp.LpVariable(
        f"lambda_{t}_{k}",
        lowBound=0
    )
    for t in range(T)
    for k in range(len(pct_breakpoints))
}
cool_cost_t = pulp.LpVariable.dicts(
    "cool_cost",
    range(T),
    lowBound=0
)
lp_req_t = pulp.LpVariable.dicts(
    "lp_req",
    range(T),
    lowBound=0
)
mp_req_t = pulp.LpVariable.dicts(
    "mp_req",
    range(T),
```

```
    lowBound=0
)

# ============================================================
# 6. OBJECTIVE FUNCTION
# ============================================================
model += (
    # Recycle operating cost
    pulp.lpSum(
        c_R * (1 + alpha) * R[t]
        for t in range(T)
    )
    # Cooling cost
    + pulp.lpSum(
        cool_cost_t[t]
        for t in range(T)
    )
    # LP and MP utility purchases
    + pulp.lpSum(
        lp_price * LP[t]
        + mp_price * MP[t]
        for t in range(T)
    )
)

# ============================================================
# 7. CONSTRAINTS
# ============================================================
for t in range(T):
    # ------------------------------------------------------
    # Distillation limits
    # ------------------------------------------------------
    model += D[t] >= Dmin
    model += D[t] <= Dmax
    # ------------------------------------------------------
    # Distillation ramp-rate limits
    # ------------------------------------------------------
    if t > 0:
        model += (
            D[t] - D[t - 1]
            <= ramp
        )

        model += (
            D[t - 1] - D[t]
            <= ramp
        )
    # ------------------------------------------------------
    # Recycle material balance
    # ------------------------------------------------------
    # Feed + recycled material = distillation rate
    model += (
        D[t]
        == F[t] + (1 + alpha) * R[t]
```

```
    )
    # ------------------------------------------------------------
    # Utility purchase constraints
    # ------------------------------------------------------------
    model += (
        LP[t]
        >= lp_req_t[t] - LP_avail_hr[t]
    )
    model += (
        MP[t]
        >= mp_req_t[t] - MP_avail_hr[t]
    )
    # ------------------------------------------------------------
    # Linear interpolation constraints
    # ------------------------------------------------------------
    # Interpolation weights sum to unity
    model += pulp.lpSum(
        lambda_cont[t, k]
        for k in range(
            len(pct_breakpoints)
        )
    ) == 1
    # Distillation operating point
    model += (
        D[t]
        == pulp.lpSum(
            lambda_cont[t, k]
            * x_break[k]
            for k in range(
                len(pct_breakpoints)
            )
        )
    )
    # Cooling requirement
    model += (
        cool_cost_t[t]
        == pulp.lpSum(
            lambda_cont[t, k]
            * cooling_break[k]
            for k in range(
                len(pct_breakpoints)
            )
        )
    )
    # LP steam requirement
    model += (
        lp_req_t[t]
        == pulp.lpSum(
            lambda_cont[t, k]
            * lp_req_break[k]
            for k in range(
                len(pct_breakpoints)
            )
        )
```

```
    )
    # MP steam requirement
    model += (
        mp_req_t[t]
        == pulp.lpSum(
            lambda_cont[t, k]
            * mp_req_break[k]
            for k in range(
                len(pct_breakpoints)
            )
        )
    )

# ============================================================
# 8. SOLVE
# ============================================================
solver = pulp.PULP_CBC_CMD(
    msg=True
)
model.solve(solver)

# ============================================================
# 9. RESULTS
# ============================================================
D_vals = [
    pulp.value(D[t])
    for t in range(T)
]
R_vals = [
    pulp.value(R[t])
    for t in range(T)
]
LP_vals = [
    pulp.value(LP[t])
    for t in range(T)
]
MP_vals = [
    pulp.value(MP[t])
    for t in range(T)
]
cool_vals = [
    pulp.value(cool_cost_t[t])
    for t in range(T)
]
lp_req_vals = [
    pulp.value(lp_req_t[t])
    for t in range(T)
]
mp_req_vals = [
    pulp.value(mp_req_t[t])
    for t in range(T)
]

# ============================================================
```

```
# 11. COST SUMMARY
# ============================================================
recycle_opex = sum(
    c_R * v
    for v in R_vals
)
cooling_cost = sum(
    cool_vals
)
lp_cost = sum(
    lp_price * v
    for v in LP_vals
)
mp_cost = sum(
    mp_price * v
    for v in MP_vals
)
total_cost = pulp.value(
    model.objective
)

# ============================================================
# 13. PRINT RESULTS
# ============================================================
print(
    "STATUS:",
    pulp.LpStatus[model.status]
)
print("\n----- COSTS -----")
print(
    "Recycle OPEX:",
    recycle_opex
)
print(
    "Cooling Cost:",
    cooling_cost
)
print(
    "LP Cost:",
    lp_cost
)
print(
    "MP Cost:",
    mp_cost
)
print(
    "\nTOTAL COST:",
    total_cost
)
print(
    "\nSaved: Recycle_Only.xlsx"
)
```

7.2.4 Hybrid Model Optimization

The model considers the selection of recycling and storage options using binary variables and evaluates K variable coefficients of storage size from 1 to 20. For each K value, the optimization model is solved independently. subsubsection 4.3.5

Listing 4: Python implementation of the Hybrid Model optimisation

```
import pandas as pd
import pulp
import numpy as np

def run_optimization(K_value):

    # ============================================================
    # 1. LOAD DATA
    # ============================================================
    df0 = pd.read_excel(
        "Crude Methanol yearly Profile.xlsx",
        sheet_name="Nordics or South America"
    )
    map_df = pd.read_excel(
        "Distillation Feed ASPEN DATA.xlsx",
        sheet_name="Vacuum vs Base Case"
    ).sort_values("Percentage")

    F_full = df0["Ft"].to_numpy()
    pct_breakpoints = (
        map_df["Percentage"].to_numpy()
    )
    cooling_break = (
        map_df["CoolingCost"].to_numpy()
    )
    lp_req_break = (
        map_df["LP_req"].to_numpy()
    )
    mp_req_break = (
        map_df["MP_req"].to_numpy()
    )
    lp_avail_break = (
        map_df["LP_avail"].to_numpy()
    )
    mp_avail_break = (
        map_df["MP_avail"].to_numpy()
    )
    max_capacity = 32166.467
    x_break = (
        pct_breakpoints
        * max_capacity
    )

    # ============================================================
    # Only use valid operating range
    # ============================================================
```

```
    valid_mask = (
        (pct_breakpoints >= 0.60)
        & (pct_breakpoints <= 1.00)
    )
    pct_breakpoints = (
        pct_breakpoints[valid_mask]
    )
    cooling_break = (
        cooling_break[valid_mask]
    )
    lp_req_break = (
        lp_req_break[valid_mask]
    )
    mp_req_break = (
        mp_req_break[valid_mask]
    )
    x_break = x_break[valid_mask]
    n_break = len(
        pct_breakpoints
    )

    # ============================================================
    # 2. FT-DEPENDENT AVAILABILITY
    # ============================================================
    def interpolate_ft_dependent(ft):
        pct = np.clip(
            ft / max_capacity,
            0.20,
            1.00
        )
        lp_avail = np.interp(
            pct,
            map_df["Percentage"].to_numpy(),
            lp_avail_break
        )
        mp_avail = np.interp(
            pct,
            map_df["Percentage"].to_numpy(),
            mp_avail_break
        )
        return lp_avail, mp_avail

    LP_avail_full, MP_avail_full = zip(
        *(
            interpolate_ft_dependent(ft)
            for ft in F_full
        )
    )
    LP_avail_full = list(
        LP_avail_full
    )
    MP_avail_full = list(
        MP_avail_full
    )
```

```
    # ============================================================
    # 3. START ROW
    # ============================================================
    START_ROW = 3
    df = df0.iloc[
        START_ROW:
    ].reset_index(drop=True)

    F = F_full[
        START_ROW:
    ]
    LP_avail_hr = LP_avail_full[
        START_ROW:
    ]
    MP_avail_hr = MP_avail_full[
        START_ROW:
    ]
    T = len(F)

    # ============================================================
    # 4. PARAMETERS
    # ============================================================
    x_val = 0.6334
    x_rec = 0.99995
    alpha = (
        (x_rec - x_val)
        / x_val
    )
    Dmax = float(
        np.max(F)
    )

    Dmin = 0.60 * Dmax
    ramp = 0.05 * Dmax
    # Scale K by maximum feed
    K = K_value * Dmax
    c_R = 0.0005
    c_store = 0.0005
    lp_price = 9    # 9 for South America, 44 for Nordics
    mp_price = 11   # 11 for South America, 45 for Nordics
    i_val = 0.06
    n_val = 30
    CRF = (
        i_val
        * (1 + i_val) ** n_val
        / (
            (1 + i_val) ** n_val
            - 1
        )
    )
    capex_storage = (
        600.0 / 894.9
    )
```

```
155
156     # ============================================================
157     # 5. MODEL
158     # ============================================================
159     model = pulp.LpProblem(
160         "Superstructure_Model",
161         pulp.LpMinimize
162     )
163
164     # ============================================================
165     # Configuration variables
166     # ============================================================
167     z_recycle = pulp.LpVariable(
168         "z_recycle",
169         cat="Binary"
170     )
171     z_storage = pulp.LpVariable(
172         "z_storage",
173         cat="Binary"
174     )
175     model += (
176         z_recycle
177         + z_storage >= 1
178     )
179     model += (
180         z_recycle
181         + z_storage <= 2
182     )
183
184     # ============================================================
185     # 6. DECISION VARIABLES
186     # ============================================================
187     D = pulp.LpVariable.dicts(
188         "D",
189         range(T),
190         lowBound=0
191     )
192     R = pulp.LpVariable.dicts(
193         "R",
194         range(T),
195         lowBound=0
196     )
197     S = pulp.LpVariable.dicts(
198         "S",
199         range(T),
200         lowBound=0
201     )
202     LP = pulp.LpVariable.dicts(
203         "LP",
204         range(T),
205         lowBound=0
206     )
207     MP = pulp.LpVariable.dicts(
208         "MP",
```

```
        range(T),
        lowBound=0
    )

    # ============================================================
    # Interpolation variables
    # ============================================================
    lambda_cont = {
        (t, k): pulp.LpVariable(
            f"lambda_{t}_{k}",
            lowBound=0
        )
        for t in range(T)
        for k in range(n_break)
    }
    cool_cost_t = (
        pulp.LpVariable.dicts(
            "cool_cost",
            range(T),
            lowBound=0
        )
    )
    lp_req_t = (
        pulp.LpVariable.dicts(
            "lp_req",
            range(T),
            lowBound=0
        )
    )
    mp_req_t = (
        pulp.LpVariable.dicts(
            "mp_req",
            range(T),
            lowBound=0
        )
    )
    Smax = pulp.LpVariable(
        "Smax",
        lowBound=0
    )
    S0 = 0

    # ============================================================
    # 7. OBJECTIVE FUNCTION
    # ============================================================
    model += (
        # Storage and recycling operating costs
        pulp.lpSum(
            c_R * R[t]
            + c_store * S[t]
            for t in range(T)
        )
              # Annualised storage capital expenditure
        + CRF
```

```
        * capex_storage
        * Smax
            # Cooling cost
        + pulp.lpSum(
            cool_cost_t[t]
            for t in range(T)
        )
            # LP and MP utility purchases
        + pulp.lpSum(
            lp_price * LP[t]
            + mp_price * MP[t]
            for t in range(T)
        )
    )

    # ============================================================
    # 8. CONSTRAINTS
    # ============================================================
    # K storage activation
    model += (
        Smax
        <= K * z_storage
    )
    for t in range(T):

        # ------------------------------------------------------
        # Distillation limits
        # ------------------------------------------------------
        model += (
            D[t] <= Dmax
        )
        model += (
            D[t] >= Dmin
        )

        # ------------------------------------------------------
        # Recycle activation
        # ------------------------------------------------------
        model += (
            R[t]
            <= K * z_recycle
        )

        # ------------------------------------------------------
        # Inventory balance
        # ------------------------------------------------------
        if t == 0:
            model += (
                S[t]
                == S0
                + F[t]
                - D[t]
                + (1 + alpha) * R[t]
            )
```

```
        else:
            model += (
                S[t]
                == S[t - 1]
                + F[t]
                - D[t]
                + (1 + alpha) * R[t]
            )
            # Distillation ramp-rate constraints
            model += (
                D[t] - D[t - 1]
                <= ramp
            )
            model += (
                D[t - 1] - D[t]
                <= ramp
            )

        # ------------------------------------------------------
        # Storage capacity
        # ------------------------------------------------------
        model += (
            S[t] <= Smax
        )

        # ------------------------------------------------------
        # Distillation feasibility
        # ------------------------------------------------------
        model += (
            D[t]
            <= F[t]
            + S[t]
            + K * z_recycle
        )

        # ------------------------------------------------------
        # Utility purchase constraints
        # ------------------------------------------------------
        model += (
            LP[t]
            >= lp_req_t[t]
            - LP_avail_hr[t]
        )
        model += (
            MP[t]
            >= mp_req_t[t]
            - MP_avail_hr[t]
        )

        # ------------------------------------------------------
        # Linear interpolation constraints
        # ------------------------------------------------------
        model += pulp.lpSum(
            lambda_cont[t, k]
```

```
            for k in range(n_break)
        ) == 1
        model += (
            D[t]
            == pulp.lpSum(
                lambda_cont[t, k]
                * x_break[k]
                for k in range(n_break)
            )
        )
        model += (
            cool_cost_t[t]
            == pulp.lpSum(
                lambda_cont[t, k]
                * cooling_break[k]
                for k in range(n_break)
            )
        )
        model += (
            lp_req_t[t]
            == pulp.lpSum(
                lambda_cont[t, k]
                * lp_req_break[k]
                for k in range(n_break)
            )
        )
        model += (
            mp_req_t[t]
            == pulp.lpSum(
                lambda_cont[t, k]
                * mp_req_break[k]
                for k in range(n_break)
            )
        )

    # ============================================================
    # 9. SOLVE
    # ============================================================
    solver = pulp.PULP_CBC_CMD(
        msg=False
    )
    model.solve(solver)

    # ============================================================
    # 10. RESULTS
    # ============================================================
    if (
        pulp.LpStatus[model.status]
        == "Optimal"
    ):
        D_vals = [
            pulp.value(D[t])
            for t in range(T)
        ]
```

```
        R_vals = [
            pulp.value(R[t])
            for t in range(T)
        ]
        S_vals = [
            pulp.value(S[t])
            for t in range(T)
        ]
        LP_vals = [
            pulp.value(LP[t])
            for t in range(T)
        ]
        MP_vals = [
            pulp.value(MP[t])
            for t in range(T)
        ]
        cool_vals = [
            pulp.value(cool_cost_t[t])
            for t in range(T)
        ]

        # ------------------------------------------------------
        # Cost components
        # ------------------------------------------------------
        cooling_cost = sum(
            cool_vals
        )
        lp_purchase = sum(
            lp_price * v
            for v in LP_vals
        )
        mp_purchase = sum(
            mp_price * v
            for v in MP_vals
        )
        recycle_opex = sum(
            c_R * v
            for v in R_vals
        )
        storage_opex = sum(
            c_store * v
            for v in S_vals
        )

        # ------------------------------------------------------
        # Storage CAPEX
        # ------------------------------------------------------
        smax_val = pulp.value(
            Smax
        )
        storage_capex = (
            CRF
            * capex_storage
            * smax_val
```

```
        )

        # ------------------------------------------------------
        # Store results
        # ------------------------------------------------------
        results = {
            "K": K_value,
            "status": "Optimal",
            "z_recycle": pulp.value(
                z_recycle
            ),
            "z_storage": pulp.value(
                z_storage
            ),
            "distillation_opex": (
                cooling_cost
                + lp_purchase
                + mp_purchase
            ),
            "hybrid_opex": (
                recycle_opex
                + storage_opex
                + cooling_cost
                + lp_purchase
                + mp_purchase
            ),
            "storage_capex": storage_capex
        }
    else:
        results = {
            "K": K_value,
            "status": pulp.LpStatus[
                model.status
            ],
            "z_recycle": None,
            "z_storage": None,
            "distillation_opex": None,
            "hybrid_opex": None,
            "storage_capex": None
        }
    return results

# ============================================================
# MAIN: LOOP OVER K VALUES 1 TO 20
# ============================================================
if __name__ == "__main__":
    print("\n" + "=" * 90)
    print(
        "SUPERSTRUCTURE OPTIMISATION "
        "- K SENSITIVITY (KEY COSTS)"
    )
    print("=" * 90)
    all_results = []
    for b in range(1, 21):
```

```
        res = run_optimization(b)
        all_results.append(res)

    # ============================================================
    # SUMMARY TABLE
    # ============================================================
    print("\n" + "=" * 90)
    print("SUMMARY TABLE")
    print("=" * 90)
    print(
        f"{'K':>5} | "
        f"{'z_recycle':>10} | "
        f"{'z_storage':>10} | "
        f"{'Distillation OPEX':>17} | "
        f"{'Hybrid OPEX':>13} | "
        f"{'Storage CAPEX':>14}"
    )
    print("-" * 90)

    for res in all_results:
        if res["status"] == "Optimal":
            print(
                f"{res['K']:5d} | "
                f"{res['z_recycle']:10.0f} | "
                f"{res['z_storage']:10.0f} | "
                f"{res['distillation_opex']:17.2f} | "
                f"{res['hybrid_opex']:13.2f} | "
                f"{res['storage_capex']:14.2f}"
            )
        else:
            print(
                f"{res['K']:5d} | "
                f"{'N/A':>10} | "
                f"{'N/A':>10} | "
                f"{'N/A':>17} | "
                f"{'N/A':>13} | "
                f"{'N/A':>14}"
            )
    print("=" * 90)
```

7.3 Heat Pump Sample Calculation for 100 % Electrolyser Capacity (South American Case)

This appendix traces one operating hour end-to-end. Hour 151 of the 8 784 h data set is used because the electrolyser delivers its full nameplate waste heat in that hour. subsubsection 4.4.1

Table 36: Step-by-step calculation of heat pump performance for the sizing hour (hour 151).

Description	Formula	Calculation
Step 0 — Selection of the Operating Point		
Raw waste heat	—	$\dot{Q}_{\mathrm{ELY,raw}} = 71.5234$ MW
Rounded waste heat	$\dot{Q}_{\mathrm{ELY}} = \mathrm{ROUND}(\dot{Q}_{\mathrm{ELY,raw}}, 0)$	$\dot{Q}_{\mathrm{ELY}} = 72.00$ MW
Utilisation	$\eta = \dot{Q}_{\mathrm{ELY,raw}}/\dot{Q}_{\mathrm{ELY,nom}}$	$\eta = 71.5234/72.00 = 99.3\%$
Step 1 — Single-Point Cycle Definition		
Condensation temp.	$T_{\mathrm{cond}} = T_{\mathrm{reb}} + \Delta T_{\mathrm{min,cond}}$	$85.0 = 75.0 + 10.0$ °C
Evaporation temp.	$T_{\mathrm{evap}} = T_{\mathrm{w,out}} - \Delta T_{\mathrm{min,evap}}$	$51.5 = 61.5 - 10.0$ °C
Temperature lift	$\Delta T_{\mathrm{lift}} = T_{\mathrm{cond}} - T_{\mathrm{evap}}$	$33.5 = 85.0 - 51.5$ K
Carnot COP	$\mathrm{COP}_{\mathrm{Carnot}} = (T_{\mathrm{cond}} + 273.15)/\Delta T_{\mathrm{lift}}$	$358.15/33.5 = 10.6910$
Real COP	$\mathrm{COP}_{\mathrm{real}} = \eta \cdot \mathrm{COP}_{\mathrm{Carnot}}$	$0.45 \times 10.6910 = 4.8110$
Applied COP	$\mathrm{COP}_{\mathrm{app}} = \min(\mathrm{COP}_{\mathrm{real}}, \mathrm{COP}_{\mathrm{max}})$	$\min(4.8110, 5.00) = 4.8110$
Step 2 — Split of Reboiler Duty		
Direct fraction	$f_{\mathrm{direct}} = (T_{\mathrm{ELY,in}} - T_{\mathrm{lim}})/(T_{\mathrm{ELY,in}} - T_{\mathrm{ELY,out}})$	$(85 - 80)/(85 - 50) = 0.142857$
Direct duty	$\dot{Q}_{\mathrm{direct}} = \min(\dot{Q}_{\mathrm{reb}},\ \dot{Q}_{\mathrm{ELY}} f_{\mathrm{direct}})$	$\min(22.7917,\ 72.00 \times 0.142857) = 10.2857$ MW
HP boost duty	$\dot{Q}_{\mathrm{HP}} = \dot{Q}_{\mathrm{reb}} - \dot{Q}_{\mathrm{direct}}$	$22.7917 - 10.2857 = 12.5060$ MW
Step 3 — Compressor Work & Evaporator Feasibility		
Compressor power	$P_{\mathrm{comp}} = \dot{Q}_{\mathrm{HP}}/\mathrm{COP}_{\mathrm{app}}$	$12.5060/4.8110 = 2.5995$ $\mathrm{MW_{el}}$
Evaporator duty	$\dot{Q}_{\mathrm{evap}} = \dot{Q}_{\mathrm{HP}} - P_{\mathrm{comp}}$	$12.5060 - 2.5995 = 9.9065$ MW
Available heat	$\dot{Q}_{\mathrm{avail}} = \dot{Q}_{\mathrm{ELY}} \cdot \Delta T_{\mathrm{leg}}/35$	$72.00 \times 18.5/35 = 38.0571$ MW
Feasibility	$\dot{Q}_{\mathrm{avail}} - \dot{Q}_{\mathrm{evap}} > 0$	$38.0571 - 9.9065 = 28.1506\,\mathrm{MW} > 0$
Step 4 — Economics of the Hour		
Electricity cost	$C_{\mathrm{el}} = P_{\mathrm{comp}} \cdot p_{\mathrm{grid}}$	$2.5995 \times 9.1605 = 23.81$ €/h
Avoided steam cost	$C_{\mathrm{steam}} = \dot{Q}_{\mathrm{HP}} \cdot p_{\mathrm{steam}}$	$12.5060 \times 9.00 = 112.55$ €/h
Net saving	$\Delta C = C_{\mathrm{steam}} - C_{\mathrm{el}}$	$112.55 - 23.81 =$ **88.74** €/h
Step 5 — Cooling-Water Balance		
Residual heat	$\dot{Q}_{\mathrm{res}} = \dot{Q}_{\mathrm{ELY}} - \dot{Q}_{\mathrm{direct}} - \dot{Q}_{\mathrm{evap}}$	$72.00 - 10.2857 - 9.9065 = 51.8078$ MW
CW mass flow	$\dot{m}_{\mathrm{CW}} = \dot{Q}_{\mathrm{res}} \cdot 10^6/(c_p \Delta T_{\mathrm{CW}})$	$51.8078 \times 10^6/(4180 \times 15) = 826.3$ kg/s
CW cost	$C_{\mathrm{CW}} = \dot{m}_{\mathrm{CW}} \cdot 3.6 \cdot p_{\mathrm{CW}}$	$826.3 \times 3.6 \times 0.05 = 148.73$ €/h
Avoided CW cost	$C_{\mathrm{CW,av}} = \dot{Q}_{\mathrm{evap}} \cdot 10^6 \cdot 3.6 \cdot p_{\mathrm{CW}}/(c_p \Delta T_{\mathrm{CW}})$	$9.9065 \times 10^6 \times 3.6 \times 0.05/(4180 \times 15) = 28.44$ €/h
Step 6 — Sizing & Annual Economics		
Design duty	$\dot{Q}_{\mathrm{design}} = \dot{Q}_{\mathrm{HP,peak}}(1 + m)$	$12.5060 \times 1.10 = 13.7566$ $\mathrm{MW_{th}}$
CAPEX (mid)	$\mathrm{CAPEX} = \dot{Q}_{\mathrm{design}} \times 300$ €/$\mathrm{kW_{th}}$	$13\,757 \times 300 = 4\,126\,975$ €

Hour 151 is the sizing hour: its boost duty of 12.5060 MW is the annual maximum. The vendor COP ceiling does not bind.

Table 37: Summary of sample hour (hour 151, 100% electrolyser capacity).

Symbol	Quantity	Value	Unit
$\dot{Q}_{\mathrm{ELY}}$	Electrolyser waste heat	72.00	MW
$\dot{Q}_{\mathrm{reb}}$	Reboiler duty required	22.7917	MW
$\dot{Q}_{\mathrm{direct}}$	Direct HX duty (free)	10.2857	MW
$\dot{Q}_{\mathrm{HP}}$	Heat-pump boost duty	12.5060	MW
ΔT_{lift}	Compressor lift	33.50	K
COP	Applied COP	4.8110	—
P_{comp}	Compressor power	2.5995	$\mathrm{MW_{el}}$
$\dot{Q}_{\mathrm{evap}}$	Evaporator heat drawn	9.9065	MW
$\dot{Q}_{\mathrm{avail}}$	Heat water leg can give	38.0571	MW
ΔC	Net saving in the hour	88.74	€/h